THE GENERATION AND PROPAGATION OF PLANETARY ROSSBY WAVES

by

Glenn John SHUTTS

Atmospheric Physics Group
Department of Physics
Imperial College, London

A thesis submitted for the degree of
Doctor of Philosophy
to the University of London

September 1976

ABSTRACT

The problem of stationary planetary wave forcing by orography and longitudinal asymmetry of heating and cooling is re-examined in the light of recent observations and theories of stratospheric motion. It is deduced that the region between *30* and *60* km is a sink of planetary wave energy for wavenumbers *1* and *2* in winter and that — in contrast to many theoretical descriptions — the transmission of wave energy to those levels is unimpeded.

Quasi-geostrophic theory expressed in spherical polar geometry suggests that in winter wave energy should be able to propagate freely into the upper stratosphere for the largest scales of motion. The uncertainty in the absorption mechanism is avoided by the use of an energy-transmitting boundary condition at a suitably chosen level and attention is concentrated on the structure of the wave motion below. Features of the January mean contour charts such as the Siberian and Aleutian anticyclones are shown to be consistent with the theory of untrapped, thermally forced motion. Close agreement of the structure of wavenumber *1* in the theoretical solutions with existing observations is obtained for all heights below *30* km vindicating the use of energy-transmitting boundary conditions. An important consequence of the ability of forced waves to propagate energy into the stratosphere is the poleward transport of heat which is particularly strong for thermally-forced motion near the level of non-adiabatic heating. The calculations suggest that the contribution of stationary, thermally-generated waves to the total poleward eddy heat transport is a major one in the lower troposphere.

Some attempt to describe the monsoonal circulation of the summer (northern) hemisphere is made with the inclusion of a stratosphere

dominated by easterly mean zonal winds. The presence of a critical layer where the mean zonal wind vanishes introduces some interesting problems as regards the 'realism' of the linearized solution. Observations below 5 km in July show the phases of low wavenumber disturbances tilting rapidly *eastward* with height in marked contrast to the westward tilt in winter. Solutions with critical layer absorption are in poor agreement with observation in the lower troposphere with westward tilt though the rapid attenuation of all waves in the stratospheric easterlies is well represented.

CONTENTS

INTRODUCTION

Synoptic meteorologists have long recognised that apart from the constant progression of depressions and anticyclones on surface pressure charts, there are some areas that are persistently associated with cyclonic or anticyclonic flow. In winter, the cold, continental anticyclones are a regular feature of the surface pressure pattern, particularly the 'Siberian High' whose central pressure is often far in excess of that found in typical 'travelling anticyclones'. Other persistent stationary pressure perturbation phenomena at the surface are the Icelandic and Aleutian 'lows' in winter and the summertime Azores High and Asiatic (monsoonal) low. Stationary, high pressure anomalies of the surface mean pressure charts tend to occur over the continental land masses in winter and over the oceans in summer. This fact provides some indication of a relationship between the differing heating and cooling effects of land and sea, and the large-scale flow patterns. The eastern sides of the continents are intensely cold near the surface in winter through the prolonged cooling of air travelling from west to east.

The mean, winter contour height charts of the *100* and *200* mb surfaces show pronounced low wavenumber troughs and ridges which appear in roughly the same place from year to year, which again points to some relation to the underlying topography. With the advent of regular high altitude rocket soundings into the high stratosphere it soon became apparent that these quasi-stationary troughs and ridges extend upwards to above *50* km, where they completely dominate the motion. Typically, the wave motion is made of wavenumbers *1* (off-pole circulation) and *2* with the short-wavelength baroclinic eddies, characteristic of the tropospheric flow, generally absent above *20* km. The January mean contours near *30* km show a well-defined ridge over the Aleutian Islands (~*150*°W) which is the result of the constructive interference of wavenumber *1* and *2* disturbances.

Stratospheric motion remains fairly steady in the northern winter hemisphere except for the dramatic sudden warming events when the circumpolar vortex becomes highly distorted, usually splitting into two distinct eddies and finally changing to a steady easterly flow similar to that of the summertime flow. We shall be primarily interested in the steady, planetary wave structure arising from lower tropospheric forcing and not strongly time-dependent phenomena.

The important questions arising are:

(1) By what physical mechanism does the surface topography influence the flow ?

(2) How does the tropospheric forcing make its influence felt in the upper atmosphere above *20* km ?

A wave description of the perturbed motion and its forcing is adopted for a number of reasons. The basic periodicity of the horizontal co-ordinates and the scale of the motion suggest an elementary representation by the superposition of a few Fourier components in the linearized analysis. Furthermore, the dispersive properties of large-scale motion are clearly revealed by the wave description, through the relationship of frequency to wavenumber and basic state parameters, and hence group velocity and energy propagation are well-defined.

The daily hemispheric charts of contour height can be imagined to be composed of stationary and transient components such that the 'stationary' part represents the average over some interval of time and the transient part is the departure from this. The choice of the time interval over which averaging should take place depends obviously on the time scale of motion under consideration and for our case must be greater than the typical period of transient Rossby wave motion. The monthly-mean

contour chart is taken as representing the stationary component of planetary wave motion and its year to year similarity confirms the suitability of this choice.

In the theoretical description of forced, stationary planetary wave motion that follows, all unsteady motion is excluded. Some implicit inclusion is inevitable in the origins of areas of large-scale heating and cooling through the transport and convergence of sensible and latent heat fluxes (e.g. in boundary layer convection and baroclinic wave transfer). Attempts to couple the action of small-scale boundary-layer turbulence to the planetary wave are made via the Ekman theory. It is quite feasible that the transfer of energy between the baroclinic eddies and long planetary waves will be important in the troposphere but not in the stratosphere where baroclinic instability is much less evident. Inclusion of these other interacting scales through parameterization would be difficult and so it is assumed that they are in some sort of balance with each other and that the stationary wave problem can be treated in isolation.

In Chapter 1 we discuss previous work and ideas on the relationship between the underlying topography and the causes of longitudinal climate variation. Emphasis is placed on pictorial representation of the dynamics in terms of vortex tube arguments. Observations of zonal wind distribution and low wavenumber disturbances are described and compared briefly with existing theories.

Chapter 2 is a re-examination of the work of Charney and Drazin (1961) concerning the reflectivity of stratosphere to upward propagating planetary waves described in spherical polar geometry. The inapplicability of energy-reflecting upper boundary conditions is stressed and is regarded as the major defect in previous attempts to model large-scale forcing with the quasi-geostrophic equations.

In Chapter 3 we put forward theoretical models of orographic and thermal forcing for the simplest cases that admit analytic solution. An 'energy-transmitting' upper boundary condition (closely related to the Sommerfeld-Radiation condition) is devised which is judiciously applied to a level above which the observations suggest there is considerable wave energy absorption. Close similarity in structure to the existing observational data suggests the correctness of the chosen upper boundary condition, and low-level features such as the Siberian anticyclone are well-described. The significantly large transfer of heat polewards in thermally-forced waves indicates its importance in the total poleward eddy heat transport.

Chapter 4 complements the analytic solutions of the previous chapter with numerical calculations for various profiles of zonal wind and static stability. Numerical integration is particularly useful for calculating the forced motion in summer where the complicated zonal wind structure rules out simple analytic solution. The changeover from westerly to easterly winds in the stratosphere causes the differential equation for the vertical structure to contain a singular point where $\bar{U} = 0$. This 'critical layer' is excluded from the region of numerical integration and the analytic result is used there. The rapid upward decay (in the easterly winds) of the wave is predicted by the model solutions.

Chapter 5 is concerned with the interaction of slowly-varying (in time) stationary waves with the zonal current. The main conclusions of the study are that the sum of the specific zonal kinetic energy and the total wave energy are locally constant in time and that this implies no *net* propagation energy — merely a local conversion from zonal kinetic energy to disturbance energy. Some physical insight is gained into the transfer of momentum and its relation to the sudden warming phenomenon. Observational evidence supporting these ideas is given.

CHAPTER 1 OBSERVATIONS AND THEORIES OF LARGE-SCALE FORCING

(i) Observations

In the last twenty years or so, sufficient information has been compiled to produce a description of large-scale motion from the ground up to at least *40* km, with the data above this level being fairly scanty. The westerly zonal winds of the winter troposphere continue to increase up to about *60* km with well-defined jet-structure occurring near *10* km at *30*°N and *80* km at *40*°N. Above *80* km the zonal wind becomes easterly though we shall not be concerned with the atmosphere at these heights (Fig.1.1). In summer the zonal tropospheric westerlies are lighter and become easterly above *20* km reaching a maximum between *60* and *80* km. It should be noted that the mean stratospheric winds appear to be much more variable in magnitude than the tropospheric winds with a factor of *2* difference between years being not uncommon. As a consequence of thermal wind balance we infer that the polar regions of the stratosphere are very cold in winter (*-60*°C at *25* km) but in summer are the warmest regions (*-40*°C at *25* km).

One of the most striking examples of large-scale forced motion in the troposphere is the wintertime Siberian anticyclone which dominates the circulation of Asia. The continental land mass near the surface is characterised by intense cold, especially on the eastern side where temperatures of *-50* to *-60*°C are frequently reported. On the *500* mb charts there is little trace of the anticyclone over Siberia though the contour charts are not zonally symmetric with the presence of marked troughs extending southwards across Japan and the Great Lakes region. A third smaller trough extends across Eastern Europe. These patterns of waves in the mean January contour charts become even more pronounced in the stratosphere. The *10* mb (*30* km) contour heights show an intense polar vortex displaced away from the north pole and a persistent anticyclone

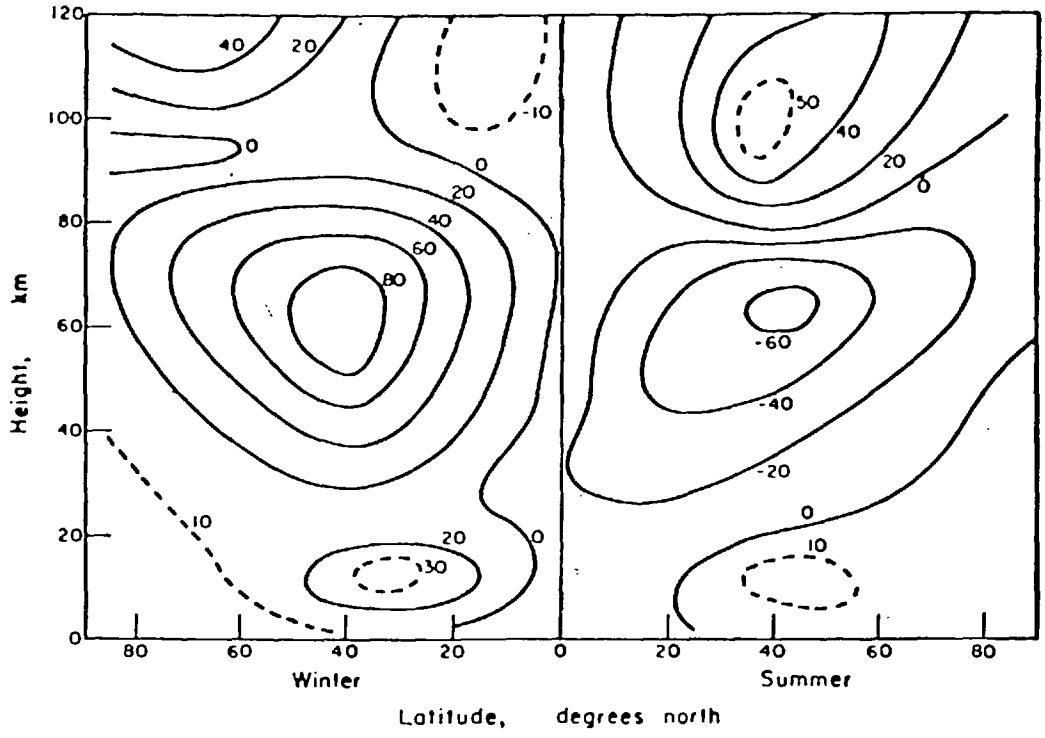

Figure 1-1 Meridional Cross-Section of Mean Zonal Wind (m/sec). (After R.E. Newell, 1969)

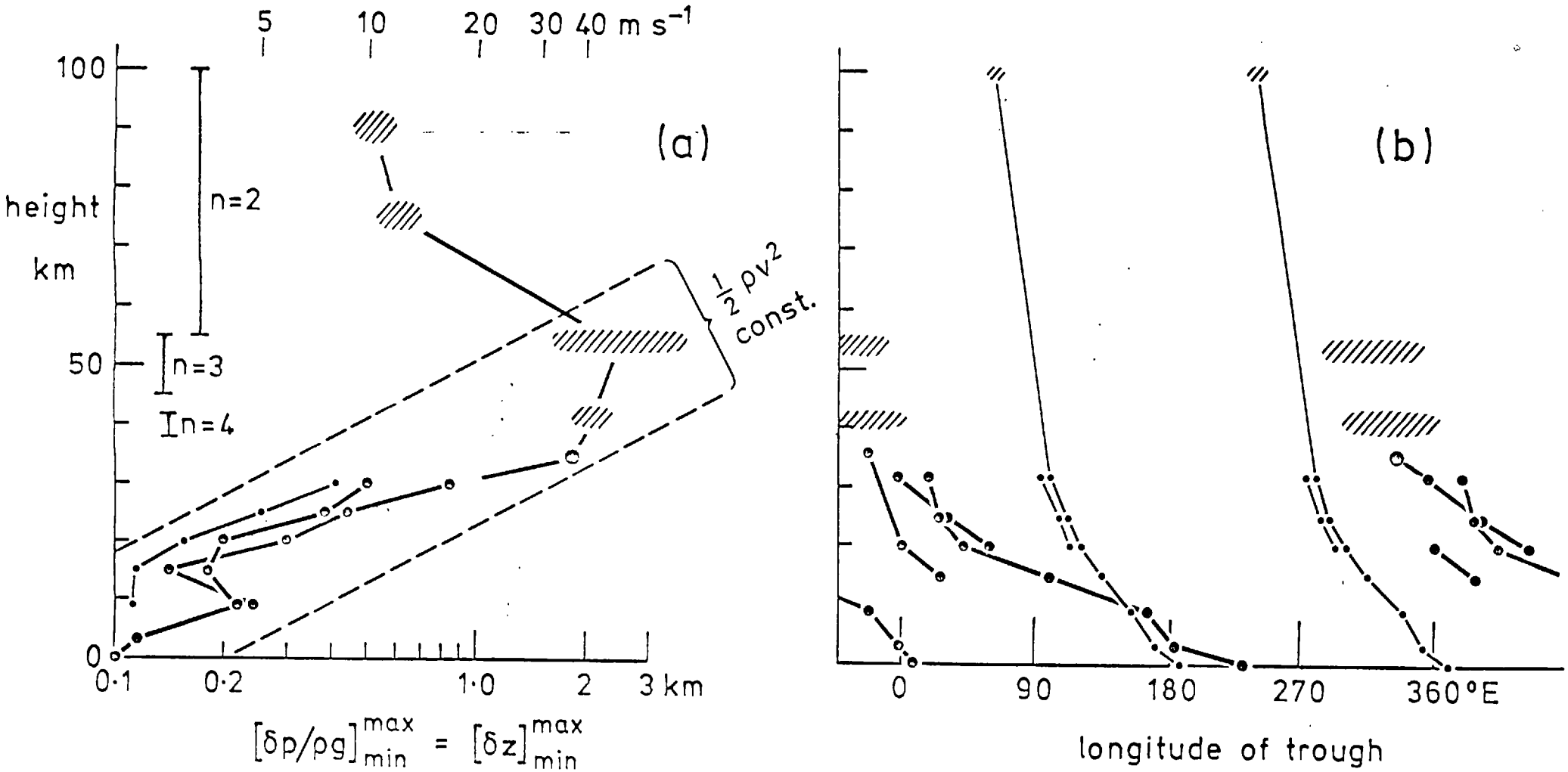

Fig.1.2 Variation with height of (a) the amplitude and (b) the phase of the January mean eddy motion at 50°N. (a) Amplitude, defined as the difference between maximum and minimum contour height is plotted on a logarithmic scale. Where the specific kinetic energy is constant the variation is parallel to the thin broken line. Also shown are levels where, for several values of n, $\frac{1}{2}\rho v^2$ should begin to decrease upwards (lower limit) and where the amplitude 'n' should begin to decrease upwards (upper limit). (b) Phase, defined as longitude of trough. Thick line, $s = 1$; thin line, $s = 2$; undetermined component ... For origin of data see Green, J.S.A., Phil.Trans.R.Soc.Lond. A 271, p.570 (1972).

near *150*°W which is well-known as the 'Aleutian High'. The 'eddy velocities' associated with these waves are considerably larger than their tropospheric counterparts exceeding *30* m s^{-1} frequently. The most outstanding difference between the tropospheric and stratospheric flow patterns is the virtual absence of wavenumbers greater than *3* above *20* km and wavenumber *1* usually makes the dominant contribution. Since the low zonal wavenumber disturbances form the major part of the deviation from zonal symmetry in the mean contour charts for both the stratosphere and troposphere we shall concentrate on their description.

Contour heights and temperatures are Fourier-analysed along latitude circles and the amplitudes and phases are given as a function of height and longitude in the usual observational analyses of large-scale phenomena (e.g. Muench, 1965). For our purposes a description in terms of a spherical harmonic expansion might be more appropriate since we shall treat the forcing of planetary wave motion as a hemispheric phenomenon and since the linearized quasi-geostrophic equations are separable in terms of associated Legendre functions.

Green (1972) has summarised recent data and theories of stratospheric motion and presents amplitude and phase of wavenumber *1* and *2* up to *100* km. though the description above *50* km is rather sketchy (Fig.1.2). Both waves tilt uniformly to the west with height with vertical wavelengths of about *50* km typically. Green shows that the specific kinetic energy of the wave motion tends to remain constant with height (or even increases) up to *40* to *50* km above which it rapidly decreases. These points will be enlarged upon further and at this stage it will suffice to recognise that the stationary perturbations are of great vertical extent.

(ii) Theories of planetary wave motion and forcing

Substantial advances in large-scale, dynamical meteorology have been made with the approximated, vertical component of vorticity equation:

$$\frac{D}{Dt_H}(\zeta + f) = \frac{f_0}{\rho_0}\frac{\partial}{\partial z}(\rho_0 w) \qquad \text{——(1.1)}$$

where D/Dt_H is the rate of change of absolute vorticity following the horizontal projection of the motion, f is the coriolis parameter (with f_0 being a constant middle-latitude value), $\rho_0(z)$ is the basic state density field, w is the vertical velocity and z is the height. This equation as it stands contains no twisting of vorticity (from horizontal to vertical), no stretching of relative vorticity and the baroclinic generation term has been ~~rejected~~ neglected (though in practice we may include it in the derivation of the quasi-geostrophic set; see appendix or White, 1976). Vorticity is generated primarily through the stretching term (on the R.H.S. of 1.1) by the forced differential vertical displacement of air and subsequent compression or stretching.

We now briefly review the behaviour of two-dimensional barotropic flow on a rotating sphere by setting the R.H.S. to zero in equation (1.1). Horizontally-non-divergent motion allows the definition of a streamfunction such that

$$\underline{V}_H = \underline{k} \wedge \nabla\psi \qquad (\underline{k} \text{ is the unit vector pointing along the local vertical})$$

If we express the vorticity equation in spherical polar co-ordinates (see sketch)

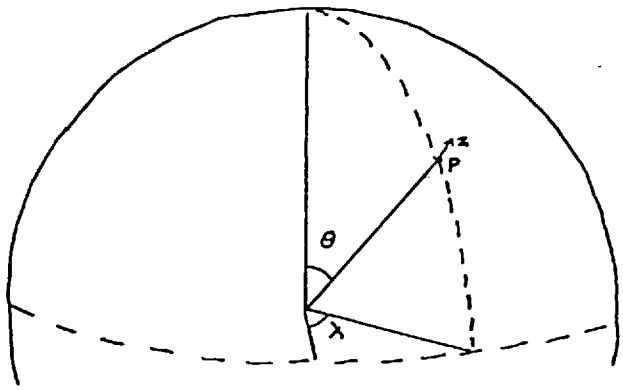

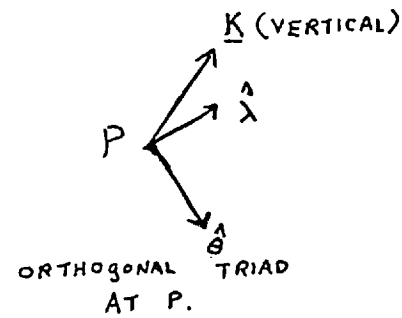

we have: $$\left(\frac{\partial}{\partial t} + \underline{V}_H.\underline{\nabla}\right)\left(\nabla_H^2\psi + 2\Omega\cos\theta\right) = 0$$

which admits solutions:

$$\psi = A\exp im(\lambda - ct)P_n^m(\cos\theta) \qquad \text{with} \quad c = \frac{-2\Omega}{n(n+1)}$$

where m (zonal wavenumber) and n are integers (subject to the condition $n \geq m$) and $P_n^m(\cos\theta)$ is an associated Legendre polynomial.

We note that all spherical harmonic wave patterns propagate westward relative to the atmosphere and that the P_1^1 mode ($= \sin\theta\cos(\lambda + \Omega t)$) remain stationary in space. In the high n limit, $c \to 0$ and the wave pattern moves with almost the same angular velocity of the atmosphere.

The meridional structure given by $P_n^m(\cos\theta)$ is complicated generally (examples given in Fig.1.3) and although we will not be concerned with the details, some useful rules of thumb exist. The number of 'peaks and troughs' encountered along a meridian from pole to pole is given by $n - m + 1$ and all the modes with $n = m$ peak at the equator. The $P_{m+1}^m(\cos\theta)$ modes are of zero amplitude at the pole and equator with one middle latitude peak and it is this class of waves that we assume to be most relevant to the discussion of planetary wave forcing though other modes will be considered.

Since the phase speed of the waves depends on the n parameter, the motion is dispersive.

Large-scale motion therefore has a strong tendency to move westwards with high angular speed (120°longitude/day for $n = 2$) and can remain stationary with respect to the earth only if the angular speed of the atmosphere relative to the earth is equal and opposite in direction. Typical angular speeds of the atmosphere relative to the earth are about

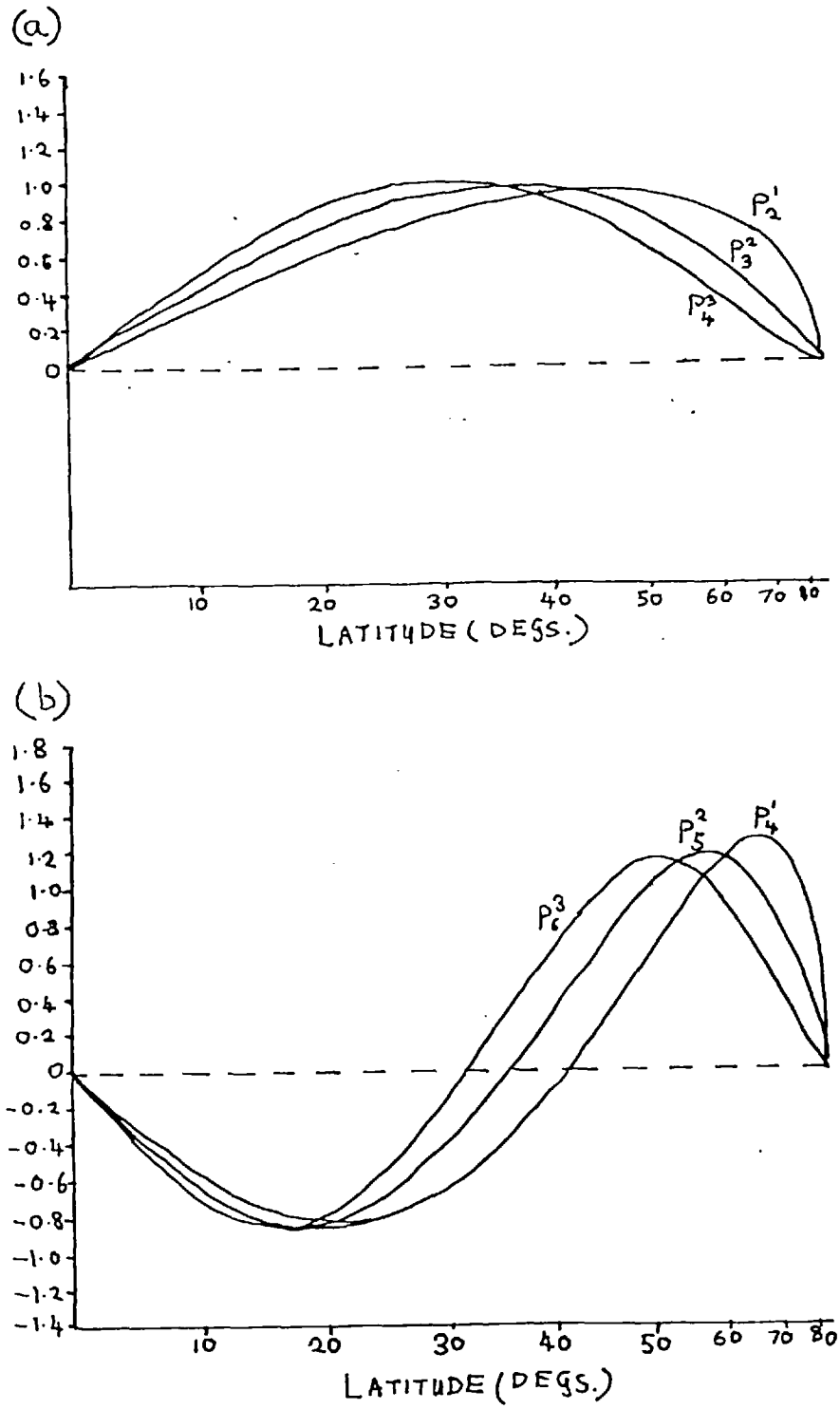

FIG. 1.3

(a) THE NORMALISED ASSOCIATED LEGENDRE FUNCTIONS, $P_{m+1}^m(\text{SIN(LAT.)})$

(b) " " " " " $P_{m+3}^m(\text{SIN(LAT.)})$

20°longitude/day and therefore unable to balance the rapid retrogression of low n mode planetary waves. Fast moving planetary waves are not observed in the real atmosphere ~~which is due mainly to the divergence of horizontal motion.~~ if only because at very large scales the horizontal divergence can no longer be neglected, even for rough qualitative purposes.

Charney and Eliassen (1949; referred to hereafter as CE) made a quantitative study of the effects of middle-latitude orography on the mean motions with an equivalent barotropic model of the atmosphere. They considered a constant zonal flow bounded at the northern and southern sides and found the response of the stationary, linearized barotropic vorticity equation to a realistic orography at the lower boundary. Those frictional effects that are of importance to the amplitude of the wave motion were included through an implicit representation of an 'Ekman boundary layer' entering the lower boundary condition. The calculated amplitude distribution was compared to the January 500 mb contours at 45°N and was found to be in very good agreement with the observed stationary pattern *only* when an excessively large eddy diffusivity was used to describe the boundary layer turbulence. Anomalously large amplitude motion occurred with typical eddy diffusivities and the phases of the lowest wavenumber components were not consistent with the observed. The response was essentially close to resonance and this tends to detract from the usefulness of the results since small changes in the system parameters produce large changes in amplitude.

Sankar-Rao (1965) attempted to extend the CE analysis to spherical geometry using the harmonic expansion of surface elevation and quasi-geostrophic theory with pressure as a vertical co-ordinate. An upper free surface boundary condition was used and the resulting amplitude and phase was found to be in poorer agreement with observed motion than that given by CE. The most serious deficiencies in the wave description

were the vertical phase lines and resonant response for wavenumber 5.

The orographically generated planetary waves with which this thesis is mainly concerned are those of low wavenumber that penetrate the high stratosphere. We are interested in the continental elevations which force wavenumbers *1*, *2* and *3* rather than the mountain range scale (e.g. Rockies, Alps etc) features which are best treated as isolated forcing agencies. Sankar-Rao gives the spherical harmonic expansion of the surface elevation up to *15*th order and typical amplitudes of low wavenumber orographic forcing are inferred.

The oldest theories of thermally forced stationary wave motion date back to the 17th century when Halley accounted for the trade wind belts and monsoons in terms of the large scale buoyant ascent of warm air in the regions of strongest heating. Hadley, later (1735) recognised the importance of the earth's rotation in modifying the direction of flow of the air as it moves towards the heating regions (this type of reasoning is still used in geography books of today to explain the Asiatic monsoon).

Smagorinsky (1953) argues that such an explanation is not even consistent with observation since the surface Siberian anticyclone does not coincide with the region of maximum cooling. Classical 'land and sea breeze' reasoning breaks down not only because the wind field is in geostrophic balance with the pressure field on the large scale but also because all large-scale planetary motion is dispersive. In Chapters 2 and 3, it will be shown how wave energy can propagate vertically ~~due to~~ because of the 'β-effect' and how this can produce motion quite different from that suggested by vortex compression arguments alone, for both orographic and thermal forcing.

A simple vortex tube description of the formation of 'cold surface

anticyclones' on an f-plane (dishpan for instance) however gives some insight into the mechanics. (SEE SKETCH)

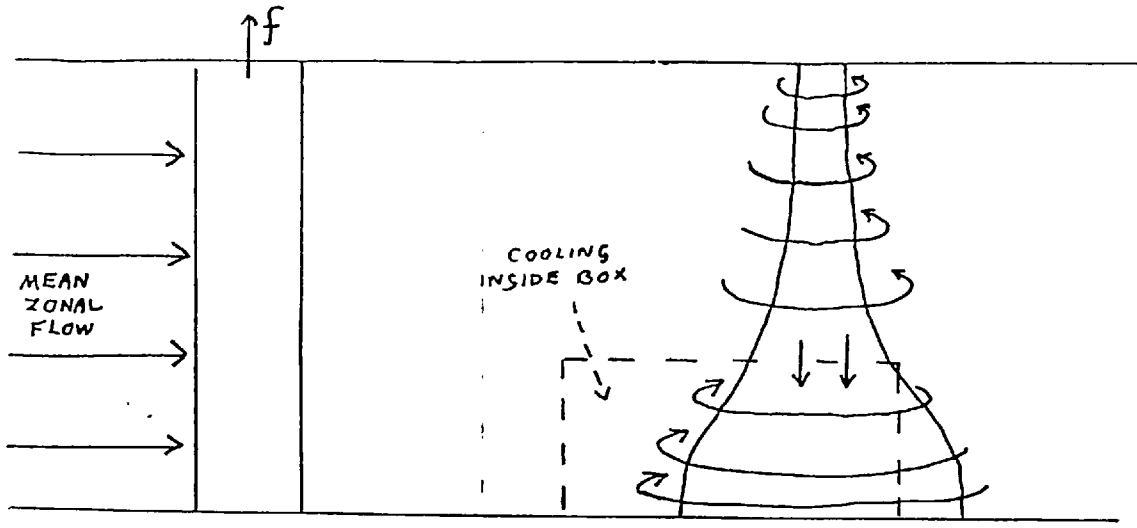

A cylindrical vortex tube in a uniform westerly current between upper and lower plane rigid surfaces will be distorted and become bottle-neck shaped as it enters a region of low level cooling and subsides. Vortex compression will generate an anticyclone at low levels and stretching causes a depression aloft. The amplitude of the motion will be greatest as the distorted tube leaves the cooling region. The changeover from anticyclone to depression will occur somewhere near the top of the cooling region. The assumption of a rigid upper boundary in this model is a rather artificial representation of the sudden increase in static stability in the stratosphere though it suffices for this qualitative argument. In Chapter 2 we investigate the effect of the discontinuous change in static stability at the tropopause on the long planetary Rossby waves and show that a rigid or free surface representation is inappropriate for the largest horizontal scale of wave motion which propagates energy upwards. The ~~vortex tube~~ f-plane description is useful only for the shortest horizontal scales of motion.

Smagorinsky (1953) studied the effect of lower tropospheric zonal asymmetries of heating and cooling on a uniform shear baroclinic zonal current.

The quasi-geostrophic, vertical component of the vorticity equation on a middle-latitude β-plane:

$$\frac{D\zeta}{Dt_H} + \beta v = \frac{f_0}{\rho_0}\frac{\partial}{\partial z}(\rho_0 w)$$

is linearized about a zonal wind $U = U(0) + \Lambda z$, and w is eliminated using the thermodynamic equation (with a source term). Smagorinsky finds solutions for the perturbed steady motion resulting from low-level heating between upper and lower plane rigid surfaces and contrasts these with the corresponding solutions allowing for a stratosphere where perturbations tend to zero at great heights. An 'Ekman boundary layer' was included in a similar manner to that introduced by CE such that the vertical velocity at the lower boundary is proportional to the geostrophic perturbation vorticity. The flow consistent with a sinusoidal heating function $Q(x,y,z) = \chi(z)\sin kx \sin \mu y$ was found for various profiles of $\chi(z)$ peaking near 2 km. Using estimates of the magnitude of the vertically integrated heating rate taken from other workers (e.g. London, 1952) he found that the forced perturbation amplitude to be of the correct order of magnitude only with the inclusion of friction which was essential to avoid near-resonance. The inclusion of a stratosphere improved the upper troposphere wave amplitude agreement with observed and tended to remove the response further away from resonance. Phase lines are vertical in non-frictional cases (except for sign changes) and westward tilt with height occurs *only* in the lower troposphere with Ekman friction. Smagorinsky concluded that the amplitudes of thermally and orographically forced motion were comparable near the surface and that the 'thermal influence' becomes relatively less important in the upper atmosphere. A detailed comparison of the theory with observation is not justified in view of the lack of knowledge of the heating function, though many qualitative features are correct including the formation of a Siberian anticyclone downstream of the area of maximum cooling rate.

The work of Chapters 3 and 4 will extend the description of thermally-forced motion by Smagorinsky to spherical geometry in which planetary wave energy is allowed to propagate into the high stratosphere and be absorbed there. The wave energy sink at upper levels prevents resonance in the system for propagating waves and Ekman friction has relatively little effect on the motion because of the largness of the horizontal scale of wave motion. Orographic forcing is treated in a similar way and the structure of low-wavenumber motion up to *40* km is determined.

(iii) The nature of the heating function

The heating function is given by the time-average of the longitudinal variations of heating (and cooling) rate that are related to the underlying topography in some way. Quasi-stationary long waves are forced by regions of heating or cooling that are persistent for at least several weeks and the month provides a convenient averaging time scale for this motion. All scales of motion smaller than the planetary scale can contribute to the heating function if related to the topography and the task of finding the sum of these contributions must be tackled indirectly.

Clapp (1961) calculates the spatial distribution of heating averaged between *1000* and *500* mb by two different methods and finds poor agreement between them, as regards amplitude. The 'thermodynamic energy method' which he and other workers used involves the evaluation of potential temperature advection from the mean gradient wind distribution and potential temperature field. Vertical motion is crudely obtained from the horizontal divergence of the gradient wind (for the details of the approximations made by different authors, see Clapp, 1961). The other method he uses is an energy budget technique to estimate the three main heating components:

(1) Release of latent heat of condensation

The time-mean longitudinal variation in precipitation rate is a useful measure of the total heating rate due to condensation, integrated throughout the atmospheric column above. Möller (1950) shows that the heating rate due to latent heat of condensation reaches a maximum at about 2 km (probably associated with frontal rain).

(2) Divergence of the net radiation field

Heating in the atmosphere due to the absorption of short-wave (solar) radiation and long (terrestrial) wave radiation is also difficult to estimate. Short wave radiation from the sun is absorbed by ozone, water vapour and solid impurities and is probably dependent on longitude (through the topography) to a lesser extent than long wave radiation.

(3) Divergence of heat transport by eddy motion

Fluid transport of sensible heat, particularly due to boundary-layer convection forms an important component of the heating function.

The energy balance method requires the use of climatological means and empirical expressions for sensible heat transport from the surface. Long wave radiation field divergence is calculated using standard radiation chart methods.

Clapp gives the mean *1000/500* mb heating rate averaged between *30°* and *60°*N as a function of longitude for the two methods and the following results were obtained from the Fourier analysis of these curves:

Heat balance method

Wave no.	Amplitude (heating rate)	Phase (longitude of maximum heating)
1	~0.5 °C/day	87°W
2		20°W
3		47°W

Thermodynamic equation method

Wave no.	Amplitude (heating rate)	Phase (longitude of maximum heating)
1	~0.5 °C/day	124°W
2	1.5 °C/day	33°W
3		44°E

Amplitudes of the higher wavenumber components of heating rapidly become smaller and we shall only be interested in the first three zonal wavenumbers. Consistency between the two methods is not particularly good with the calculated amplitudes of the wavenumber 2 heating rate differing by a factor of 3.

CHAPTER 2 PROPAGATION OF ENERGY IN STATIONARY ROSSBY WAVES AND 'REFLECTIVITY' OF THE STRATOSPHERE

In discussions of the dynamics of Rossby waves with vertical structure the standard quasi-geostrophic potential vorticity equation provides much information. Briefly, the quasi-geostrophic equations are derived as follows:

the vertical component of the vorticity equation is simplified to

$$\frac{D\zeta}{Dt_H} + \beta v = \frac{f_0}{\rho_0}\frac{\partial}{\partial z}(\rho_0 w) \qquad \left(\beta = \frac{df}{dy}\right)$$

neglecting vertical advection, twisting, non-linear stretching and baroclinic generation of vorticity.

The conservation of entropy is expressed as:

$$\frac{D\delta\phi}{Dt_H} + wB = 0 \qquad \phi = \log(\text{potential temperature})$$

where the vertical entropy gradient $\partial\phi/\partial z$ is replaced by ~~the fixed value B.~~ $B(z)$.

(N.B. all thermodynamic variables are of the form $Q = Q_0(z) + \delta Q(x,y,z,t)$.)

The horizontal wind is approximated by the non-divergent part of the real wind so that:

$$\underline{V}_H = \underline{k}\wedge\underline{\nabla}_H\psi \quad \text{and the thermal wind relation} \quad \frac{\partial \underline{V}_H}{\partial z} = \frac{g}{f_0}\,\underline{k}\wedge\underline{\nabla}\,\delta\phi$$

which gives a relation between the entropy perturbation and streamfunction,

$$\delta\phi = \frac{f_0}{g}\frac{\partial\psi}{\partial z} \qquad (\underline{k} \text{ is the vertical unit vector}).$$

Eliminating w from the vorticity equation and using the streamfunction expressions for relative vorticity ζ and entropy $\delta\phi$ yields the quasi-geostrophic potential vorticity equation

$$\frac{D}{Dt_H}\left\{\nabla_H^2\psi + \frac{f_0^2}{g}\frac{1}{\rho_0}\frac{\partial}{\partial z}\left(\frac{\rho_0}{B}\frac{\partial\psi}{\partial z}\right) + \beta y\right\} = 0 \qquad \text{——(2.1)}$$

In the literature, the derivation of the quasi-geostrophic potential vorticity theorem is confused and two distinct sets of approximations lead to identical theorems. White (1976) has clarified the situation by showing how the conventional Boussinesq approximation demands a rigorous application of the relations:

$$\delta\phi, \frac{\delta p}{p_0}, \frac{\delta\rho}{\rho} << 1$$

and $$BH_0 << 1 \qquad (H_0 \text{ is the density scale height})$$

yet this second condition may be omitted and the same equation derived from more complete continuity, hydrostatic and vorticity equations (see Appendix). Although a formally identical potential vorticity equation results, the improved set embodies elastic potential energy as well as gravitational potential energy. White shows that the only modification that arises in the use of the improved set occurs through the application of upper and lower boundary conditions (on vertical velocity) and then only for time-dependent problems.

For the stationary problems which we shall be dealing with the mathematical problems are identical, though the entropy perturbation is now given by:

$$\delta\phi = \frac{f_0}{g}\left(\frac{\partial}{\partial z} - B\right)\psi$$

Much of the rest of this chapter will be a re-examination of the work of Charney and Drazin (1961) with an emphasis on the change to spherical polar geometry.

Linearizing the equation (2.1) about a basic state of uniform zonal wind $\bar{U}$ (and static stability) in a β-plane, channel flow gives:

$$\left(\frac{\partial}{\partial t} + \bar{U}\frac{\partial}{\partial x}\right)\left\{\nabla^2\psi' + \frac{f_0}{gB\rho_0}\frac{\partial}{\partial z}\left(\rho_0\frac{\partial\psi'}{\partial z}\right)\right\} + \beta\frac{\partial\psi'}{\partial z} = 0$$

and $\psi = -\bar{U}y + \psi'(x,y,z)$.

Choosing stationary solutions of the form $\psi' = \underline{\text{Real}}\ F(z)e^{i\lambda x}\cos \mu y$ and re-arranging gives an equation for the complex height structure $F(z)$:

$$\frac{d^2F}{dz^2} - \frac{1}{H_0}\frac{dF}{dz} + \frac{gB}{f_0^2}\left(\frac{\beta}{\bar{U}} - (\lambda^2 + \mu^2)\right)F = 0$$

which admits a solution

$$F(z) = \left\{C_1\exp(i\nu z) + C_2\exp(-i\nu z)\right\}\exp\left(\frac{z}{2H_0}\right)$$

with $$\nu^2 + \frac{1}{4H_0^2} = \frac{gB}{f_0^2}\left(\frac{\beta}{\bar{U}} - (\lambda^2 + \mu^2)\right)$$

If parameters are chosen such that $\nu^2 < 0$ then

$$F(z) = \left\{C_1\exp(-|\nu|z) + C_2\exp(|\nu|z)\right\}\exp\left(\frac{z}{2H_0}\right)$$

and it would be natural to select the bounded mode only (put $C_2 = 0$) in an infinite atmosphere. When $\nu^2 > 0$ the choice of wave mode is less obvious with both waves having bounded specific kinetic energy at infinity.

Setting C_1 to zero gives an eastward tilting system of troughs and ridges and a westward tilting wave results from putting C_2 to zero. Analogous problems exist in electromagnetic field theory where the stationary solution to the field equations for a radiating antenna is sought. The choice rests ultimately on the direction of energy propagation and the amount of reflection. For instance, the component $C_1\exp\left(i(\lambda x + \nu z) + \frac{z}{2H_0}\right)$ corresponds to pure upward energy propagation and the other to pure downward propagation. That this is so may be shown by a consideration of the group velocity obtained from the time-dependent, linearized quasi-geostrophic equation (2.1).

The direction of energy flow may also be ascertained by calculating the horizontally averaged pressure-work term $\overline{\delta p w}^{x,y}$ since if this is positive, the atmosphere below a certain level is doing work on the atmosphere above. The observations of low wavenumber planetary waves

show strong westward tilt and upward energy propagation is implied.

Upward energy propagation in stationary wave systems can occur only when $\nu^2 > 0$ and Charney and Drazin show how this imposes a condition on the zonal wind speed $\bar{U}$ such that propagation is only possible if:

$$0 < \bar{U} < \frac{\beta}{\left\{(\lambda^2 + \mu^2) + \frac{f_0^2}{gB4H_0^2}\right\}} = \bar{U}_c \quad \text{(critical wind speed)} \qquad \text{——(2.2)}$$

Stationary Rossby waves propagate wave energy upwards only when the zonal mean winds are westerly and less than some upper bound. That this should be the case is borne out at least by the summer hemisphere easterlies of the stratosphere which are free from the large stationary wave distortions of the polar vortex observed in the westerlies of the winter hemisphere. Wave energy is unable to penetrate far into the easterlies and hence the amplitude dies away rapidly with height. Charney and Drazin concluded that for typical values of λ and μ, all waves would eventually be reflected by the strong polar night westerlies at some height by a local application of the criterion (2.2).

They infer from the theory that conditions would be right for a catastrophic upward flow of energy into the stratosphere near the equinoxes when the zonal winds are light and westerly though there is no evidence of such abnormal behaviour then. If anything, the greatest transmission of wave energy appears to prevail when the zonal winds are at their strongest, in the winter months.

Their analysis in β-plane geometry was extended to spherical polar geometry though they discount the importance of the modification on the grounds that the harmonic modes $P_n^m(\cos\theta)\exp im\phi$ for small n will be energetically unimportant for orographic forcing. (m is the zonal wavenumber, θ is co-latitude and ϕ is longitude.) The Q-G potential

vorticity equation with entropy source term is now given in spherical polar geometry and a separable solution for perturbations to an atmosphere of constant angular rotation is found.

The transformation from the rectangular cartesian set (x,y,z) to the curvilinear set (ϕ,θ,z) is made ~~where the approximation that the geometric height above the surface is much less than the earth's radius is neceessary~~. In contrast to the β-plane analysis the full variation of the coriolis parameter is permitted in the absolute vorticity, though again a mid-latitude value is assumed in association with the stretching term and geostrophic wind equation so that the streamfunction $\psi = \frac{\delta p}{f_0 \rho_0}$.

The potential vorticity equation is found to be: (including a source term)

$$\frac{D}{Dt_H}\left\{\zeta + 2\Omega\cos\theta + \frac{f_0}{\rho_0}\frac{\partial}{\partial z}\left(\frac{\rho_0}{B}\delta\phi\right)\right\} = \frac{f_0}{\rho_0}\frac{\partial}{\partial z}\left(\frac{\rho_0}{B}S\right)$$

when the thermodynamic equation is: $\frac{D\delta\phi}{Dt_H} + wB = S$

and the conservation of potential vorticity is recovered when the entropy source S is zero.

All symbols in the above equations have the same meaning as before and Ω is the angular rotation rate of the earth.

In terms of the rotational streamfunction the above equation becomes:

$$\frac{D}{Dt_H}\left\{\nabla_H^2\psi + 2\Omega\cos\theta + \frac{f_0^2}{g\rho_0}\frac{\partial}{\partial z}\left(\frac{\rho_0}{B}\frac{\partial\psi}{\partial z}\right)\right\} = \frac{f_0}{\rho_0}\frac{\partial}{\partial z}\left(\frac{\rho_0}{B}S\right) \qquad (2.3)$$

with $\frac{D}{Dt_H} = \frac{\partial}{\partial t} + \underline{V}_H\cdot\underline{\nabla}$

(for scalars)

The gradient operator in spherical curvilinear co-ordinates is:

$$\underline{\nabla} = \frac{\hat{\phi}}{R\sin\theta}\frac{\partial}{\partial\phi} + \frac{\hat{\theta}}{R}\frac{\partial}{\partial\theta} + \hat{k}\frac{\partial}{\partial z}$$

where the radial co-ordinate has been replaced by z under the assumption of its smallness compared to the earth's radius, and the unit vectors $\hat{\phi}$, $\hat{\theta}$ and $\hat{k}$ form an orthonormal triad pointing eastward, southward and upward respectively.

The horizontal velocity vector $\underline{V}_H$ is given by:

$$\underline{V}_H = \hat{k} \wedge \left(\frac{\hat{\theta}}{R} \frac{\partial \psi}{\partial \theta} + \frac{\hat{\phi}}{R \sin\theta} \frac{\partial \psi}{\partial \phi} \right)$$

and with the relations $\hat{k} \wedge \hat{\theta} = \hat{\phi}$ and $\hat{k} \wedge \hat{\phi} = -\hat{\theta}$, we define the curvilinear velocities in the eastward and northward sense (as of the cartesian horizontal wind) u and v respectively so that:

$$u\hat{\phi} - v\hat{\theta} = \frac{\hat{\phi}}{R} \frac{\partial \psi}{\partial \theta} - \frac{\hat{\theta}}{R \sin\theta} \frac{\partial \psi}{\partial \phi}$$

and $u = \frac{1}{R} \frac{\partial \psi}{\partial \theta}$, $v = \frac{1}{R \sin\theta} \frac{\partial \psi}{\partial \phi}$

It can be shown that the relative vorticity $\nabla_H^2 \psi$ is given by:

$$\nabla_H^2 \psi = \frac{1}{R^2 \sin\theta} \frac{\partial}{\partial \theta} \left(\sin\theta \frac{\partial \psi}{\partial \theta} \right) + \frac{1}{R^2 \sin^2\theta} \frac{\partial^2 \psi}{\partial \phi^2}$$

and the substantial derivative following the horizontal motion D/Dt_H becomes:

$$\frac{D}{Dt_H} = \frac{\partial}{\partial t} + \frac{1}{R^2 \sin\theta} \left(\frac{\partial \psi}{\partial \theta} \frac{\partial}{\partial \phi} - \frac{\partial \psi}{\partial \phi} \frac{\partial}{\partial \theta} \right)$$

Linearizing (2.3) about an atmosphere in differential solid rotation for small stationary perturbations so that:

$$\psi = -\bar{\psi}(z)\cos\theta + \psi'(\theta, \phi, z)$$

and

$$\bar{U}(\theta, z) = \frac{\sin\theta}{R} \bar{\psi}(z)$$

gives after algebraic manipulation

$$\frac{\bar{\psi}}{R^2} \frac{\partial}{\partial \phi} \left\{ \frac{1}{R^2 \sin\theta} \left[\frac{\partial}{\partial \theta} \left(\sin\theta \frac{\partial \psi'}{\partial \theta} \right) + \frac{1}{\sin\theta} \frac{\partial^2 \psi'}{\partial \phi^2} \right] + \frac{f_0^2}{g\rho_0} \frac{\partial}{\partial z} \left(\frac{\rho_0}{B} \frac{\partial \psi'}{\partial z} \right) \right\}$$

$$+ \frac{1}{R^2} \frac{\partial \psi'}{\partial \phi} \left\{ \frac{2\bar{\psi}}{R^2} + 2\Omega - \frac{f_0^2}{g\rho_0} \frac{d}{dz} \left(\frac{\rho_0}{B} \frac{d\bar{\psi}}{dz} \right) \right\} = \frac{f_0}{\rho_0} \frac{\partial}{\partial z} \left(\frac{\rho_0}{B} S \right)$$

A separation of variables is possible when ψ' and S are chosen so that:

$$\psi' = \underline{\text{Real}}\ F(z)\Theta(\theta)\exp im\phi$$

$$S = \underline{\text{Real}}\ -iS_0(z)\Theta(\theta)\exp im\phi$$

and substitution in the linearized potential vorticity equation leads to:

$$\left\{\frac{d}{d\theta}\left(\sin\theta\frac{d\Theta}{d\theta}\right) - \frac{m^2}{\sin\theta}\Theta\right\}\Big/ R^4\sin\theta.\Theta = -\frac{f_0^2}{gR^2\rho_0}\frac{d}{dz}\left(\frac{\rho_0}{B}\frac{dF}{dz}\right)\frac{1}{F(z)}$$

$$-\left\{2\left(\Omega+\frac{\bar{\psi}}{R^2}\right) - \frac{f_0^2}{g\rho_0}\frac{d}{dz}\left(\frac{\rho_0}{B}\frac{d\bar{\psi}}{dz}\right)\right\}\Big/\bar{\psi}(z) - \frac{f_0}{m\rho_0\bar{\psi}F(z)}\frac{d}{dz}\left(\frac{\rho_0}{B}S_0\right)$$

The left hand side of the equation is a function of θ alone and the right hand side of z alone, therefore:

$$\frac{1}{R^4}\left\{\frac{d}{d\theta}\left(\sin\theta\frac{d\Theta}{d\theta}\right) - \frac{m^2}{\sin\theta}\Theta\right\}\Big/\Theta\sin\theta = \alpha \quad \text{(a constant)}$$

Using the transformation $P = \cos\theta$ we obtain:

$$\frac{d}{dP}\left\{(1-P^2)\frac{d\Theta}{dP}\right\} + \left\{n(n+1) - \frac{m^2}{1-P^2}\right\}\Theta(P) = 0$$

$$\text{if}\quad \alpha R^4 = -n(n+1)$$

This equation has solutions $\Theta(\cos\theta) = P_n^m(\cos\theta)$ which are the associated Legendre polynomials and exist only for $n \geq m$, when Θ is non-singular at $P=\pm1$. (perturbations vanish at the poles).

The equation for the complex vertical structure $F(z)$ becomes:

$$\frac{d^2F}{dz^2} + \frac{B}{\rho_0}\frac{d}{dz}\left(\frac{\rho_0}{B}\right)\frac{dF}{dz} + \frac{gB}{f_0^2}\left\{\frac{2\Omega}{\bar{\psi}} - \frac{f_0^2}{\rho_0 g}\frac{1}{\bar{\psi}}\frac{d}{dz}\left(\frac{\rho_0}{B}\frac{d\bar{\psi}}{dz}\right) - \frac{(n-1)(n+2)}{R^2}\right\}F$$

$$= -\frac{gBR^2}{f_0 m\bar{\psi}}\frac{1}{\rho_0}\frac{d}{dz}\left(\frac{\rho_0}{B}S_0\right) \qquad \text{——(2.4)}$$

For adiabatic motion of an atmosphere in solid rotation which is uniformly stratified, (B = a constant): (2.4) reduces to:

$$\frac{d^2F}{dz^2} - \frac{1}{H_0}\frac{dF}{dz} + \frac{gB}{f_0^2}\left(\frac{2\Omega}{\bar{\psi}} - \frac{(n-1)(n+2)}{R^2}\right)F(z) = 0$$

Comparing this vertical structure equation with the corresponding one for constant zonal flow in cartesian geometry shows that the only change is the replacement of the total horizontal wavenumber squared $(\lambda^2 + \mu^2)$ by $\frac{(n-1)(n+2)}{R^2}$.

An algebraic point worth mentioning is that the Charney/Drazin derivation of this equation omits the term $\frac{2\bar{\psi}}{R^4}\frac{\partial \psi'}{\partial \phi}$ which represents the eddy poleward advection of the potential vorticity of the mean flow. Consequently, their interpretation of $(\lambda^2 + \mu^2)$ in the transformation to spherical geometry becomes $n(n+1)/R^2$ which is significantly larger only for very small n ($n = 1$, 2 and 3).

Although the horizontal structure is represented by Legendre functions of global extent, the arguments are strictly only valid for one hemisphere since one of the primary approximations of the quasi-geostrophic theory is the replacement of f in the stretching term and geostrophic wind relation by a constant middle-latitude value. The mid-latitude value $-f_0$ might be thought to apply to the southern hemisphere though this would imply pressure discontinuities etc at the equator and so only those wave modes that vanish at the equator are selected. It is found that all modes satisfying the condition $n - m$ = an odd integer vanish at the equator and it is these in which this study is concerned. Particularly, those wave modes with one middle latitude peak. (P_2^1, P_3^2 and P_4^3 ($\cos\theta$) for the first three zonal wavenumbers.)

Typical values used by Charney and Drazin for $(\lambda^2 + \mu^2)$ were 10^{-12} and 4×10^{-13} m^{-2} and these lead to critical zonal wind speeds $\bar{U}_c$ of 15 and 32 $m\,s^{-1}$. For spherical harmonic modes $n = 2$ and 3, the equivalent total square wavenumbers $\left((n-1)(n+2)/R^2\right)$ are 10^{-13} and 2.5×10^{-13} m^{-2}

which lead to average critical zonal wind speeds of *80* $m\,s^{-1}$ and *46* $m\,s^{-1}$, and hence the largest scale waves associated with $n = 2$ and *3* can propagate upwards in much stronger zonal westerlies than their analysis suggests. Referring to Fig.1.1 which shows the distribution of mean zonal wind in winter up to *100* km and assuming that a local application of the propagation criterion (2.2) is valid, it is clear that the $P_2^1(\cos\theta)$ mode should be able to penetrate the whole depth of the mesosphere in the wintertime circulation. Pure propagating modes (C_1 or C_2 equals zero in previous expression for the height structure) are such that the horizontally averaged specific kinetic energy is uniform with height and a $P_2^1(\cos\theta)$ wave mode associated with an eddy velocity of *1* $m\,s^{-1}$ at the surface would be of the order of *1000* $m\,s^{-1}$ at *96* km if unreflected. Clearly, the linearization would become invalid long before this amplitude was reached and even if it were permissible the smallness of the pressure perturbation compared to the basic state would be violated. Eddy velocities become comparable to the mean zonal wind speed at about *30* km and consequently one might expect the assumption of linearity to break down above this level. The theory of wave/mean flow interaction of Chapter 5 confirms this viewpoint.

Smagorinsky's quasi-geostrophic model of thermal forcing produced a strongly evanescent stratospheric wave through the choice of a narrow channel flow and fairly short zonal wavelength (he selected a horizontal wavenumber equivalent to a wavelength of *160*°longitude). The total square wavenumbers $(\lambda^2 + \mu^2)$ used in his analysis were 2.8×10^{-12} m^{-2} and 1.2×10^{-12} m^{-2} which are at least an order of magnitude larger than those for $n = 2$ and *3* of the spherical harmonic modes. The thermally forced planetary waves studied by Smagorinsky must be regarded as a description of high order $(n > 4)$ wave motion and this study will be concerned with low n modes.

Before going on to examine planetary scale forcing by orography

and differential heating and cooling for various vertical profiles of zonal wind and static stability it will be instructive to see to what extent a 'lid' approximation at the tropopause is justified as is the case for baroclinic instability problems. The two-layer model of the Charney/Drazin paper is re-analysed with the modification of the β-plane description, by the use of spherical polar geometry, accounted for.

The reflective properties of the interface between two unbounded regions of constant zonal wind and static stability, for various values in each case is determined.

A two-layer model

Suppose that the height of the interface is given by:

$$h(x,y,t) = \bar{h}(y) + h'(x,y,t)$$

then the unperturbed state will satisfy Margules relation for the slope of a frontal surface:

$$\frac{d\bar{h}}{dy} = -f_0[\bar{\rho}\,\bar{U}] \,/\, g[\bar{\rho}]$$

where [ ] indicates the difference across the interface

i.e. $$[a] = \lim_{\varepsilon \to 0}\left\{a(h+\varepsilon) - a(h-\varepsilon)\right\}$$

Solutions in the upper and lower layers must be connected at the interface in a way that satisfies certain kinematical and dynamical conditions. The interface must behave as a material surface so that:

$$\frac{D}{Dt}(z-h) = 0 \quad \text{at } z=h \qquad \text{(A)}$$

and also, the pressure must be continuous across the interface.

$$[p] = 0 \qquad \text{at } z=h \qquad \text{(B)}$$

Linearizing (A) about constant zonal wind $\bar{U}$ yields:

$$w' = \frac{\partial h'}{\partial t} + \bar{U}\frac{\partial h'}{\partial x} + v'\frac{\partial \bar{h}}{\partial y} \qquad \text{at } z = \bar{h}$$

where the expression is now applied at $z = \bar{h}$.

All aspects of the cartesian geometry analysis are retained except in the interpretation of $(\lambda^2 + \mu^2)$ so that:

$$\nu^2 + \frac{1}{4H_0^2} = \frac{gB}{f_0^2}\left(\frac{\beta}{\bar{U}} - \frac{(n-1)(n+2)}{R^2}\right)$$

The results will be equivalent to that of the complete spherical polar analysis since the only change that occurs is in the horizontal normal mode structure ($\cos \mu y \rightarrow P_n^m(\cos\theta)$) and this merely complicates the notation.

Choosing $h' = h_0 \exp i\lambda(x - ct)\cos \mu y$ then we may write (A) as:

$$w' = (\bar{U} - c)i\lambda h' + v'\frac{d\bar{h}}{dy} \qquad \text{at } z = \bar{h}$$

re-arrangement and application of [ ] leads to:

$$\left[\frac{w' - v'\frac{d\bar{h}}{dy}}{\bar{U} - c}\right] = [i\lambda h'] = 0 \qquad \text{at } z = \bar{h} \qquad \text{——(2.5)}$$

The continuity of pressure condition (B) is expanded as follows:

$$[p] = \left[\bar{p}(z) + \delta p(x,y,z,t)\right] = 0 \qquad \text{at } z = h$$

$$\simeq \left[\bar{p}(\bar{h}) + h'\frac{d\bar{p}}{dz} + \delta p\right] = 0 \qquad z = \bar{h}$$

and since the undisturbed pressure $\bar{p}$ is continuous across the interface we have:

$$\left[h'\frac{d\bar{p}}{dz} + \delta p\right] = 0 \qquad \text{at } z = \bar{h}.$$

Using the geostrophic and hydrostatic approximations:

$$\frac{d\bar{p}}{dz} = -\bar{\rho}g \qquad \text{and} \qquad v' = i\lambda\frac{\delta p}{\bar{\rho}f_0}$$

we have:

$$-gh'[\bar{\rho}] + \frac{f_0}{i\lambda}[\bar{\rho}v'] = 0 \qquad \text{at } z = \bar{h} \qquad \text{——(2.6)}$$

which reduces to the continuity of the perturbed pressure only when the mean state density is continuous (and hence the continuity of the zonal mean wind).

This condition can be simplified and h' eliminated using the linearized kinematical relation (A), so that after multiplication by $\bar{\rho}$ and application of [ ] we have:

$$\left[\bar{\rho}\omega\right] = \left[\bar{\rho}\,\bar{U}\right] i\lambda h' + \left[\rho v'\right]\frac{d\bar{h}}{dy}$$

(where the phase-speed c is set to zero since we are interested in stationary problems) and (2.6) can be reduced to:

$$\left[\bar{\rho}\omega\right] = 0 \qquad \text{——(2.7)}$$

with the use of the Margules formula.

Equations (2.5) and (2.7) are used to connect solutions at the interface of two layers with different static stabilities B and zonal wind $\bar{U}$.

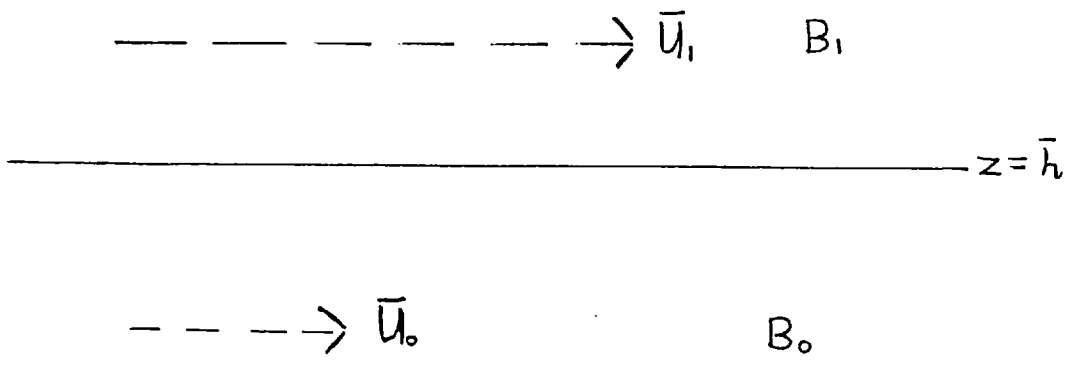

The transmissivity of stationary planetary Rossby waves to a two-layer atmosphere (as depicted in the above diagram) is determined for solutions to the linearized, stationary, Q-G potential vorticity equation:

$$\bar{U}\frac{\partial}{\partial x}\left\{\nabla_H^2\psi' + \frac{f_0^2}{gB}\left(\frac{\partial^2\psi'}{\partial z^2} - \frac{1}{H_0}\frac{\partial\psi'}{\partial z}\right)\right\} + \beta\frac{\partial\psi'}{\partial x} = 0$$

For a wave source located in the lower layer and an upper layer in which energy transmission is unimpeded and upward, solutions will be of the form:

$$\psi_0 = \underline{\text{Real}}\left\{C_1\exp(i\nu_0 z) + C_2\exp(-i\nu_0 z)\right\}\exp\left(i\lambda x + \frac{z}{2H_0}\right)\cos\mu y$$

and

$$\psi_1 = \underline{\text{Real}}\ C_3\exp\left\{i(\lambda x + \nu_1 z) + \frac{z}{2H_0}\right\}\cos\mu y$$

with the subscripts $_0$ and $_1$ referring to the lower and upper layers respectively.

The scale heights in each layer are necessarily different because continuity of undisturbed pressure $\bar{p}$ implies $[\bar{\rho}\,\bar{T}]$ and a discontinuous mean temperature $\bar{T}$, so that the scale height H_0 $\left(=\frac{R\bar{T}}{g}\right)$ is different in each layer. The difference is small however and forms an unimportant contribution to the reflectivity.

The interfacial conditions (2.5) and (2.7) relate the streamfunction in the upper and lower layers and a transmission and reflection coefficient can be defined. The upward energy flux given by the vertical pressure work term averaged zonally, $\overline{\delta p\omega}^x$, and is equal to $\frac{1}{2}\underline{\text{Real}}\,(\delta p'\omega'^*)$ where $\delta p'$ and ω' are the complex quantities and the asterisk denotes the complex conjugate. The vertical velocity ω is found in terms of ψ from the thermodynamic equation and is found to be

$$\omega' = -\frac{f_0}{gB}\bar{U}\frac{\partial}{\partial x}\left(\frac{\partial\psi}{\partial z}\right)$$

so that the upward energy flux is given by:

$$\overline{\delta p'\omega'}^x = -\frac{1}{2}\underline{\text{Imag.}}\,\frac{f_0}{gB}\rho_0\bar{U}\lambda\psi\left(\frac{\partial\psi}{\partial z}\right)^*$$

(Imag. denotes 'the imaginary part of').

For the pure propagating mode $\psi = \underline{\text{Real}}\ a\exp\left\{i(\lambda x + \nu z) + \frac{z}{2H_0}\right\}$ this simplifies to:

$$\overline{\delta p' w'} = \frac{1}{2}\frac{f_0^2}{gB}\rho_{0s}\bar{U}\lambda\nu|a|^2 \qquad \left(\text{with } \rho_0 = \rho_{0s}\exp\left(-\frac{z}{H_0}\right)\right)$$

An energy transmission coefficient T is defined as the ratio of the energy propagation in the upper layer to that of the upward propagating component in the lower layer so that:

$$T = \frac{\frac{\bar{U}_1}{B_1}|C_3|^2\nu_1}{\frac{\bar{U}_0}{B_0}|C_1|^2\nu_0}$$

and a reflection coefficient R is similarly defined as:

$$R = \frac{|C_2|^2}{|C_1|^2}$$

Using (2.5), (2.7) and the expressions for ψ_0 and ψ_1 to eliminate C_1, C_2 and C_3 in the transmission and reflection coefficients gives:

$$T = \frac{\bar{U}_0}{\bar{U}_1}\frac{B_1}{B_0}\frac{\nu_1}{\nu_0}\frac{\left(\nu_0^2 + \frac{1}{4H_0^2}\right)}{\left(\nu_0^2 + \frac{1}{4H_0^2}\right)}\left(A^2 - 2A\cos\chi + 1\right)$$

and $R = A^2$

with $A\exp i\chi = U + iV$

where
$$U = \left\{\left(P - \frac{1}{2H_0}(Q-R)\right)^2 - \left(\nu_0^2R^2 - \nu_1^2Q^2\right)\right\}\Big/W$$

$$V = 2\nu_0 R\left(P - \frac{1}{2H_0}(Q-R)\right)\Big/W$$

$$W = \left\{P + \frac{1}{2H_0}(Q-R)\right\}^2 - \left(\nu_1 Q + \nu_0 R\right)^2$$

and
$$P = \frac{\Delta\bar{\rho}}{\bar{\rho}B_1} \qquad Q = \frac{\bar{U}_0/\bar{U}_1}{\nu_1^2 + \frac{1}{4H_0^2}} \qquad R = \frac{\frac{\bar{U}_1}{\bar{U}_0}\frac{B_0}{B}}{\nu_0^2 + \frac{1}{4H_0^2}}$$

A graph of T and R for wave modes $n = 2$ to 5 is plotted in Fig.2.1 showing their dependence on the mean zonal wind of the upper layer (stratosphere). The zonal wind speed of the lower layer is fixed at 10 m s^{-1} and the static stability of the two layers is chosen to be representative of

troposphere and stratosphere. For $\bar{U}_1 = 10$ m s^{-1} the zonal wind speeds of each layer are identical and it can be seen that the fraction of energy reflected by the discontinuity in stratification at the tropopause is about 20 %. Reflection is large only when the waves are close to evanescence. Green, in an unpublished calculation, shows the parameter $2H_0\nu$ to be important in determining the transmissive properties of a model tropopause and reflection is large when $2H_0\nu < 1$.

Reflection of wave energy is much more sensitive to the value of the mean zonal wind speed than static stability as can be seen from Fig.2.1 with total reflection occurring when the critical wind speed $\bar{U}_c$ is exceeded or if $\bar{U}_1 \leq 0$.

The cut-off in the transmission curves is very sharp particularly for higher n values.

An interesting point that is brought out in the calculation of the transmissivity is that the wave extracts energy from the mean flow as it passes across the interface to stronger zonal winds and loses energy to the flow in passing to lighter zonal winds. In these cases the sum of the transmission and reflection coefficients is not unity and T may be greater than one. An atmosphere of two layers rotating at different speeds requires a density difference between them and a sloping interface to maintain geostrophic equilibrium. The availability of gravitational potential energy due to the sloping of the density surfaces enables a propagating mode to exchange energy with the flow. This is consistent with the more general ideas on wave-mean flow interaction given in Chapter 5.

The rate of propagation of wave energy in each layer is given by the vertical component of group velocity and the reflectivity is strongly connected with the difference of group velocity between each layer.

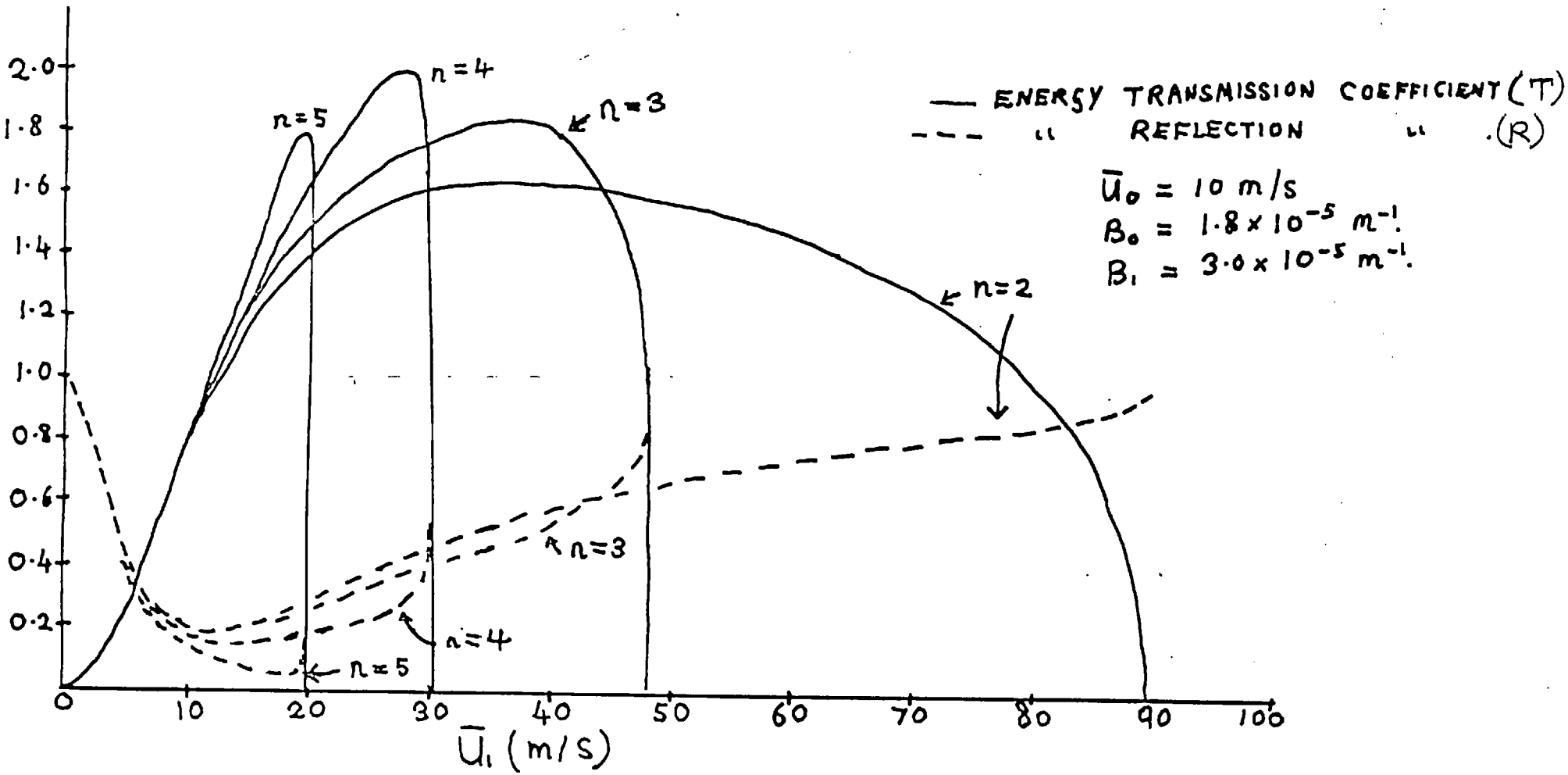

FIG. 2.1 REFLECTIVITY (R) AND TRANSMISSIVITY (T) OF A TWO-LAYER ATMOSPHERE FOR DIFFERENT N MODES. THEIR VARIATION IS PLOTTED AGAINST THE ZONAL WIND SPEED OF THE UPPER LAYER, $\bar{U}_1$ FOR FIXED VALUES OF $\bar{U}_0$ ($= 10 ms^{-1}$), B_0 ($= 1.8 \times 10^{-5} m^{-1}$) AND B_1 ($= 3.0 \times 10^{-5} m^{-1}$).

The dispersion relation for quasi-geostrophic planetary waves is:

$$\sigma = \bar{U}\lambda - \frac{\beta\lambda}{\lambda^2 + \mu^2 + \frac{f_0^2}{gB}\left(\nu^2 + \frac{1}{4H_0^2}\right)}$$

where σ is the frequency and the vertical component of group velocity is obtained by differentiating with respect to ν giving:

$$C_{gz} = \frac{\partial\sigma}{\partial\nu} = \frac{2\beta\lambda\frac{f_0^2}{gB}\nu}{\left\{\lambda^2 + \mu^2 + \frac{f_0^2}{gB}\left(\nu^2 + \frac{1}{4H_0^2}\right)\right\}^2}$$

For stationary waves ($\sigma = 0$) this simplifies to:

$$C_{gz} = \frac{2\bar{U}^2\frac{f_0^2}{gB}\lambda\nu}{\beta}$$

and for the largest wave scales (with n small) such that $\frac{\beta}{\bar{U}} >> \frac{(n-1)(n+2)}{R^2}$

we find $$C_{gz} \propto \frac{\bar{U}^{3/2}}{\sqrt{B}}$$

showing the stronger dependence of group velocity on zonal wind.

It may be concluded from the reflectivity graphs that the $n = 2$ and 3 are very effectively transmitted into the stratosphere and a rigid boundary approximation would be quite inappropriate in modelling these waves in stationary forcing problems. Existing theories of large-scale forcing appear to be unrealistic in their artificial restriction of the horizontal scale through the choice of a narrow, β-plane channel flow which causes the wave motion to be trapped (Smagorinsky, 1953 and Charney/Eliassen, 1949).

Studies which do not have this restriction such as that of Sankar-Rao (1965) apparently fail through the imposition of an energy-reflecting upper boundary condition. We now proceed to set up models of orographic and thermal forcing without this restriction by imposing an energy-transmitting boundary condition in the upper stratosphere.

CHAPTER 3 SIMPLE QUASI-GEOSTROPHIC MODELS OF OROGRAPHIC AND THERMAL FORCING

(i) Constant zonal wind solutions

(a) Orographic forcing

On the scale in which we are interested, the orography represents the departure of the earth's surface from its basic oblate spheriodal shape rather than mountain ranges such as the Himalayas. Sankar-Rao (1965) has calculated the spherical harmonic coefficients of the elevation of the land surface above sea-level up to *15*th degree and these values give some idea of the amplitude of orographic forcing for the first three wavenumbers. Typically amplitudes are of the order of *100-200* gpm for $m < 4$, $n < 6$. A substantial proportion of the orographic 'forcing function' will be by-passed in this work because only the low n spherical harmonic modes are to be considered and, for instance, features such as the Himalayas make strong contributions to wavenumber *1* in the orography through the high n modes reflecting the short meridional scale. Such isolated orographic features land themselves more readily to treatment by Fourier transform techniques on a β-plane and an unpublished calculation by Green shows that pressure perturbations near the surface of as much as *10* mb are to be expected just upstream of the Rockies in the presence of a uniform westerly flow of *10* $m\,s^{-1}$. Similarly, flow around 'tall' orographic objects such as the Himalayas can be shown to generate large amplitude laterally propagating Rossby waves.

It is instructive to examine the solution corresponding to orographic forcing of a 'solid-rotation' atmosphere of uniform static stability since this carries most of the physical information relevant to this type of problem.

The differential equation for the height structure has already been derived in Chapter 2 and upward energy propagating solutions are

of the form

$$\psi' = \underline{\text{Real}}\ A \exp\left\{i(m\phi + \nu z) + \frac{z}{2H_0}\right\} P_n^m(\cos\theta)$$

where A is a constant to be determined from the lower boundary condition on vertical velocity.

Air flowing over the lower surface will remain at the surface during the motion and this is expressed by the equation:

$$\frac{D}{Dt}(z - z_0) = 0 \qquad \text{at } z = z_0 \qquad \text{——(3.1)}$$

where $z_0 = z_0(\phi,\theta)$ is the surface elevation function. Linearizing (3.1) and evaluation at $z = 0$ gives the condition

$$w = \frac{\bar{\psi}}{R^2} \frac{\partial z_0}{\partial \phi} \qquad \text{at } z = 0$$

where $\bar{\psi}/R$ = a constant and represents the zonal wind speed at the equator, and vertical velocity is related to the streamfunction through the thermodynamic equation by:

$$\frac{\bar{\psi}}{R^2} \frac{f_0}{g} \frac{\partial}{\partial \phi}\left(\frac{\partial \psi'}{\partial z}\right) + wB = 0 \ .$$

Combination of these two equations gives the relation:

$$\frac{f_0}{gB} \frac{\partial \psi'}{\partial z} + z_0 = 0 \quad \text{at } z = 0. \qquad \text{——(3.2)}$$

Considering one spherical harmonic component of the expansion of the surface elevation so that:

$$z_0 = a\, P_n^m(\cos\theta) \exp im\phi$$

then (3.2) can be used to evaluate A and gives the solution:

$$\psi' = -\underline{\text{Real}}\ \frac{agB}{f_0\left\{\nu^2 + \frac{1}{4H_0^2}\right\}^{1/2}} \exp\left\{i(m\phi + \nu z - \varepsilon) + \frac{z}{2H_0}\right\} P_n^m(\cos\theta)$$

——(3.3)

where $\varepsilon = \tan^{-1}(2H_0\nu)$ and $\nu^2 + \frac{1}{4H_0^2} = \frac{gB}{f_0^2}\left(\frac{2\Omega}{\bar{\psi}} - \frac{(n-1)(n+2)}{R^2}\right)$. We take values for the relevant parameters which represent averages for the troposphere and stratosphere; with $a = 200$ m, $n = 3$, $B = 3.0 \times 10^{-5}$ m^{-1} and $\bar{\psi} = 12.8 \times 10^7$ m^2 s^{-1} (equivalent to a zonal wind speed of 10 m s^{-1} at 30°N) the surface amplitude can be shown to be of the order of 5 mb and the westward phase tilt is $\sim 9°$/km. At 30 km the contour height perturbation is ~ 270 m. All the general aspects of the structure of the untrapped low-wavenumber disturbances observed are contained in this elementary solution and the selection of the upward propagating mode alone is justified.

It is evident from the surface phase shift ε ($\sim 66°$) that the flow exerts an eastward drag on the orography since the higher pressure occurs on the upwind slopes and low pressure on the eastern slopes.

By correlating first order perturbation quantities, several important second-order flux terms can be calculated. For instance, the latitude-average of the pressure-work term $\overline{\delta p'w'}$, which determines the rate of upward transmission of wave energy, can be evaluated from:

$$\overline{\delta p'w'} = -\rho_0 \frac{f_0^2}{gB}\frac{\bar{\psi}}{R^2}\overline{\psi' \frac{\partial}{\partial\phi}\left(\frac{\partial\psi'}{\partial z}\right)} \qquad \text{——(3.4)}$$

$$= -\rho_0 \frac{\bar{\psi}}{R^2} m \frac{f_0^2}{gB}\frac{1}{2}\,\underline{\text{Imag.}}\left\{\psi'\left(\frac{\partial\psi'}{\partial z}\right)^*\right\}$$

$$\overline{\delta p'w'} = \frac{1}{2}\frac{\bar{\psi}}{R^2} m\nu\rho_0 \frac{f_0^2}{gB}|\psi'|^2 = \frac{1}{2}\rho_{0s}\frac{ma^2 gB\nu}{\left(\nu^2 + \frac{1}{4H_0^2}\right)}\left(\frac{\bar{\psi}}{R^2}\right)|P_n^m|^2$$

Substituting typical values into the above gives upward energy fluxes of ~ 0.3 W m^{-2}. It can be seen immediately that had the eastward tilting wave been selected, then ν would be replaced by $-\nu$ and energy propagation would be downwards.

Westward tilting waves in geostrophic and hydrostatic balance transport entropy polewards as can be inferred from a re-arrangement of (3.4):

$$\overline{\delta p'w'} = \frac{\bar{\psi}}{R}\frac{\rho_0 f_0}{B}\overline{\delta\phi'\frac{1}{R}\frac{\partial\psi'}{\partial\phi}} = \frac{f_0\bar{U}(\theta)}{B}\rho_0\overline{\delta\phi'v'}$$

For a zonal wind speed of 10 m s^{-1} at 30°N this implies an entropy flux of ~ 0.1 m s^{-1} and in an atmosphere of mean temperature ~ 250°K implies a poleward heat flux $\rho_0 C_p\overline{v'\delta T'}$ of $\sim 2.5\times 10^3$ W m^2 which is equivalent to about 1.7 solar constants. Since the total poleward heat flux required to offset the radiational imbalance of heating is ~ 6 solar constants there is good reason to believe that untrapped stationary wave heat transport is an important component of the total poleward fluid transport of heat.

Lastly, the drag exerted by the wave on the lower surface can be evaluated by correlating the pressure perturbation with the slope of the surface so that the eastward drag is given by $\overline{\delta p'\frac{1}{R\sin\theta}\frac{\partial z_0}{\partial\phi}}$ at $z=0$ which is identical to $\frac{\overline{\delta p'w'}}{\bar{U}(\theta)}$ at $z=0$. Surface stress is calculated to be ~ 0.03 N m^{-2} at 30 °N which is about an order of magnitude smaller than typical boundary layer turbulent stress, though the comparison of the hemispheric averages of surface drag might be similar in size (since the subtropical westward torque due to the easterlies tends to balance the middle and high latitude westerly drag).

The ability of planetary wave motion to exert drag on the orography is intimately related to the upward propagation of energy and poleward transport of entropy and therefore to the zonal wind speed. Wave drag occurs only for a limited range of zonal wind speeds corresponding to the criterion for propagation and implies a drag law quite unlike that for the diffusive transfer of momentum. Indeed the linearized analysis demands that momentum transfer between atmosphere and earth due to stationary Rossby waves should occur only for westerly zonal winds.

Specific kinetic energy of the wave motion is constant with height (characteristic of pure energy transmission) and this is consistent with observed wavenumber 1 and 2 motion (Fig.1.2). In fact, wave energy tends

to increase with height which is explained later as a wave/mean flow interaction resulting from the increase of zonal wind with height.

It is remarkable how successful this simple solution is in representing the general features of planetary wave motion observed up to *30* km when sophisticated models such as that of Sankar-Rao fail. The selection of the upward, radiating solution seems to be crucial in this respect. Upper boundary conditions commonly used in general circulation models, such as $\omega\left(\frac{Dp}{Dt}\right) = 0$ at $p = p_0$ and $\frac{D\sigma}{Dt} = 0$ at $\sigma = \sigma_0$ reflect energy and their application below *40* km might be expected to lead to a distortion of planetary wave structure in view of the observed transmission of energy above these heights.

Examination of the solid-rotation atmosphere solution to the problem of orographic forcing with an upper rigid lid provides useful information relevant to this effect and the streamfunction is found to be:

$$\psi' = \underline{\text{Real}} \frac{gBa}{f_0\left(\nu^2 + \frac{1}{4H_0}\right)^{1/2}} \frac{\sin\{\nu(z-H) - \delta\}}{\sin \nu H} \exp\left(im\phi + \frac{z}{2H_0}\right) P_n^m(\cos\theta) \qquad (3.5)$$

A stationary standing wave results from the reflection of wave energy at $z = H$ so that there is no net upward propagation of energy and the phase lines are vertical. The associated absence of surface wave drag and poleward transport of entropy are important deficiencies and the presence of resonant peaks when $\nu H = n\pi$ would result in unrealistic modelling by general circulation experiments.

Evidence of this type of modelling deficiency can be inferred from the results of numerical simulations of the stratosphere. The *11*-level model of the circulation of the stratosphere used by Mahlman and Manabe (1972) was unsuccessful in the description of the mean zonal wind and temperature structure, with winds too strong by a factor of two and

polar night temperatures colder than observed by 25-30°K. Planetary wave transfer of heat is the dominant mechanism offsetting the polar cooling of the stratosphere in winter (Green 1972) and the absence of this transport process (through the forced reflection of energy at the upper boundary at 10 mb) could account for the coldness there. Thermal wind balance demands that the shear should be greater there and hence excessive zonal wind speeds result. The effect of spurious energy reflection could also seriously upset the tropospheric circulation through the reduced stationary wave transport of heat and build up of wave energy. Numerical modellers frequently complain of 'excessive blocking' in weather prediction schemes and it is quite possible for this to be a manifestation of the forced trapping of waves and their resonant behaviour. The treatment of large-scale forced waves in climate models presents a formidable problem to the modeller with the tropospheric wave motion suffering considerable distortion in the absence of a realistic stratosphere.

(b) Thermal forcing

As explained earlier, planetary Rossby waves can be generated by the extension or contraction of vortex tubes associated with the vertical motion induced by a field of heating and cooling. Two 'thermal effects' that generate quasi-geostrophic waves can be distinguished, and they are:

(1) Heating near a rigid boundary.

(2) Differential heating in the vertical.

In an atmosphere of uniform static stability, if the energy heating function $\rho_0 S$ is independent of height then the inhomogeneous term in equation (2.3) associated with the forcing vanishes and the equation is identical to that for adiabatic flow. Wave forcing enters through the boundary condition on vertical velocity w which is obtained from the thermodynamic equation. Vorticity is generated by the forced compression of vortex tubes against a rigid boundary and this will be shown to be

the dominating mechanism in the formation of the Siberian anticyclone. Differential cooling in the vertical tends to cause subsidence at differing rates which also leads to vortex compression and wave motion.

The *Q-G* potential vorticity equation can again be used to write down a simple solution representing the thermal forcing of an atmosphere in solid rotation ($\bar{\psi}/R$ = a constant, which represents the equatorial zonal wind speed for the solid rotation atmosphere). Low-level heating is conveniently represented by a source function $S' = a \sin m\phi \, P_n^m(\cos\theta)\exp(-bz)$ so that equation (2.4), for the vertical structure of the wave, becomes:

$$\frac{d^2F}{dz^2} - \frac{1}{H_0}\frac{dF}{dz} + \frac{gB}{f_0^2}\left\{\frac{2\Omega}{\bar{\psi}} - \frac{(n-1)(n+2)}{R^2}\right\}F(z) = \frac{ga(b + 1/H_0)}{f_0 m(\bar{\psi}/R^2)}\exp(-bz)$$

Selecting the pure upward energy radiating component of the solution to the homogeneous equation and imposing a lower boundary condition that vertical velocity vanishes at $z = 0$ (through the thermodynamic equation) leads to the perturbation streamfunction solution:

$$\psi' = \frac{\left(\frac{gaR^2}{f_0 m\bar{\psi}}\right)P_n^m(\cos\theta)}{b^2 + \frac{b}{H_0} + \nu^2 + \frac{1}{4H_0^2}} \underline{\text{Real}}\left\{\left(b + \frac{1}{H_0}\right)e^{-bz} + \left(i\nu - \frac{1}{2H_0}\right)e^{i(\nu + 1/2H_0)z}\right\}\exp im\phi$$

Figs. 3.1 and 3.2 show the amplitude and phase of contour height and temperature fields for the P_{m+1}^m modes with $m = 1$, 2 and 3. Contour height perturbations are largest for wavenumber 1 and a heating function equivalent to 3°C/day at the surface produces a pressure perturbation of 15 mb at the ground. An amplitude minimum in contour height occurs near 4 km for all three waves, above which the disturbance increases steadily to give a 600 gpm disturbance amplitude at 30 km for wavenumber one. Phase tilt in all three waves is very similar with the strongest tilt below 4 km.

A strong surface temperature perturbation is indicated, again being largest for the lowest zonal wavenumber, with amplitude of 12°C for

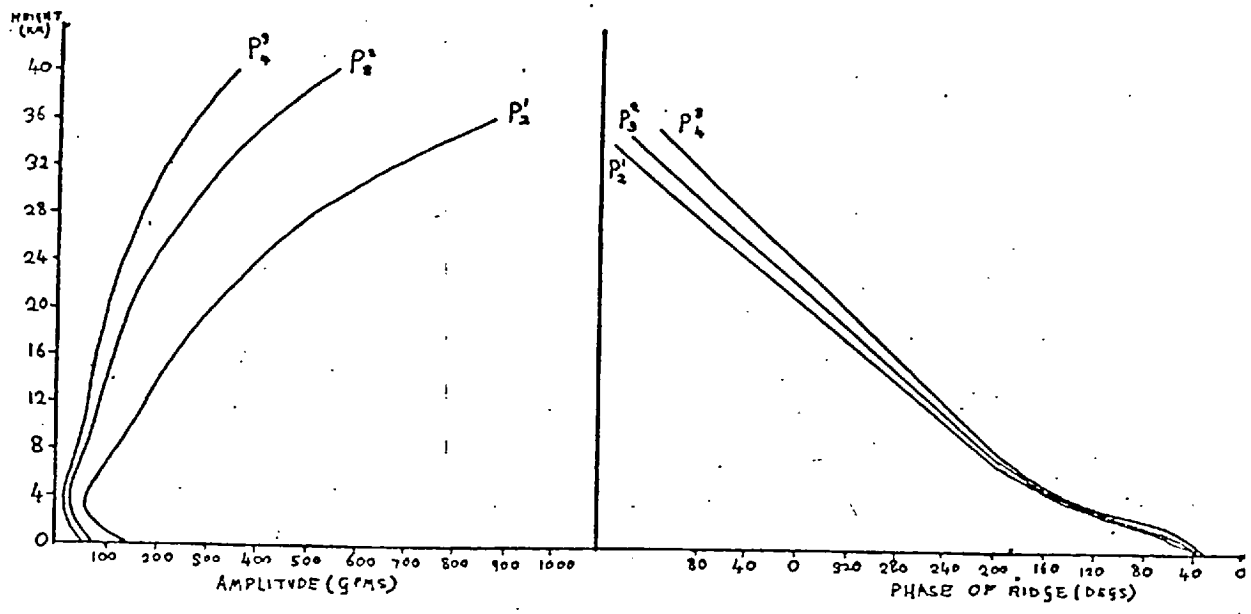

FIG. 3.1 AMPLITUDE AND PHASE OF THE CONTOUR HEIGHT FIELD RESULTING FROM THE FORCING OF THE P^m_{m+1} MODES ($m = 1, 2$ AND 3) IN A 'SOLID-ROTATING' ATMOSPHERE.

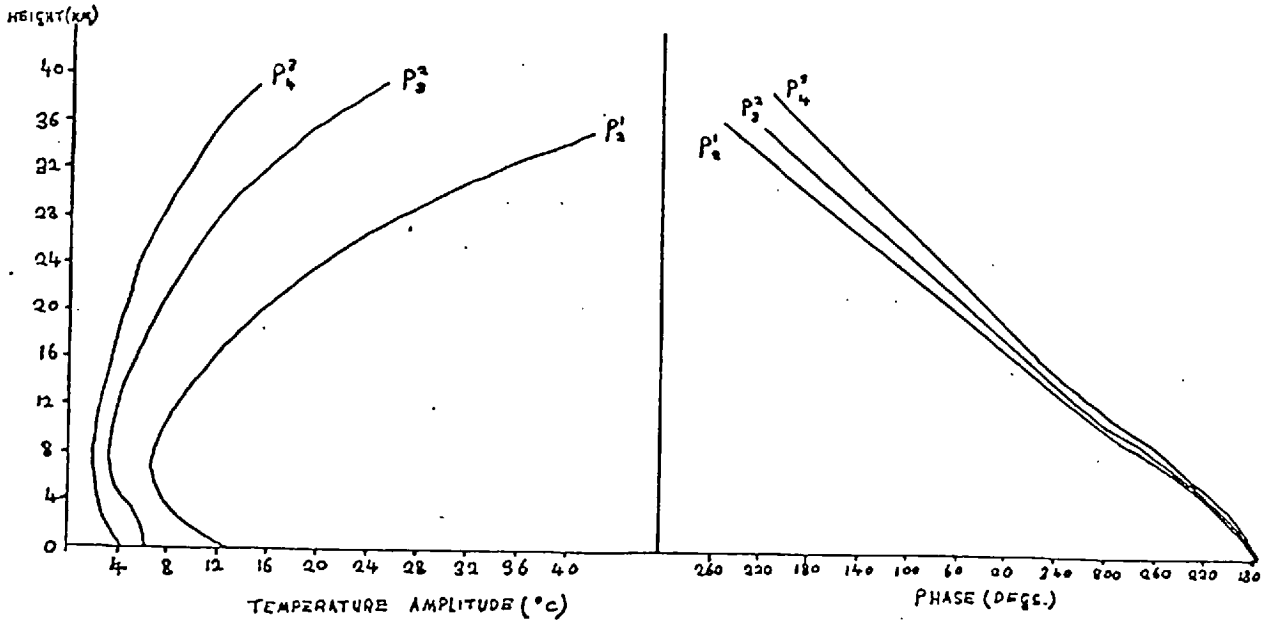

FIG 3.2 TEMPERATURE FIELD CORROSPONDING TO 3.1.

$B = 3.0 \times 10^{-5}\ m^{-1}$, $S_0(z) = \left(\frac{3.0°c/DAY}{260°K}\right) \exp\left(-\frac{z}{4\,KM.}\right)$

AND $\bar{u} = 10\ ms^{-1}$ AT 45°N.

wavenumber one. All perturbation quantities increase rapidly in amplitude with height in the stratosphere which is associated with the inertial effect of density. Predicted temperature amplitudes over *20* km are too large even though the contour height disturbance amplitudes are reasonable. Some interesting points regarding the surface phase relationships of pressure and temperature to the source function are brought out by Figs. 3.1 and 3.2. The 'model equivalent' of the Siberian anticyclone appears about *60°* downstream of the region of maximum cooling whereas the coldest spot is *90°* downstream. This is, at first glance, consistent with synoptic experience with the lowest Siberian temperatures being recorded to the east of the region of intense high pressure. From this it is worth remarking that the coldest air will be associated with northerly winds and the warmest with southerlies from which the poleward transport of heat can be inferred. The general qualitative agreement with observation suggests that the model assumptions are correct.

For a given magnitude of heating function, the amplitude of the resulting wave depends inversely on the zonal wavenumber m and the angular velocity of solid rotation of the atmosphere. Parcels of air travelling through the heating regions will remain there for a time inversely proportional to the zonal wind speed and hence will suffer the greatest effect of the cooling for the slowest zonal wind speed. The angular extent of the zone of heating or cooling is inversely dependent on the zonal wavenumber and the larger this region the longer the time a parcel spends in each heating phase and hence the larger the amplitude of the temperature perturbation.

We might deduce from these simple arguments that thermally forced motion in the atmosphere is most likely to be observed in the lowest wavenumbers (given that the spectral distribution of forcing $S_0(m)$ is uniform).

Spherical harmonic modes of high n are evanescent and their amplitude changes sign near the top of the heating layer. For these modes (3.6) may be approximated to:

$$\psi' \simeq \frac{gaR^2}{f_0 m\bar{\psi}} \frac{(be^{-bz} - \nu e^{-\nu z})}{b^2 - \nu^2} \cos m\phi \, P_n^m(\cos\theta)$$

(when $\frac{2\Omega R^2}{\bar{\psi}} + 2 \ll n(n+1)$) and it is clear that the wave is relatively large at the ground and decreases to change sign at a particular height, thereafter tending back to zero at infinity. This type of wave structure conforms with the classical picture of a cold anticyclone changing to a cold low aloft. This is applicable only for disturbances of short horizontal scale for which the dispersive properties of the fluid are unimportant and for continental scale anticyclones the notion is quite misleading. The temperature perturbations of such disturbances are $90°$ out of phase with the heating field from which can be inferred that there is no generation of available potential energy since the zonal average of $S'\delta\phi$ is zero. Parcels assume their lowest temperatures after traversing the whole of the cooling region, unlike the propagating modes in general (see Figs. 3.1 and 3.2).

A realistic model of thermally-forced motion, that is self-consistent with regard to the wave-structure in the troposphere and stratosphere must include the basic increase of zonal wind with height. The magnitude of tropospheric forcing is critically dependent on the zonal wind speed in the vicinity of the heating function whereas the ability to propagate energy and the vertical structure depend essentially on some average zonal wind characteristic of the stratosphere.

It is desirable, therefore, to consider the analytic problem of forcing in uniform shear flow which is the next simplest case.

(ii) Constant angular shear solutions

Having examined the simple analytic solutions to the potential vorticity equation for stationary forcing of an atmosphere in solid rotation and identified the important physical processes, we shall now deal with constant angular shear models that are sufficiently realistic to allow comparison with the real atmosphere with more confidence. Although analytic solutions are obtainable, their evaluation is considerably more difficult.

(a) Orographic forcing

Analytic solution to (2.4) is possible when the angular rotation of the atmosphere is a linear function of height and the static stability is uniform, so that letting:

$$\bar{\psi} = \bar{\psi}_0 + \Lambda z, \qquad \rho_0 = \rho_{0s} \exp\left(-\frac{z}{H_0}\right)$$

and $S_0 = 0$ in (2.4) gives:

$$\frac{d^2F}{dz^2} - \frac{1}{H_0}\frac{dF}{dz} + \frac{gB}{f_0^2}\left\{\frac{2\Omega}{\bar{\psi}_0 + \Lambda z} + \frac{f_0^2}{gB}\frac{\Lambda}{H_0(\bar{\psi}_0 + \Lambda z)} - \frac{(n-1)(n+2)}{R^2}\right\}F = 0$$

Transforming the dependent and independent variables by the relations:

$$\left.\begin{aligned} F(z) &= Z(z)\exp\left(\frac{z}{2H_0}\right) \\ \text{and} \quad h &= \left(\frac{\bar{\psi}_0}{\Lambda} + z\right)\delta_* \\ \text{with} \quad \delta_* &= 2\left\{\frac{gB}{f_0^2}\frac{(n-1)(n+2)}{R^2} + \frac{1}{4H_0^2}\right\}^{1/2} \end{aligned}\right\} \qquad \text{——(3.7)}$$

then we have:

$$\frac{d^2Z}{dh^2} + \left\{-\frac{1}{4} + \frac{k}{h}\right\}Z(h) = 0 \qquad \text{with} \quad k = \left(\frac{gB}{f_0^2}\frac{\beta}{\Lambda} + \frac{1}{H_0}\right)\Big/\delta_*$$

This is a special case of Whittaker's Equation:

$$\frac{d^2w}{dz^2} + \left[-\frac{1}{4} + \frac{k}{z} + \frac{(\frac{1}{4} - \mu^2)}{z^2}\right]w = 0$$

which has two independent solutions $M_{k,\mu}(z)$ and $W_{k,\mu}(z)$ such that:

$$M_{k,\mu}(z) = \exp\left(-\frac{z}{2}\right) z^{\frac{1}{2}+\mu}\, M(\tfrac{1}{2}+\mu-k,\ 1+2\mu,\ z)$$

and

$$W_{k,\mu}(z) = \exp\left(-\frac{z}{2}\right) z^{\frac{1}{2}+\mu}\, U(\tfrac{1}{2}+\mu-k,\ 1+2\mu,\ z)$$

as given by Abramowitz and Stegun (1964).

$M(a,b,c)$ and $U(a,b,c)$ are confluent hypergeometric functions and their series expansions are given in most text books of special functions. The functions $M_{k,\frac{1}{2}}(z)$ and $W_{k,\frac{1}{2}}(z)$, in which we are interested, are not generally tabulated and in practice the latter is quite difficult to evaluate. By a combination of asymptotic expansions and limiting cases it is possible to evaluate the functions on a computer to a high degree of accuracy in regions where the series summation is difficult, and also get some insight into the behaviour of the solutions.

For instance, at large positive z:

$$M_{k,\frac{1}{2}}(z) \underset{z\to\infty}{\longrightarrow} \frac{z^{-k}}{(-k)!} \exp\left(\frac{z}{2}\right)\left[1+O(z^{-1})\right]$$

and

$$W_{k,\frac{1}{2}}(z) \underset{z\to\infty}{\longrightarrow} z^{-k} \exp\left(-\frac{z}{2}\right)\left[1+O(z^{-1})\right]$$

and they both represent trapped waves with $M_{k,\frac{1}{2}}(z)$ becoming unbounded at infinity and $W_{k,\frac{1}{2}}(z)$ tending to zero.

Rejecting the $M_{k,\frac{1}{2}}(z)$ solution on the grounds of physical inadmissibility for an unbounded atmosphere gives the height structure $F(z) = W_{k,\frac{1}{2}}(h)\exp(z/2H_0)$ and it can be seen that the specific kinetic energy density (which is proportional to $\rho_0|F|^2$) also tends to zero at infinity.

The expression for the streamfunction ψ becomes:

$$\psi = \underline{\text{Real}}\ A\ W_{k,\frac{1}{2}}(h)\exp\left(im\phi + \frac{z}{2H_0}\right) P_n^m(\cos\theta) \qquad \text{——(3.8)}$$

where A must be determined from the lower boundary condition on w.

Again, the forced vertical velocity at the surface is determined by the surface zonal wind speed and the slope of the orography, and is related to the streamfunction through the thermodynamic equation. The uniform westerly shear will be balanced by an equatorward gradient of entropy (thermal-wind equation) and this introduces an extra term into the thermodynamic equation.

The stationary, linearized thermodynamic equation becomes:

$$\frac{f_0}{gR^2}\left\{\bar{\psi}(z)\frac{\partial^2\psi'}{\partial\phi\partial z} - \frac{\partial\psi'}{\partial\phi}\frac{\partial\bar{\psi}}{\partial z}\right\} + w'B = 0$$

and together with the kinematic relation for the surface vertical velocity $w = \frac{\bar{\psi}_0}{R^2}\frac{\partial z_0}{\partial\phi}$ gives:

$$\frac{f_0}{gB}\left\{\frac{\partial\psi'}{\partial z} - \frac{1}{\bar{\psi}_0}\frac{d\bar{\psi}}{dz}\psi'\right\} + z_0 = 0 \qquad \text{at } z = 0$$

Consider one spectral component of the expansion of the surface elevation in spherical harmonics and the corresponding component of the streamfunction so that:

$$z_0(\theta,\phi) = a P_n^m(\cos\theta)\cos m\phi$$

and $$\psi' = \underline{\text{Real}}\ F(z)\, P_n^m(\cos\theta)\exp im\phi$$

then substitution into the boundary condition expression above yields a linear first order boundary condition on $F(z)$ at $z = 0$ given by:

$$\frac{dF}{dz} - \frac{\Lambda}{\bar{\psi}_0}F = -\frac{gBa}{f_0} \qquad \text{at } z = 0$$

Applying the transformations (3.7) to this condition gives the transformed boundary condition:

$$\frac{dZ}{dh} + \delta_*^{-1}\left(-\frac{\Lambda}{\bar{\psi}_0} + \frac{1}{2H_0}\right)Z(h) = -\frac{gBa}{f_0\delta_*} \qquad \text{at } h = \frac{\delta\bar{\psi}_0}{\Lambda} = h_*$$

and using this to evaluate A in the streamfunction expression (3.8) leads

to the solution

$$\psi = \underline{\text{Real}} - \frac{\frac{gBa}{f_0}\exp\left(\frac{z}{2H_0}\right) W_{k,\frac{1}{2}}(h)\, P_n^m(\cos\theta)\exp im\phi}{\delta_* W_{k,\frac{1}{2}}(h_*) + \left(\frac{1}{2H_0} - \frac{\Lambda}{\bar{\psi}_0}\right) W_{k,\frac{1}{2}}(h_*)} \qquad \text{——(3.9)}$$

For all positive values of h, $W_{k,\frac{1}{2}}(h)$ is a real function and the phase of ψ will be the same at all heights apart from $180°$ changes associated with amplitude sign change. This is equivalent to saying that the phase is independent of height for all regions in the westerly winds. If the zonal wind is westerly at $z = 0$ then there is no net energy propagation in any direction and the wave motion is described as 'trapped'. If a region exists where the Charney/Drazin criterion of propagation is locally satisfied (roughly) then the disturbance motion may behave as a standing wave there with the appearance of nodes (see Simmons, 1974).

Resonance is also possible when the denominator of (3.9) vanishes and an example is given later.

These effects are summarised schematically in the following diagram:

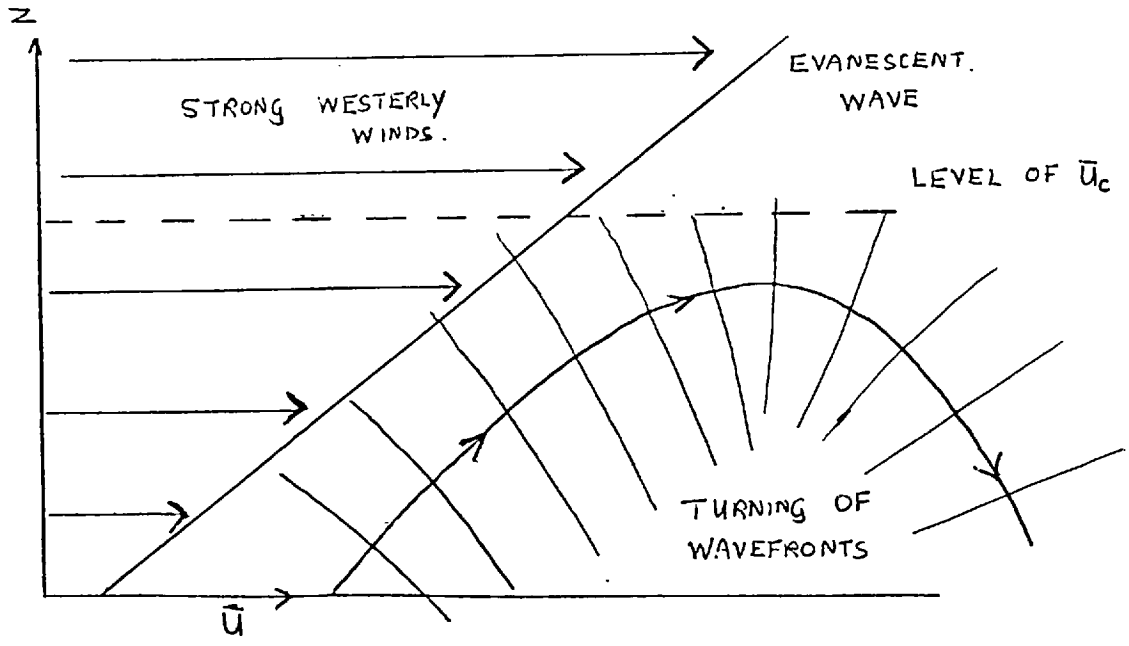

Clearly, this model is quite unlike the observed structure of wavenumber *1* and *2* wave motion in the real atmosphere with the complete absence of phase tilt. No absorption process exists in the model and

its implicit inclusion through an energy transmitting boundary condition is required.

It is appropriate at this point to review some of the theoretical work carried out on planetary wave motion in the stratosphere and interpret it in the context of the model used here.

Simmons (1974) obtained solutions to the quasi-geostrophic potential vorticity equation for the motion resulting from forcing at the base of a stratosphere with jet profiles of zonal wind in the meridional direction and constant vertical shear. In general the problem is non-separable and is only tractible for special cases; yet Simmons circumvents this by expansion of β into the horizontal eigenmodes and finds that the amplitude of the forced wave tends to mimic the shape of the zonal wind field. He calculated the stationary response of wavenumbers *1* and *2* to forcing of an atmosphere of 'realistic zonal wind' distribution up to *100* km, imposing an upper boundary condition demanding the boundedness of energy density at infinity. Although the calculated amplitude variation in the vertical is quite reasonable, the phase lines are vertical and no net upward propagation of energy occurs.

In an attempt to reproduce the westward tilting wave patterns of wavenumbers *1* and *2*, he introduces dissipation through height-independent Newtonian damping of the temperature perturbations of magnitudes, estimated by Lindzen and Goody (1965) from photochemical calculations. The destruction of available potential energy of the wave by the radiative relaxation of the temperature field is offset to a large extent by the potential energy drawn from the mean state by the wave through poleward heat transport by the wave (and hence westward tilt). Although Simmons obtains a westward tilting wave system with the introduction of Newtonian cooling it is far too abrupt with all the phase change occurring in a shallow layer ($\sim$*10* km)

above the forcing height. Muench's data indicates a much more uniform westward tilt with height of both wavenumbers *1* and *2*.

Matsuno (1970) investigated the vertical propagation of wave energy into the stratosphere in a model with realistic horizontal and vertical variation of the mean zonal wind in winter. Observed amplitudes and phases of the low zonal wavenumbers were specified at the lower boundary corresponding to the *500* mb level and a simple radiation boundary condition was applied at *65* km. Wave energy was found to propagate upwards and southwards to be absorbed at the zero-wind line (critical layer). In this way energy was prevented from reaching the high stratosphere by the strong critical layer absorption and phase tilt westward with height was quite realistic. The major deficiency of the model results was the underestimation of the amplitude of wavenumber *2* in the stratosphere with amplitude decreasing above *25* km.

Matsuno's numerical solutions appear to differ from those of Simmons who found that the critically absorbing layer (of the equatorial zero-wind line) has little effect on the penetration of wavenumbers *1* and *2* into the upper stratosphere and his predicted amplitude variation of wavenumber *2* was in better agreement with observation.

In Chapter 4, we argue that a critical-level absorption process is not desirable in stationary wave problems since it implies an infinite drag on the zonal wind at the zero-wind line which would be inconsistent with a steady basic state flow. Nevertheless, the exchange of energy between the wave and mean flow by this process is not ruled out for the non-linear system and the question of its importance remains unanswered at this stage.

An energy-transmitting upper boundary condition

In view of the uncertainty concerning the wave energy absorption mechanism in the upper stratosphere, whether it be by radiative damping of the temperature perturbations or exchange with the mean flow at the equatorial zero-wind line, we avoid the problem by imposing an energy-transmitting boundary condition below the region of observed absorption.

Energy transmission is allowed by keeping the angular rotation rate of the atmosphere fixed above *40* km and selecting the purely upward energy radiating solution there. This upper solution is connected to the motion below *40* km by demanding continuity of pressure and vertical velocity (consistent with the interfacial conditions of the previous chapter).

This allows a boundary condition to be formed as follows:

B = A CONSTANT

$\bar{u}$ = (A CONSTANT)·SIN θ

ψ_+ = REAL $C \exp\left\{ i(m\phi + \nu z) + \frac{z}{2H_0} \right\} P_n^m(\cos\theta)$

—— —— —— —— —— —— —— —— —— —— $z = H$

ψ_- = REAL $F(z) \exp im\phi \, P_n^m(\cos\theta)$

ψ ~~(AND $\bar{u}$)~~ ARE CONTINUOUS ACROSS $z = H$.

The upward radiating solution of the hypothetical upper layer is:

$$\psi_+ = \underline{\text{Real}}\, C \exp\left\{ i(m\phi + \nu z) + \frac{z}{2H_0} \right\} P_n^m(\cos\theta)$$

where C is an undetermined complex constant and the lower solution is of the form:

$$\psi_- = \underline{\text{Real}}\, F(z) \exp im\phi \, P_n^m(\cos\theta)$$

so that the connecting conditions at $z = H$ are:

$$C \exp\left\{i\nu H + \frac{H}{2H_0}\right\} = F(H) \qquad \text{(continuity of pressure)}$$

and

$$\left\{\bar{\psi}(H)\frac{dF}{dz} - F\,\frac{d\bar{\psi}}{dz}\right\}\Big|_{z=H} = \bar{\psi}(H)\left\{i\nu + \frac{1}{2H_0}\right\}C$$

(from the thermodynamic equation)

Elimination of C between them yields the complex boundary condition:

$$\frac{dF}{dz} - \left\{\frac{1}{\bar{\psi}}\frac{d\bar{\psi}}{dz} + \frac{1}{2H_0} + i\nu\right\}F(z) = 0 \qquad \text{at } z = H \qquad \text{——(3.10)}$$

with

$$\nu^2 + \frac{1}{4H_0^2} = \frac{gB}{f_0^2}\left\{\frac{2\Omega}{\bar{\psi}(H)} - \frac{(n-1)(n+2)}{R^2}\right\}$$

This type of boundary condition, which is closely related to the Sommerfeld radiation condition, will be particularly useful for numerical integration where an infinite integration region must be reduced to a finite region. When $\nu^2 < 0$, the upper wave is evanescent and the boundary condition is no longer complex which prevents the sloping of the phase lines.

The solution to the orographic forcing problem with radiation condition (3.10) is straightforward to obtain and involves the linear combination of the independent solutions $W_{k,\frac{1}{2}}(h)$ and $M_{k,\frac{1}{2}}(h)$ which satisfy the upper and lower boundary conditions. Fig.3.3 gives the amplitude and phase of wavenumbers *1* and *2* up to *40* km for a 'realistic' choice of zonal wind shear (values given at *45*°N) and average static stability*. Amplitudes of the contour height field forced by $Z_0 = 200\, P_n^m(\cos\theta)\cos m\phi$ gpm are of the order of *1* mb at the ground and ~*500* gpm near *30* km which compares favourably with observed values. Phase tilt is in good agreement with Fig.1.2 and is less rapid in the upper regions as one would expect from a local application of the constant zonal wind solution. Unevenness in the curves results from the partial internal reflection inherent in the solution, which causes interference with the propagating component.

*The static stability B in the 'hypothetical layer' is $5 \times 10^{-5}\ \mathrm{m}^{-1}$.

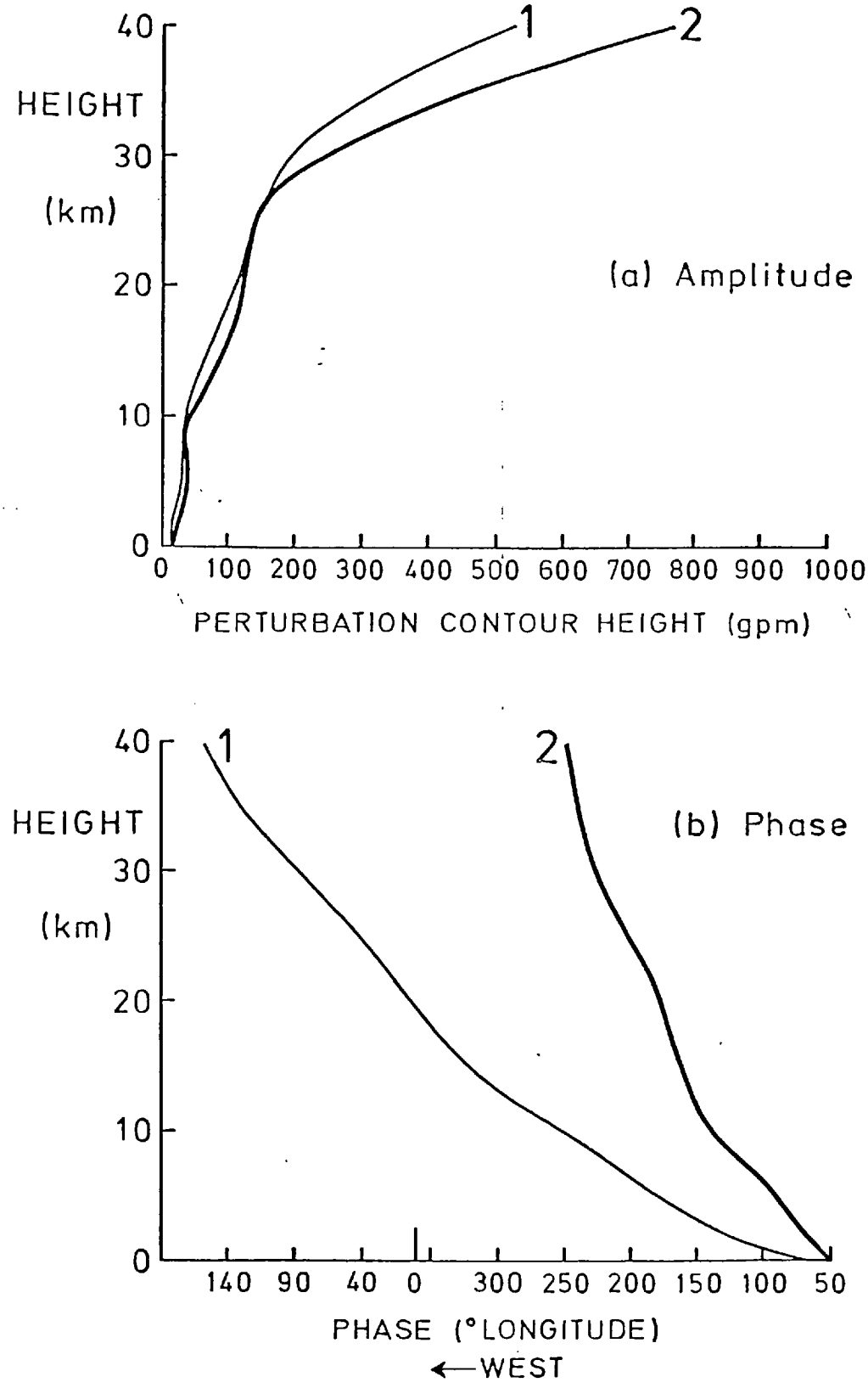

Fig.3.3 Orographic forcing in constant shear. Amplitude and phase of untrapped modes 1 (wavenumber *1*, $n = 2$) and 2 (wavenumber *2*, $n = 3$) with $\overline{u} = 2$, *30* m s^{-1} at $z = 0$, *40* km respectively for $a = 300$ m and $B = 3.0 \times 10^{-5}$ m^{-1}.

A useful test of accuracy of the solution arises from an interesting property of the differential equation for the height structure $F(z)$. Setting $S=0$ in (2.4) and re-arranging gives:

$$\frac{d}{dz}\left\{\frac{\rho_0}{B}\frac{dF}{dz}\right\} + k(z)F(z) = 0 \qquad \text{——(3.11)}$$

where the coefficient of $F(z)$ is replaced by the real function $k(z)$.

Also taking the complex conjugate (denoted by $*$) of (3.11) gives:

$$\frac{d}{dz}\left\{\frac{\rho_0}{B}\frac{dF^*}{dz}\right\} + k(z)F^*(z) = 0 \qquad \text{——(3.12)}$$

Multiplying (3.11) by F^* and (3.12) by F, subtracting the resulting equations and further re-arrangement gives:

$$\frac{d}{dz}\,\underline{\text{Imag.}}\left\{\frac{\rho_0}{B}F^*\frac{dF}{dz}\right\} = 0$$

or $\underline{\text{Imag.}}\left\{\frac{\rho_0}{B}F^*\frac{dF}{dz}\right\}$ is independent of height.

Now the poleward eddy entropy flux $\overline{v'\delta\phi'}$ is given in terms of the streamfunction by:

$$\rho_0\,\overline{v'\delta\phi'} = \underline{\text{Real}}\,\frac{\rho_0}{2}\left(\frac{im}{R}\psi\right)^*\left(\frac{f_0}{g}\left(\frac{\partial\psi}{\partial z} - B\psi\right)\right)$$

(where the overbar denotes the average about a latitude circle)

which may be simplified to:

$$\rho_0\,\overline{v'\delta\phi'} = -\frac{\rho_0 f_0 m}{2gR}\,\underline{\text{Imag.}}\,(F^*F')$$

and therefore: $\frac{\rho_0}{B}\overline{v'\delta\phi'}$ is independent of height.

The eddy heat flux $\rho_0 C_p\,\overline{v'\delta\theta}$ should be proportional to the vertical gradient of potential temperature for a propagating wave in a given zonal wind field. It must be remembered however that the ability to transport heat polewards is primarily dependent on whether or not the wave is trapped by the zonal winds. It is interesting to speculate on the possible sensitivity of stationary wave heat transport in the troposphere to the wind circulation of the stratosphere. The reduced transmissivity of

the stratosphere to upward propagating planetary waves through the increased strength of the polar night jet might have important repercussions on the tropospheric circulation through the reduction of the stationary wave heat transport.

The year to year variability of the polar night vortex strength is large with as much as a factor of *2* involved in the variation of the zonal wind speed at *10* mb and so the tropospheric response should also vary. Another interesting possibility is that of resonance of trapped planetary waves and their influence on the weather.

To demonstrate and emphasise this possibility, a trapped resonant wave was found for the orographic forcing of the $P_3^2(\cos\theta)$ mode and the surface pressure response is plotted for different uniform shear profiles in Fig.3.4. The surface (mid-latitude) zonal wind speed is fixed at *5* $m\,s^{-1}$ and the speed at *40* km is varied between *40* and *75* $m\,s^{-1}$. A highly peaked resonant state occurs when the zonal wind at *40* km is about *52* $m\,s^{-1}$.

Naturally, the growth of a near-resonant wave is limited by the availability of energy in the system and dissipation so that the response of a real (non-linear) atmosphere would be bounded. The question that must be raised is, 'Does planetary wave resonance occur naturally in the atmosphere and if so how does it manifest itself'? One hypothesis is that 'blocking', so-named by synopticians, is a persistent, resonantly amplified planetary wave. Certainly, trapping is favoured by the high n spherical harmonic modes consistent with the 'splitting of jet streams phenomenon' since $(n-m)$ determines the qualitative characteristics of the meridional wave structure and harmonic modes change sign with latitude more frequently the larger the value of $(n-m)$.

This point might form the basis of an interesting investigation

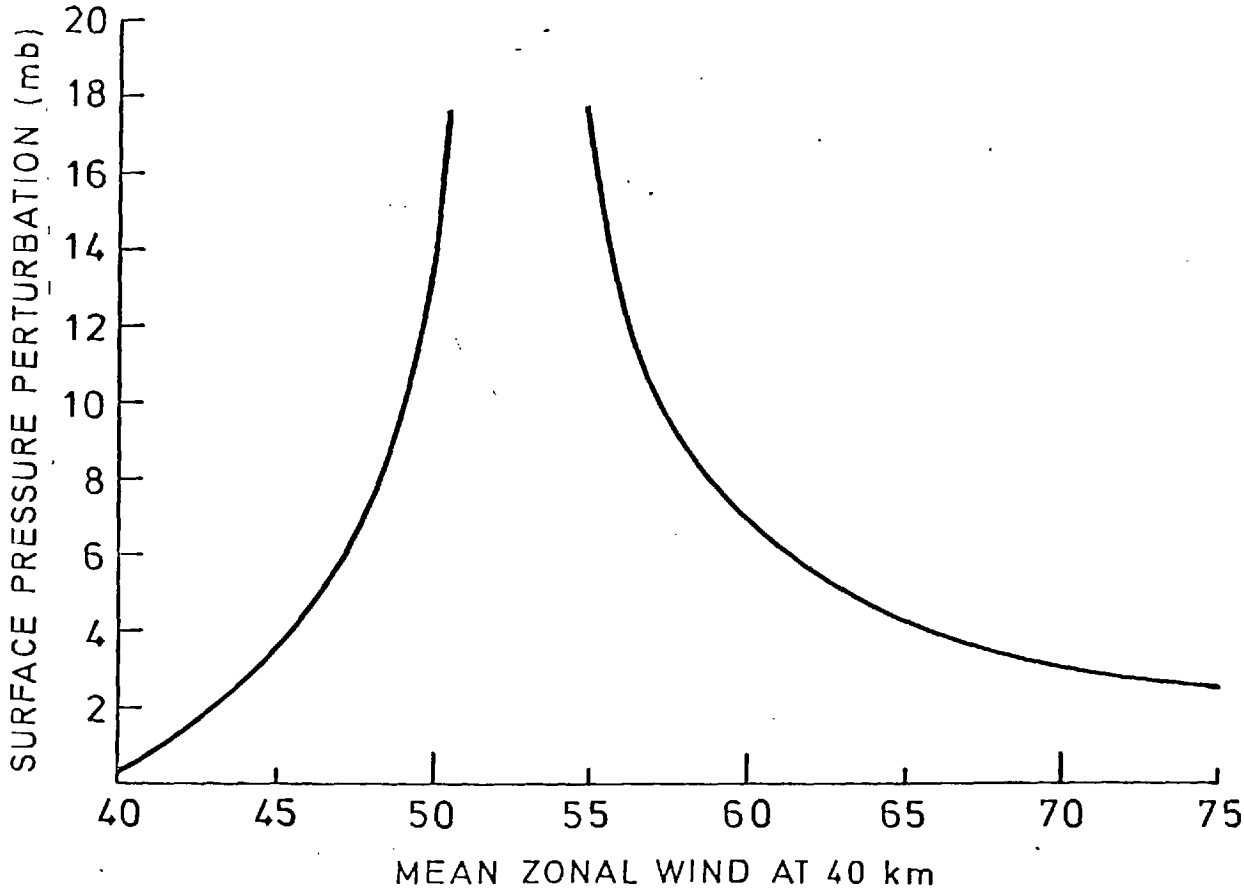

Fig.3.4 Response at the surface to different constant shear wind profiles. Wavenumber 2 (with $n = 3$) is trapped in a constant shear wind profile with $\overline{u} = 5$ m s^{-1} at the surface and various values for $\overline{u}$ at 40 km. All other parameters relevant as in Fig.2. Resonance occurs near $\overline{u} = 52$ m s^{-1} at 40 km.

into the resonant growth of planetary waves in a multi-levelled, non-linear numerical model in order to determine the meteorological significance of such waves.

Summarizing this section, we conclude that satisfactory models of orographic forcing are obtained with the use of a radiation boundary condition at *40* km and that amplitudes and phases of wavenumbers *1* and *2* are in good agreement with observed structure in the atmosphere. Using calculated spherical harmonic coefficient values for the P_2^1 and P_3^2 modes of the spherical harmonic expansion of surface elevation, we find stratospheric disturbances of realistic amplitude.

Further work on the structure of orographically forced waves will be presented in Chapter 4 where the observed variation of zonal wind and static stability in the vertical will be accounted for.

(b) Thermal forcing

Attention has been focussed so far on the propagation of energy away from the forcing regions into the upper stratosphere in winter and we have attempted to improve the tropospheric description of the wave motion by constructing a more suitable upper boundary condition. The energy transmitting boundary condition will now be used to examine the structure of thermally forced waves of the largest horizontal scale (with $n = 2$, *3* and *4*). The P_2^1 and $P_3^2(\cos\theta)$ modes should represent a substantial proportion of the thermal forcing at these zonal wavenumbers since they possess one middle-latitude peak in their meridional structure, and the higher modes P_4^1, P_6^1, P_5^2 and $P_7^2(\cos\theta)$ are trapped and are important mainly in the troposphere (choosing only modes that vanish at the equator).

The amplitude of thermally-forced motion depends critically on the strength of the zonal winds in the vicinity of the heating region and

a constant shear profile of wind allows the smallness of the westerlies near the ground to be represented without underestimating the stratospheric wind, as in the solid-rotation atmosphere solutions.

The thermal-forcing of planetary waves poses a more difficult mathematical problem through the inclusion of an inhomogeneous term in the differential equation for the height structure. Introduction of a uniform shear of the angular rotation rate into equation (2.4) such that $\bar{\psi} = \bar{\psi}_0 + \Lambda z$; letting B = a constant and $\rho_0 = \rho_{0s} \exp(-z/H_0)$) gives:

$$\frac{d^2F}{dz^2} - \frac{1}{H_0}\frac{dF}{dz} + \frac{gB}{f_0}\left\{\frac{2\Omega}{\bar{\psi}_0 + \Lambda z} + \frac{\frac{f_0^2}{gB}\frac{\Lambda}{H_0}}{\bar{\psi}_0 + \Lambda z} - \frac{(n-1)(n+2)}{R^2}\right\}F(z) = -\frac{gR^2}{f_0 m\bar{\psi}}\frac{1}{\rho_0}\frac{d}{dz}(\rho_0 S_0)$$

As before, using the transformations:

$$F(z) = Z(z)\exp\left(\frac{z}{2H_0}\right)$$

and

$$h = \delta_*\left(\frac{\bar{\psi}_0}{\Lambda} + z\right)$$

the above equation reduces to:

$$\frac{d^2Z}{dh^2} + \left\{-\frac{1}{4} + \frac{k}{h}\right\}Z(h) = -\frac{gR^2}{f_0\Lambda m}\frac{\exp\left\{-\frac{(h-h_*)}{2H_0\delta_*}\right\}}{h}\frac{1}{\rho_0}\frac{d}{dh}(\rho_0 S_0) \qquad \text{——(3.11)}$$

This is a second-order inhomogeneous linear differential equation with variable coefficients and may be intergrated by standard Green's function construction. The Green's function $G(h,h_F)$ is the solution to the equation:

$$\frac{d^2Z}{dh^2} + \left\{-\frac{1}{4} + \frac{k}{h}\right\}Z(h) = \delta(h - h_F)$$

under homogeneous boundary conditions, where δ is the Dirac delta function. In this problem the lower boundary condition is inhomogeneous if the source term S_0 does not vanish at the ground $z = 0$, and an extra term is added to the Green's function solution that originates from the 'surface term' of the generalised Green's identity. The modified radiation upper boundary condition to be used is identical to that used for orographic forcing provided that the flow is adiabatic in that region.

* the radiation condition used produces some reflection arising from the discontinuity of shear at the height of application.

The Green's function solution in our case corresponds to a step-function in energy heating rate $\rho_0 S_0$ and it will be of some interest to examine the elementary Green's function solution which corresponds to constant $\rho_0 S_0$ up to a certain height and zero elsewhere, i.e. $\rho_0 S_0(0) = H(z_F - z)$ where $H(x)$ is the unit stepfunction (i.e. lower tropospheric heating anomaly).

The Green's function method consists of constructing an upper solution from the two homogeneous solutions $W_{k,\frac{1}{2}}(h)$ and $M_{k,\frac{1}{2}}(h)$ which satisfies the upper boundary condition and a lower solution which satisfies the *homogeneous* lower boundary condition. These are connected by the condition that the streamfunction is continuous at $h = h_F$ (the non-dimensional height corresponding to z_F) and a jump condition which imposes a unit discontinuity in the derivative of $Z(h)$ at $h = h_F$. If $Z_>(h,h_F)$ and $Z_<(h,h_F)$ denote the upper and lower solutions respectively, then,

$$Z_>(h,h_F) = K_1 W_{k,\frac{1}{2}}(h) + K_2 M_{k,\frac{1}{2}}(h) \qquad \text{for } h \geq h_F$$

and

$$Z_<(h,h_F) = K_3 W_{k,\frac{1}{2}}(h) + K_4 M_{k,\frac{1}{2}}(h) \qquad \text{for } h \leq h_F$$

where K_1, K_2, K_3 and K_4 are constants to be determined from the two boundary conditions and the continuity and jump conditions at $h = h_F$.

The homogeneous upper and lower boundary conditions can be shown to be:

$$\frac{dZ}{dh} - \delta_*^{-1}\left(\frac{\Lambda}{\bar{\psi}_0 + \Lambda H} + i\nu\right) Z(h) = 0 \qquad \text{at } h = h_T$$

(radiation condition)

and

$$\frac{dZ}{dh} + \delta_*^{-1}\left(\frac{1}{2H_0} + \frac{\Lambda}{\bar{\psi}_0}\right) Z(h) = 0 \qquad \text{at } h = h_0$$

(vertical velocity is zero at the ground

with

$$h_T = \delta_*\left(\frac{\bar{\psi}_0}{\Lambda} + H\right) \quad \text{and} \quad h_0 = \frac{\delta_* \bar{\psi}_0}{\Lambda}$$

At $h = h_F$ the connecting conditions are:

$$Z_>(h_F) = Z_<(h_F) \quad \text{and} \quad \frac{dZ}{dh}_> - \frac{dZ}{dh}_< = 1$$

and after algebraic manipulation the Green function, given by $Z_>$ and $Z_<$ in their appropriate ranges, becomes:

$$G(h,h_F) = \begin{cases} \gamma\left(\alpha_1 W_{k,\frac{1}{2}}(h_F) - M_{k,\frac{1}{2}}(h_F)\right)\left(\alpha_2 W_{k,\frac{1}{2}}(h) - M_{k,\frac{1}{2}}(h)\right) & \text{for } h_0 \leq h \leq h_F \\ \gamma\left(\alpha_2 W_{k,\frac{1}{2}}(h_F) - M_{k,\frac{1}{2}}(h_F)\right)\left(\alpha_1 W_{k,\frac{1}{2}}(h) - M_{k,\frac{1}{2}}(h)\right) & \text{for } h_F \leq h \leq h_T \end{cases}$$

where
$$\alpha_1 = \frac{M'_{k,\frac{1}{2}}(h_T) + \varepsilon_1 M_{k,\frac{1}{2}}(h_T)}{W'_{k,\frac{1}{2}}(h_T) + \varepsilon_1 W_{k,\frac{1}{2}}(h_T)}$$

$$\alpha_2 = \frac{M'_{k,\frac{1}{2}}(h_0) + \varepsilon_2 M_{k,\frac{1}{2}}(h_0)}{W'_{k,\frac{1}{2}}(h_0) + \varepsilon_2 W_{k,\frac{1}{2}}(h_0)}$$

with
$$\gamma = \frac{(-k)!}{(\alpha_1 - \alpha_2)}, \qquad \varepsilon_1 = -\delta_*^{-1}\left(\frac{\Lambda}{\bar{\psi}_0 + \Lambda H} + i\nu\right)$$

$$\varepsilon_2 = \delta_*^{-1}\left(\frac{1}{2H_0} - \frac{\Lambda}{\bar{\psi}_0}\right)$$

(Primes denote the ordinary first derivative.)

In the derivation above, the property that the Wronskian of the independent solutions is constant for this homogeneous differential equation was used and is found to be such that:

$$W'_{k,\frac{1}{2}}(h)M_{k,\frac{1}{2}}(h) - M'_{k,\frac{1}{2}}(h)W_{k,\frac{1}{2}}(h) = -\frac{1}{(-k)!}$$

For a heating function $\rho_0 S_0 = \rho_0(0)S_0(0)\,H(z_F - z)$, the right-hand side of (3.11) becomes:

$$\frac{gR^2}{f_0 \Lambda m}\,\frac{\exp\left\{-\dfrac{(h_F - h_0)}{2H_0\delta_*}\right\}}{h_F}\,\frac{\rho_0(0)S_0(0)\,\delta(h - h_F)}{\rho_0(h_F)} = \frac{gR^2}{f_0\Lambda m}\exp\left\{\frac{h_F - h_0}{2H_0\delta_*}\right\}S_0(0)\delta(h - h_F)\Big/ h_F$$

To obtain the solution to (3.11) with a step-function profile of forcing, the Green function must be multiplied by the coefficient of $\delta(h - h_F)$ above and the inhomogeneous term of the lower boundary condition must be accounted for

At the lower boundary $h = h_0$, the vanishing of vertical velocity w gives:

$$\frac{dZ}{dh} + \epsilon_2 Z(h) = - \frac{gS_0(0)R^2}{f_0 \delta_* m \bar{\psi}_0}$$

(from the thermodynamic eqution using the transformations (3.7)) and the extra surface term from the Green's identity is:

$$- \frac{gS_0(0)R^2}{f_0 \delta_* m \bar{\psi}_0} G(h,h_0)$$

so that the full solution becomes:

$$Z(h) = \frac{gS_0(0)R^2}{f_0 m} \left[\frac{\exp(z_F/2H_0)}{\Lambda h_F} G(h,h_F) - \frac{G(h,h_0)}{\delta_* \bar{\psi}_0} \right]$$

Once the Green's function is known, the solution for any distribution of $S_0(z)$ may be synthesised by summing the influences from all levels, which is expressed formally by the integral:

$$Z(h) = \int_{h_0}^{h_T} G(h,h_F) \left\{ - \frac{gR^2}{f_0 \Lambda m} \frac{\exp\left\{ - \frac{(h_F - h_0)}{2H_0 \delta_*} \right\}}{h_F} \frac{1}{\rho_0(h_F)} \frac{d}{dh_F} \left(\rho_0 S_0(h_F) \right) \right\} dh_F - \frac{gR^2 S_0(0)}{f_0 m \delta_* \bar{\psi}_0} G(h,h_0)$$

——(3.12)

Having outlined the mathematical procedure, it remains to discuss those results obtained by calculating the Whittaker functions and performing numerical integrations to evaluate the above complex integral.

Firstly, consider step-function forcing in a uniform shear profile equivalent to a mid-latitude zonal wind speed of *2* m s^{-1} at the surface and *30* m s^{-1} at *40* km where the modified radiation condition is applied. The heating function $\rho_0 S_0$ is constant below *4* km and equivalent to a heating rate of *1.5*°C/day at the surface. The graphs (Fig.3.5) show the amplitude and phase of the wavenumber *1* response ($n = 2$) compared to the response with the uniform shear profile altered so that the surface wind is *10* m s^{-1} (again with zonal wind of *30* m s^{-1} and *40* km). In the case of light surface winds, the amplitude is everywhere much larger than is reasonable in the

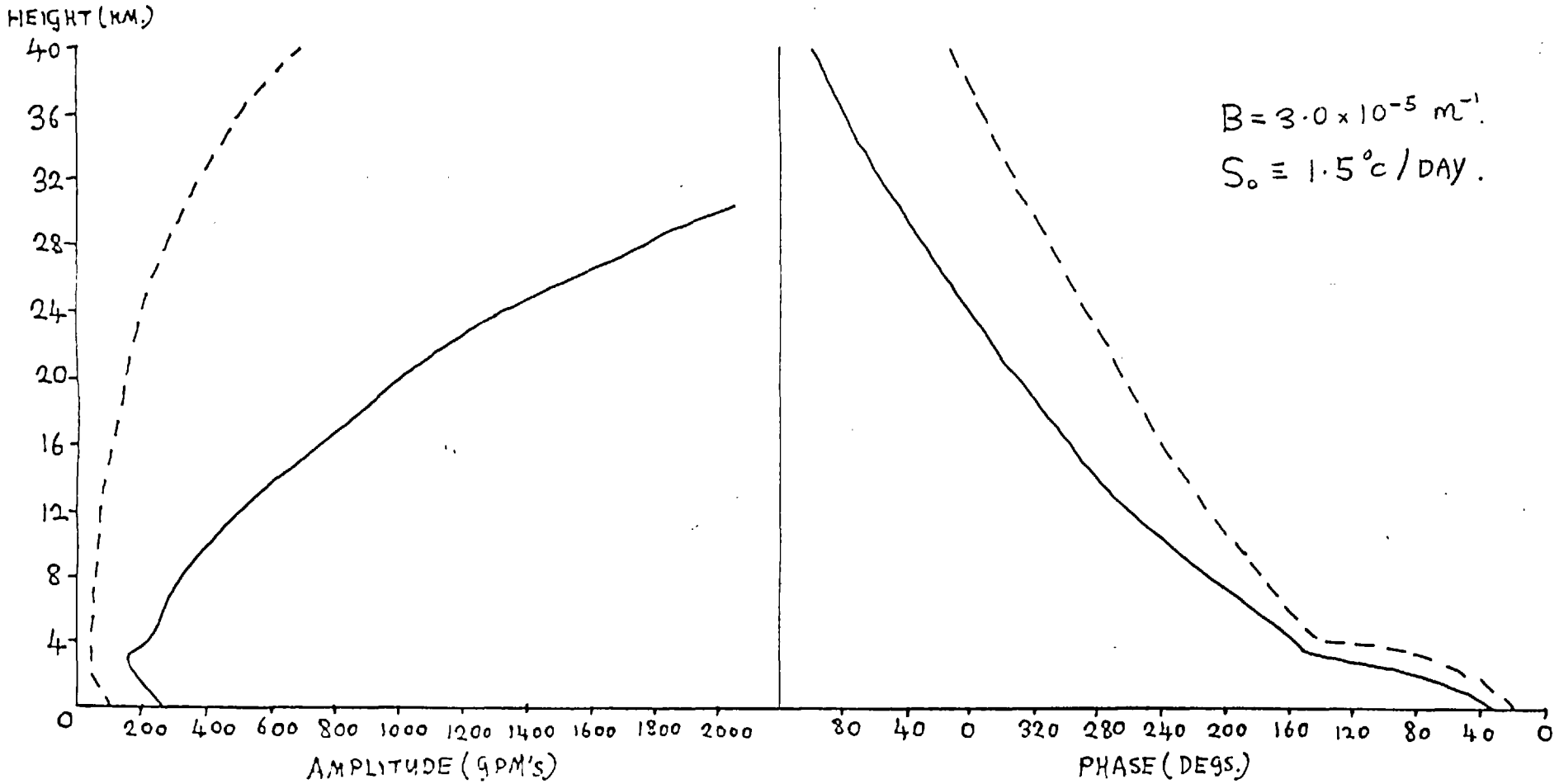

FIG. 3.5 AMPLITUDE AND PHASE OF THE P_2^1 MODE DUE TO 'STEP-FUNCTION FORCING' OF AN ATMOSPHERE IN CONSTANT ANGULAR SHEAR, FOR TWO DIFFERENT ZONAL WIND FIELDS.

——— $\bar{u}(z=0) = 2\ m s^{-1}$, $\bar{u}(z=40 KM.) = 30\ m s^{-1}$ } AT 45°N.

– – – – $\bar{u}(z=0) = 10\ m s^{-1}$, " " }

real atmosphere with a surface pressure perturbation of ~ 25 mb. When the mid-latitude surface wind is increased to 10 m s^{-1} the amplitude is greatly reduced particularly in the stratosphere and is smaller than observed magnitudes.

The difference in amplitude size between each must be attributed mainly to the reduction of the effective forcing when the zonal wind speed in the heating region is large. This is, as explained before, due to the greater time spent by air in the heating and cooling phases which allows greater compressive effects on the vortex tubes and hence larger amplitudes and upward energy propagation. In reality, these two cases probably represent extremes of the mean zonal wind in the troposphere.

Phase variation is broadly similar in both cases with the most rapid phase tilt westward occurring just below 'the step' in the heating function. Above 4 km the tilt is fairly uniform except for its slow decrease in magnitude with height. Typically, phase variation with height is observed to be about $6°$/km in the stratosphere which compares favourably with both of these curves.

The distribution of zonal wind speed in these profiles is not very representative of the tropospheric flow and so it is instructive to consider forcing in a flow with zonal wind speeds of 2 and 20 m s^{-1} at 0 and 10 km respectively with a radiation condition at 10 km. Fig.3.6 shows the amplitude and phase of the contour height field, together with the associated poleward heat flux (given by $\overline{v'\delta T'}$) for wavenumber 1 forcing of such a flow. Amplitude is largest at the ground (~ 11 mb) and rapidly decreases to a minimum at 4 km (above which the heating function is zero), strongly resembling the characteristic intense, shallow surface anticyclones of the continents in winter time. In the upper troposphere, the increase in amplitude is due mainly to the inertial effect of density associated

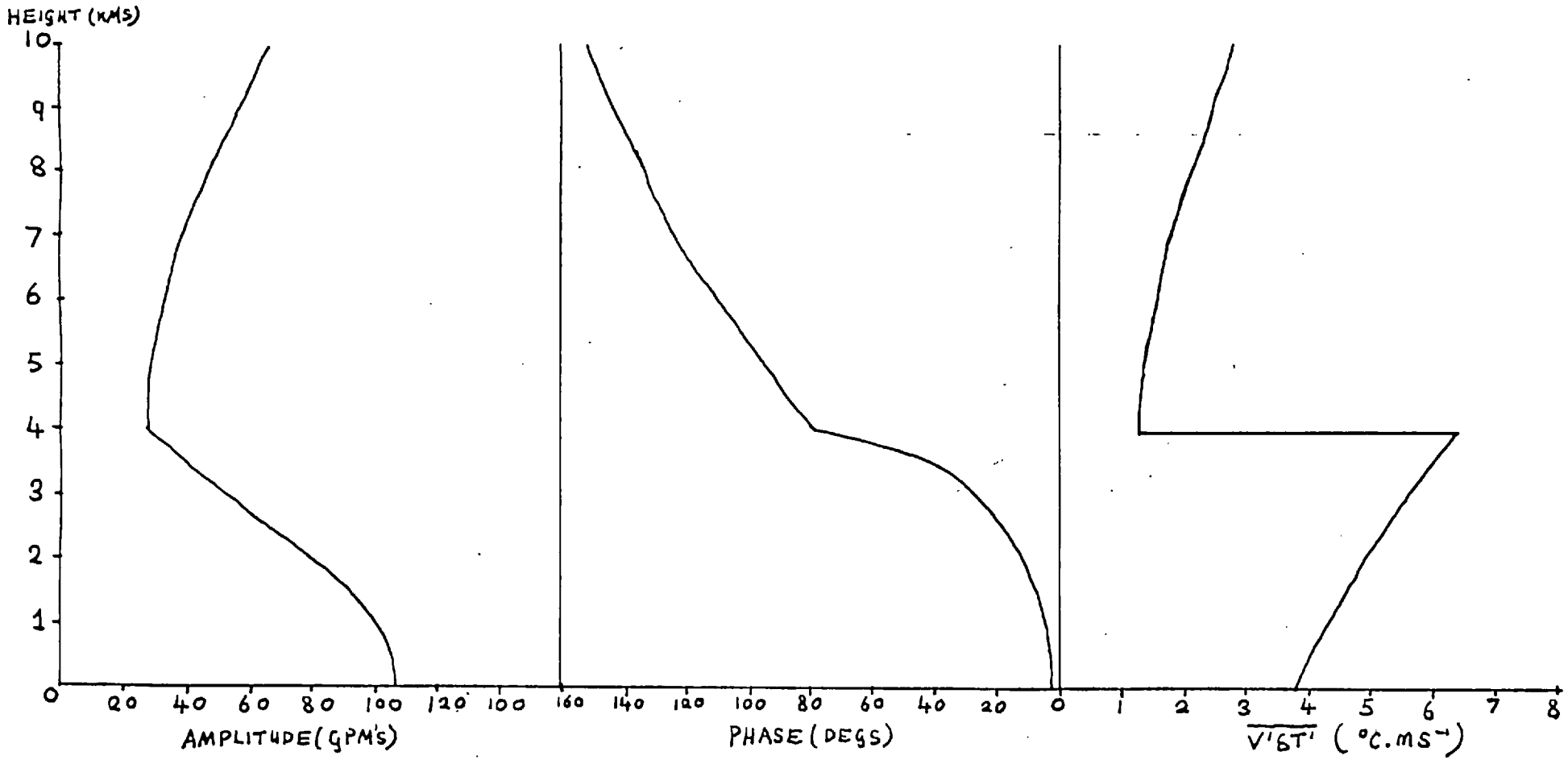

FIG. 3.6 AMPLITUDE AND PHASE OF THE P_2^1 MODE DUE TO 'STEP-FUNCTION FORCING' OF AN ATMOSPHERE IN CONSTANT ANGULAR SHEAR.
$\bar{u}(z=0) = 2\,ms^{-1}$ AND $\bar{u}(z=10KM.) = 20\,ms^{-1}$ (IN MIDDLE LATITUDES)
$S_0 \equiv 1{\cdot}5\,°C/DAY$ FOR $z \leq 4KM.$ AND ZERO ELSEWHERE.

with the factor $\exp(z/2H_0)$ in the height structure.

Phase variation with height is small below 2 km and increases to become most rapid near the top of the heating layer, with a phase difference of 90° between the 1000 and 500 mb level (this difference forms a useful yardstick when making comparison with synoptic chart data).

Poleward heat transport is greater in the heating layer and changes discontinuously at 4 km with $\rho_0 \overline{v'\delta T'}$ being constant in the regions above and below. Calculated values of $\overline{v'\delta T'}$ in the heating layer of $\sim 5^\circ$C m s^{-1} indicate the importance of stationary forced waves as transporters of heat. Looking again at the phase relationship of the pressure perturbation to the source function S, shows that the surface anticyclone is to be found nearly 90° downstream of the region of highest cooling rate which is significantly further than that for the constant rotation atmosphere solutions.

The discontinuity of the heating function in the vertical used so far allows a very crude representation of low level heating and we supplement these with constant shear calculations for an exponential heating function, $a \exp(-bz)$ of the form used in the solid rotation atmosphere solutions. The height structure is found by substituting this expression for S_0 into equation (3.12) and evaluating the integral numerically. Fig.3.7 gives the resulting amplitude and phase for the P_2^1 and $P_4^1(\cos\theta)$ modes with heating rate a equivalent to 1.5°C/day and scale height b^{-1} of 4 km. A constant shear zonal wind profile was chosen with $\bar{u}(z=0) = 5$ m s^{-1} and $\bar{u}(z=40\text{km}) = 50$ m s^{-1} (mid-latitude values) with modified radiation condition at 40 km.

Only the $n = 2$ mode is propagating with the characteristic westward tilt of the phase lines; the phase lines of the $n = 4$ mode are vertical except at the node near 4 km. The amplitude of this trapped mode actually

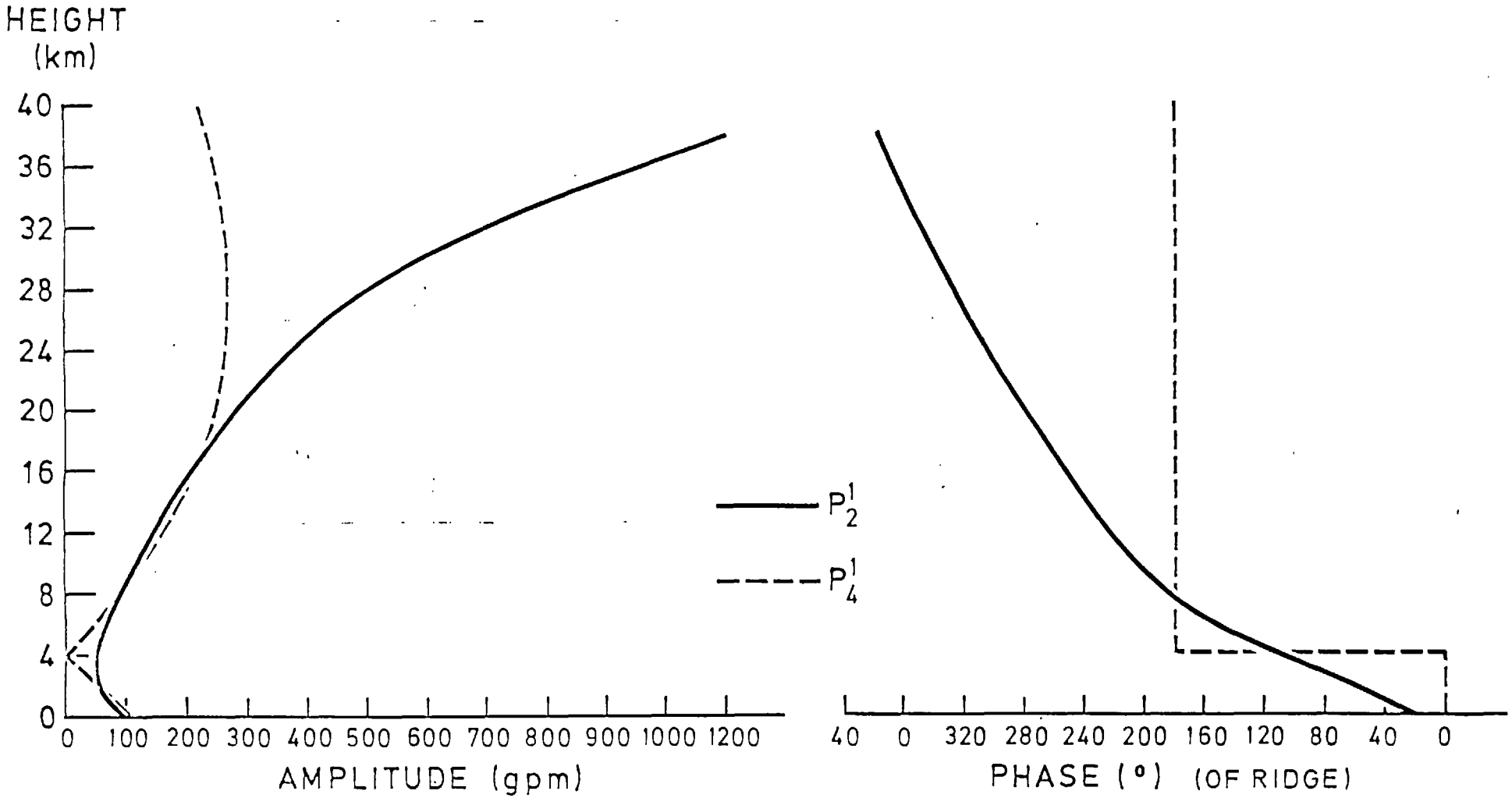

FIG. 3.7 THE STRUCTURE OF THE THERMALLY-FORCED P_2' AND P_4' MODES IN IN UNIFORM ANGULAR SHEAR,

$\bar{u}\,(z=0) = 5\ m\,s^{-1}$.
$\bar{u}\,(z=40KM.) = 50\ m\,s^{-1}$. } $45°N$ AND $B = 3.0\times10^{-5}\ m^{-1}$.

decreases above *30* km and is reminiscent of the adiabatic solutions found by Simmons. As in the step-function heating profiles the amplitude of the untrapped wave exhibits a minimum near *4* km and it is later found that this is a general feature of thermally forced motion generated by lower tropospheric heating anomalies. The amplitude of the $P_2^1(\cos\theta)$ mode increases very rapidly with height in the stratosphere consistent with the upward propagation of energy into the tenuous, upper regions of the stratosphere

Poleward heat transport by the $P_2^1(\cos\theta)$ mode is given in Fig.3.8 and shows again, a significant low-level transport of heat with a minimum in $\overline{v'\delta T'}$ occurring in mid-troposphere.

The phase relationship of heating function to pressure perturbation is such that for the trapped $n = 4$ mode they are either *90°* or *270°* out of phase. In this case, at the surface the cold anticyclone occurs *90°* downstream of the maximum cooling region. For the propagating $n = 2$ mode, the surface high is *63°* downstream of the maximum cooling spot, and is similar to that for the solid rotation atmosphere considered previously.

Fig.3.9 gives the response to the same forcing function S of an atmosphere with uniform shear such that $\bar{u}(z=0) = 5$ m s^{-1} and $\bar{u}(z=10\text{km}) = 25.0$ m s^{-1} with the radiation condition at *10* km. General features of the solution for $P_2^1(\cos\theta)$ are as before with surface amplitude of ~ 8 mb.

These more sophisticated models of thermal forcing are sufficiently realistic to allow comparison with observation and we shall briefly compare the calculated structure of wavenumber *1* with data given by Muench. The final summary of theory and observations will be given after the detailed numerical calculations of Chapter 4.

Muench (1965) presents mean amplitude and phase of contour height

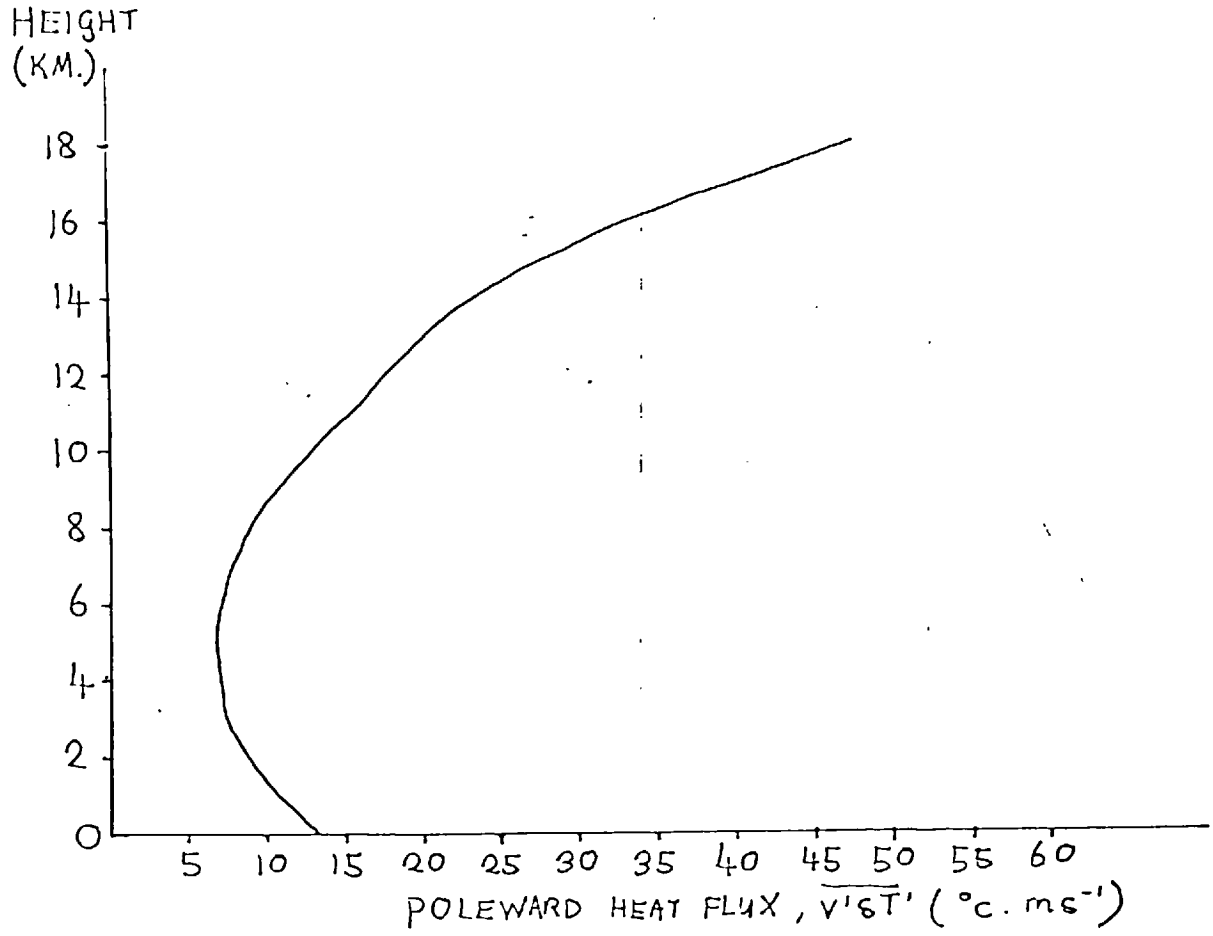

FIG. 3.8 POLEWARD EDDY HEAT TRANSPORT ($\overline{v'\theta'}$) ASSOCIATED WITH THE P_2' MODE IN FIG. 3.7. $\overline{v'\theta'} = 0$ FOR P_4' MODE.

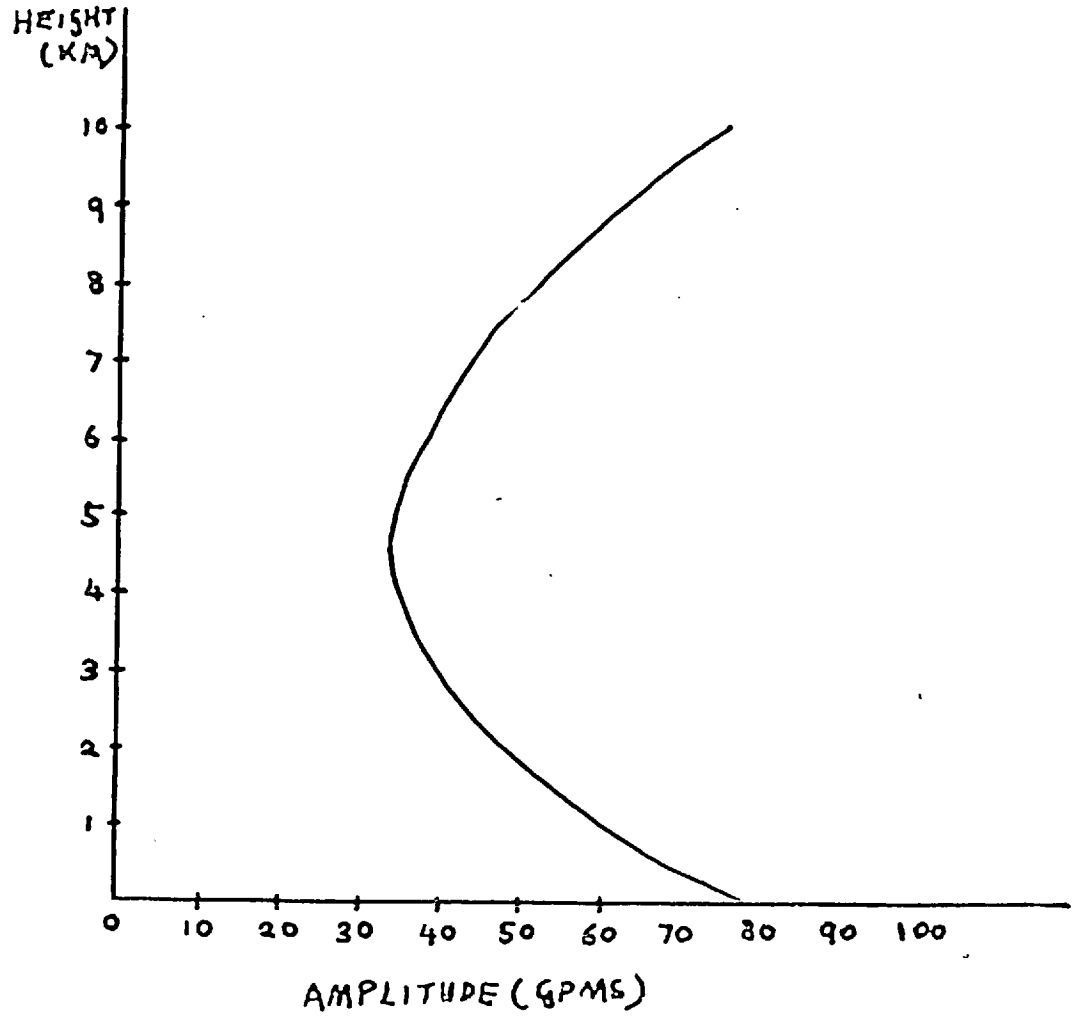

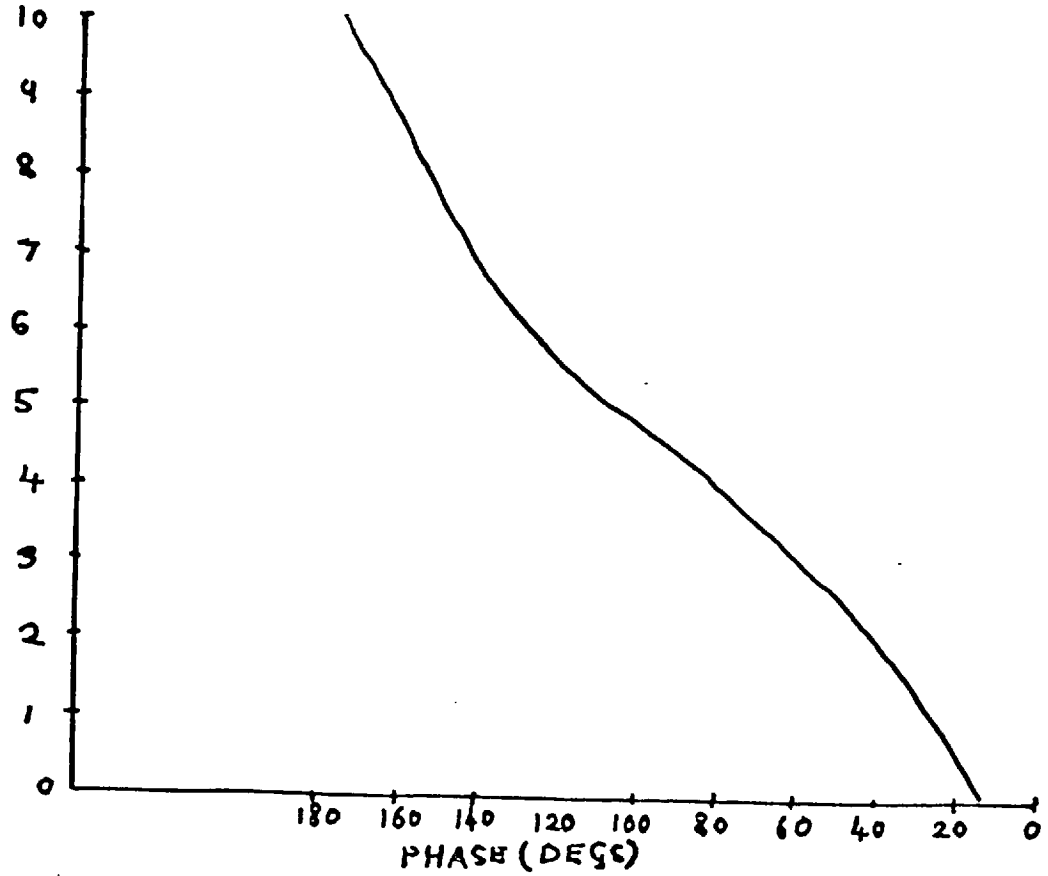

FIG. 3.9 STRUCTURE OF THE P_2^1 MODE FOR 'EXPONENTIAL THERMAL FORCING' IN CONSTANT ANGULAR SHEAR.

$S_0 \equiv \left(\frac{1.5°C/DAY}{260°K}\right) \exp\left(\frac{-z}{4KM.}\right)$, $\bar{u} = \begin{cases} 5\ ms^{-1} & AT\ z = 0 \\ 25\ ms^{-1} & z = 10\ KM. \end{cases}$

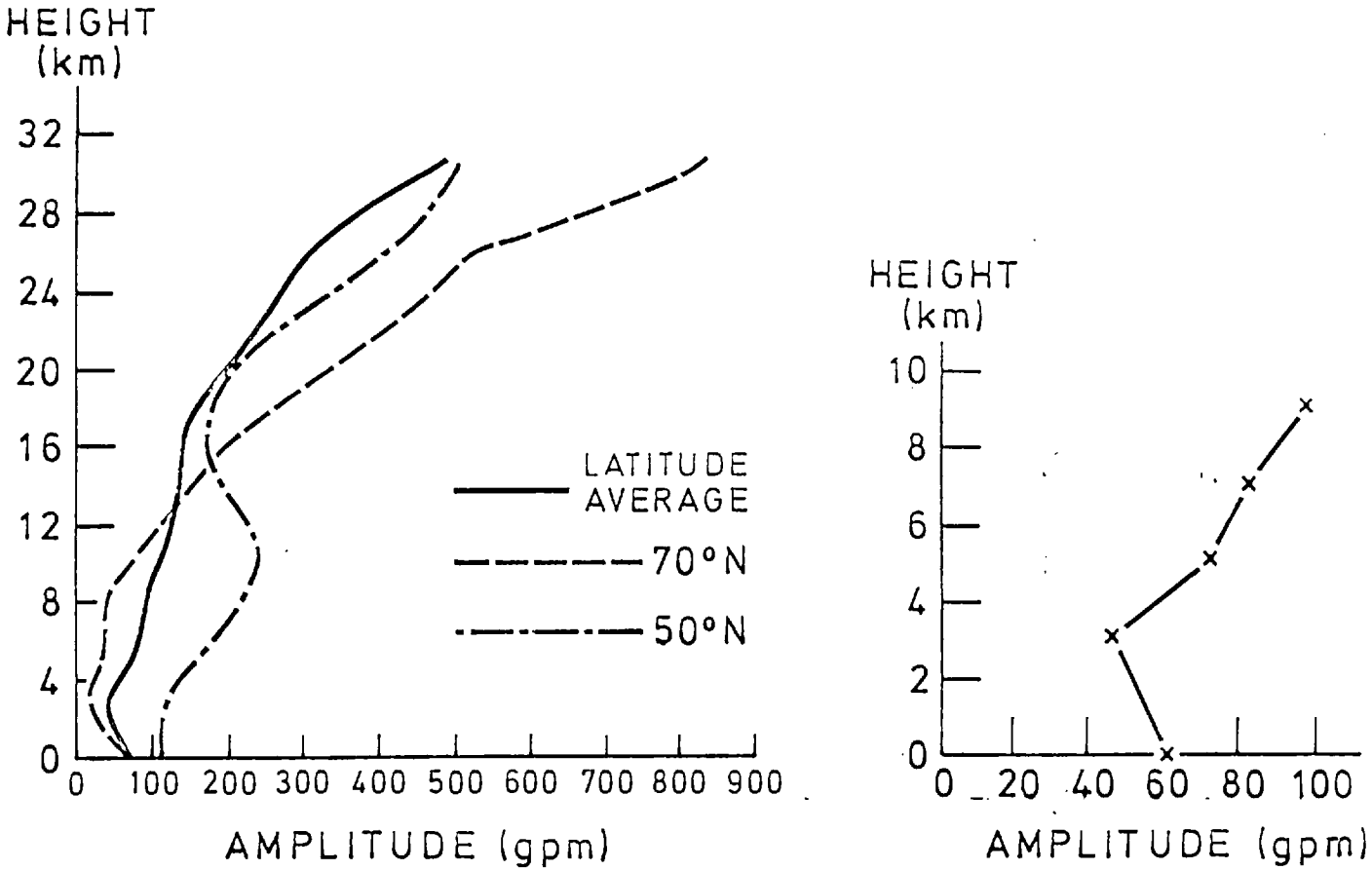

FIG. 3.10(a) LATITUDINALLY-AVERAGED AMPLITUDE OF WAVENUMBER 1 FOR JANUARY 1958 (TAKEN FROM THE DATA OF MUENCH) COMPARED TO THAT AT 70°N AND 50°N. (ON THE R.H.S. AN ENLARGEMENT OF THE LAT. AVERAGE CURVE BELOW 10 KM.)

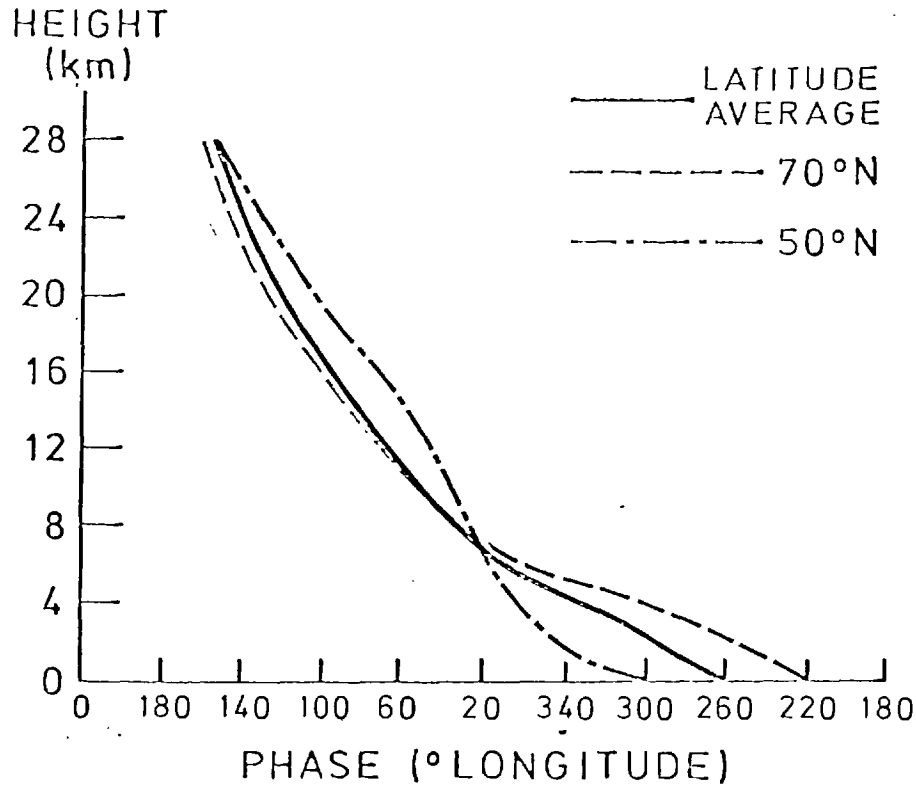

FIG. 3.10(b) PHASE VARIATION CORRESPONDING TO 3.10(a)

up to *10* mb for the wavenumbers *1* to *4* at *50*°N in January 1958. Dickinson (1972) published data (from Muench) giving the latitude/height distribution of wavenumber *1* for the same year up to *10* mb and we use this in the comparisons with the theory. The outstanding feature of the phase variation is the uniformity of westward tilt with height which is particularly large at low levels.

There is no evidence of trapping in the troposphere for wavenumbers *1* and *2* which would be reflected in the presence of vertical phase lines and nodes, as in the theoretical solutions. The vertical profile of phase is strongly latitude dependent and since the solutions have no θ dependence of phase it is appropriate to latitudinally-average the observed phase. Fig.3.10(b) gives the height variation of latitudinally-averaged phase compared with that at *70* and *50*°N (which represent extremes of phase variation) and shows that the phase tilt in the troposphere at *50*°N is much less rapid than the latitude-average. The corresponding distributions of amplitude are shown in Fig.3.10(a) and in agreement with the thermal forcing calculations - an amplitude minimum occurs near *4* km.

In Fig.3.11, the theoretical solution for 'exponential' thermal forcing in uniform shear is compared with the latitudinally-averaged curves of amplitude and phase, with the latter displaced by a constant value to give the best 'fit'*. The similarity in structure is quite surprising particularly in the phase agreement and there can now be no doubt that the imposition of an energy transmitting boundary condition at upper levels is desirable.

The behaviour of the wavenumber *1* structure north of *60*°N seems to resemble thermal forcing to a much greater extent than near *50*°N with a pronounced minimum in amplitude in mid-troposphere and rapid westward phase tilt there. It might be speculated that the orographic forcing of

* In the absence of exact knowledge of the distribution of forcing.

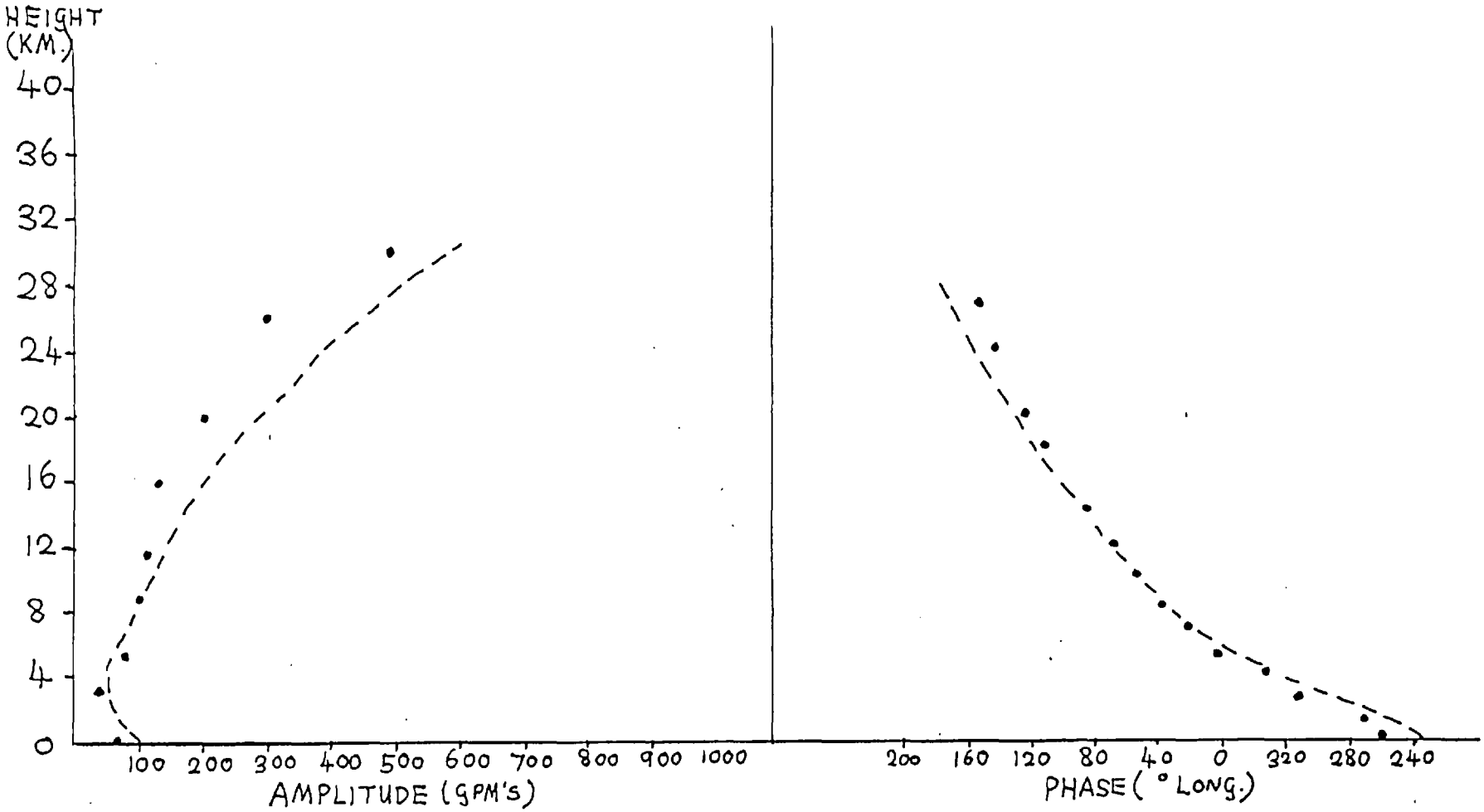

FIG. 3.11 COMPARISON OF THE STRUCTURE OF THE THERMALLY-FORCED P_2^1 MODE OF FIG. 3.7 (DASHED LINE) WITH LATITUDINALLY-AVERAGED DATA OF MUENCH. (DOTS)

wavenumber *1* dominates near *40°N* where the Himalayas exert a strong influence on the flow, and therefore the structure of wave motion is different for these latitudes. The *1000-500* mb phase difference given by the latitude-average curve is ~ *90°* which is in good agreement with the theoretical solutions given, though rather smaller than that shown in Fig.3.11.

It has already been seen that the poleward eddy heat flux associated with the above constant shear solution shows a strong low-level bias with surface correlation $\overline{v'\delta T'}$ of $\sim 12°C\ m\ s^{-1}$. Oort and Rasmussen (1971) have calculated from observation the stationary eddy heat fluxes for each month of the year and find a low-level maximum of $\overline{v'\delta T'}$ near *850* mb with typical amplitudes of *10-15*°C m s^{-1} in January. Other calculations, with realistic tropospheric shear and radiation condition at *10* km, show $\overline{v'\delta T'}$ to be $\sim 5°C\ m\ s^{-1}$ and generally comparable to observed fluxes indicating the importance of stationary planetary waves in the total wintertime poleward heat transport.

Since only the untrapped planetary waves transport heat it might be inferred that the P_2^1 and $P_3^2(\cos\theta)$ modes are the most important transporters of heat. We have failed, so far, to consider forcing by wavenumber *2* which, according to Clapp, should be just as large if not more so than the thermally-forced wavenumber *1*.

Briefly summarising this section, it has been found that the observed structure of the mean January wavenumber *1* disturbance has many of the features of an untrapped, thermally forced wave. Using a lower tropospheric heating function of magnitude consistent with calculated values given by Clapp, the resulting disturbance forced in uniform shear flow is closely comparable with observation up to *30* km where a radiation condition is applied above. Notable features of the thermally-forced waves are:

(1) An intense, shallow surface disturbance of depth ~ 3 km.

(2) An amplitude minimum near 4 km and associated rapid phase tilt westwards there.

(3) Strong low-level transport of heat.

The untrapped orographically forced waves $\left(P_2^1 \text{ and } P_3^2(\cos\theta)\right)$ are of much smaller surface amplitude and their contribution to the tropospheric poleward heat transport is small ($< 1°C\ m\ s^{-1}$). Both types of forcing appear to be important in the production of large amplitude stratospheric waves in winter.

CHAPTER 4 NUMERICAL SOLUTIONS: SOLUTION FOR VARIOUS VERTICAL PROFILES OF ZONAL WIND, STATIC STABILITY AND HEATING

The analytical solutions of the Q-G potential vorticity equation as given in Chapter 3 provide the simplest description of forced motion. The atmospheres considered so far are of isothermal basic state and uniform static stability $d\phi_0/dz$ with exponential distributions of mean state pressure and density, p_0 and ρ_0 respectively. The vertical variation of zonal wind is the most important property determining the propagation of Rossby wave energy and the constant shear solutions adequately describe this wintertime variation.

In this chapter we will further elaborate the wintertime description of forced motion by allowing a more realistic variation of zonal wind and static stability and more importantly will be able to describe the forcing in summer by numerical integration of equation (2.4). The selection of a 'realistic' profile of zonal wind is somewhat arbitrary since the angular rotation rate at any level must represent a mean latitude value and the effects of jet peaks will be excluded. Simmons (1974) found that the important modifications of allowing a horizontal jet structure were the enhanced ability to propagate wave energy vertically (through the increased meridional gradient of potential vorticity of the mean state) and the similarity in shape of contour height amplitude and zonal wind magnitude. On the hemispheric scale it is anticipated that planetary wave modes will be insensitive to the presence of jets which are essentially 'local' phenomena. One might imagine that with a realistic distribution of zonal wind on a sphere that has a mid-latitude peak and vanishes at the equator, the increased mean state potential vorticity gradient would raise the critical wind speed $\overline{u}_c$ and allow even freer transmission of energy into the stratosphere.

Some additional simplifying assumptions are made in describing the thermodynamic basic state when the static stability is allowed to vary. The basic state temperature of the atmosphere is assumed to be uniform except in the origin of the height variation of static stability B, so that the basic state fields of pressure and density decrease exponentially with height. Justification for this approximation is given as follows:

Using the perfect gas equation in the hydrostatic relation we have:

$$\frac{1}{\rho_0}\frac{d\rho_0}{dz} = -\left(\frac{g}{RT_0} + \frac{1}{T_0}\frac{dT_0}{dz}\right)$$

where $T_0(z)$ is the basic state temperature and R is the gas constant.

Comparing the terms in brackets reveals that $\left(\frac{1}{T_0}\frac{dT_0}{dz}\right)^{-1}$ is ~ 40 km in the troposphere and ~ 200 km in the stratosphere which is considerably greater than H_0 $(= RT_0/g) \sim 7$ km. Since T_0 varies by at most 15 % throughout the troposphere and stratosphere, the density stratification $\frac{1}{\rho_0}\frac{d\rho_0}{dz}$ is well approximated by $-\frac{g}{R\overline{T_0}}$, where $\overline{T_0}$ is a mean atmospheric temperature.

Now $B = \frac{1}{T_0}\left(\frac{g}{C_p} + \frac{dT_0}{dz}\right)$ and in the troposphere the two terms on the right-hand side of the equation are of comparable size so that no similar approximation is valid. It is therefore a useful simplification to assume exponential distributions of mean state pressure and density even when B varies.

The numerical integration procedure allows freedom in the choice of heating function profiles $S_0(z)$ as well as static stability B and angular rotation rate $(\overline{\psi}/R^2)$, and later in this chapter, the results of experimentation with various low-level profiles of heating are given. Little is known of the actual vertical distribution of heating in the atmosphere so that the calculations of wave structure for various profiles of $S_0(z)$ will serve as a useful guide when making comparison with observations.

Numerical integration is most useful for the evaluation of forced,

stationary motion in summer when the complicated zonal wind variation in the vertical rules out simple analytic solution. This advantage is offset to some extent by the existence of a singular point at the height where $\bar{\psi} = 0$, corresponding to the 'critical-level' for stationary waves (see Eq. (2.4)). Numerical methods fail in the neighbourhood of this point so that an analytic solution must be sought there and connected to the numerical solution.

Only thermally forced motion is considered for the summertime situation since the orographically forced component is very small and provides little further information. The introduction of Ekman friction into the summer description of thermal forcing is found to give some extra realism to the structure of the wave motion.

The details of the method of numerical integration are given next and is taken from a short article by Lindzen and Kuo (1969).

(i) Method of integration (~~Cauccian elimination~~)

All second-order linear differential equations with variable coefficients of the form:

$$\frac{d^2f}{dz^2} + g(z)\frac{df}{dz} + h(z)f(z) = r(z) \qquad \text{——(4.1)}$$

with linear first-order boundary conditions of the form:

$$\left.\begin{aligned} \frac{df}{dz} + a_1 f &= b_1 \qquad \text{at } z = z_1 \\ \frac{df}{dz} + a_2 f &= b_2 \qquad \text{at } z = z_2 \end{aligned}\right\} \qquad \text{——(4.2)}$$

are integrable by this method, provided that $g(z)$, $h(z)$ and $r(z)$ do not contain singularities in the range of integration, and only if the corresponding homogeneous problem has no non-trivial solution.

Comparison of equation (4.1) with the Q-G potential vorticity equation for the height structure (2.4) yields:

$$f(z) = F(z)$$

$$g(z) = \frac{B}{\rho_0}\frac{d}{dz}\left(\frac{\rho_0}{B}\right)$$

$$h(z) = \frac{gB}{f_0^2}\left\{\frac{2\Omega}{\bar{\psi}(z)} - \frac{f_0^2}{\rho_0 g}\frac{1}{\bar{\psi}}\frac{d}{dz}\left(\frac{\rho_0}{B}\frac{d\bar{\psi}}{dz}\right) - \frac{(n-1)(n+2)}{R^2}\right\}$$

and $$r(z) = -\frac{gB}{f_0 m}\frac{R^2}{\bar{\psi}}\frac{1}{\rho_0}\frac{d}{dz}\left(\frac{\rho_0 S_0}{B}\right)$$

Dividing the integration range into N segments of length δz, we may write $z_i = i\delta z$ with $0 \leqslant i \leqslant N$.

We adopt the convention that $f(z_i) = f_i$, $g(z_i) = g_i$ etc. and express the first and second derivative in finite difference form as:

$$\frac{df}{dz}(z_n) = (f_{n+1} - f_{n-1})/2\delta z$$

and $$\frac{d^2 f}{dz^2}(z_n) = (f_{n+1} + f_{n-1} - 2f_n)/\delta z^2$$

Substituting these expressions into equation (4.1) gives:

$$\frac{f_{n+1} + f_{n-1} - 2f_n}{\delta z^2} + \frac{g_n}{2\delta z}(f_{n+1} - f_{n-1}) + h_n f_n = r_n$$

and on collecting terms:

$$f_{n+1}\left(\frac{1}{\delta z^2} + \frac{g_n}{2\delta z}\right) + f_n\left(h_n - \frac{2}{\delta z^2}\right) + f_{n-1}\left(\frac{1}{\delta z^2} - \frac{g_n}{2\delta z}\right) = r_n$$

or $$A_n f_{n-1} + B_n f_n + C_n f_{n+1} = D_n \qquad \text{——(4.3)}$$

with $$A_n = \frac{1}{\delta z^2} - \frac{g_n}{2\delta z}, \quad B_n = h_n - \frac{2}{\delta z^2}, \quad C_n = \frac{1}{\delta z^2} + \frac{g_n}{2\delta z}$$

and $$D_n = r_n .$$

Equation (4.3) can be used at all interior points $1 \leqslant n \leqslant N-1$ since at the boundaries fictitious points are involved.

The boundary conditions, equations (4.2), are given by:

$$\frac{f_1 - f_{-1}}{2\delta z} + a_1 f_0 = b_1 \qquad \text{at} \quad z = 0 \qquad \text{——(4.4)}$$

and

$$\frac{f_{N+1} - f_{N-1}}{2\delta z} + a_2 f_N = b_2 \qquad \text{at} \quad z = iN \qquad \text{——(4.5)}$$

and involve the fictitious values f_{-1} and f_{N+1}.

Using (4.3), we may express the fictitious values in terms of two real point values and substitute these expressions into (4.4) and (4.5).

From (4.3) we have:

$$A_0 f_{-1} + B_0 f_0 + C_0 f_1 = D_0$$

and substituting in (4.4) for f_{-1} gives:

$$f_1\left(1 + \frac{C_0}{A_0}\right) + f_0\left(\frac{B_0}{A_0} + 2\delta z a_1\right) = \frac{D_0}{A_0} + 2\delta z b_1 \qquad \text{——(4.6)}$$

Similarly, eliminating f_{N+1} from (4.5) gives:

$$f_{N-1}\left(1 + \frac{A_n}{C_N}\right) - f_N\left(2\delta z a_2 - \frac{B_N}{C_N}\right) = \frac{D_N}{C_n} - 2\delta z b_2 \qquad \text{——(4.7)}$$

The upper and lower boundary conditions may now be written as:

$$A_b f_0 + B_b f_1 = D_b \qquad \text{(lower boundary condition)}$$

and

$$A_t f_{N-1} + B_1 f_N = D_t \qquad \text{(upper boundary condition)}$$

with

$$A_b = \frac{B_0}{A_0} + 2\delta z a_1 , \qquad B_b = 1 + \frac{C_0}{A_0}$$

$$B_t = \frac{B_N}{C_N} - 2\delta z a_2 \text{ and } D_t = \frac{D_N}{C_N} - 2\delta z b_2$$

from (4.6) and (4.7).

The Gaussian elimination method works by expressing the function f_n at z_n in terms of the adjacent point value so that:

$$f_n = \alpha_n f_{n+1} + \beta_n \qquad \text{——(4.8)}$$

or $$f_{n-1} = \alpha_{n-1} f_n + \beta_{n-1} \quad (\alpha_n \text{ and } \beta_n \text{ are sets of constants})$$

The above equation for f_{n-1} is substituted into equation (4.3) giving an expression for f_n in terms of f_{n+1} and:

$$f_n = \left\{ - \frac{C_n}{A_n \alpha_{n-1} + B_n} \right\} f_{n+1} + \frac{D_n - A_n \beta_{n-1}}{A_n \alpha_{n-1} + B_n}$$

which on comparison with (4.8) yields:

$$\alpha_n = \frac{- C_n}{A_n \alpha_{n-1} + B_n} \quad \text{and} \quad \beta_n = \frac{D_n - A_n \beta_{n-1}}{A_n \alpha_{n-1} + B_n} \qquad \text{——(4.9)}$$

Equations (4.9) are recurssion relations for the α_ns and β_ns with the values A_n, B_n, C_n and D_n determined by the variable coefficients of the differential equation. Once the values of α_0 and β_0 are known, the rest of the values of α and β may be generated. α_0 and β_0 can be determined from the lower boundary condition using equation (4.8) and are found to be:

$$\alpha_0 = - \frac{B_b}{A_b} \quad \text{and} \quad \beta_0 = \frac{D_b}{A_b} .$$

Knowledge of f_N will permit the calculation of all the values of f_n and this may be obtained from the upper boundary condition as follows.

Re-arranging the upper boundary condition gives:

$$f_{N-1} = \frac{D_t}{A_t} - \frac{B_t}{A_t} f_N$$

and eliminating f_{N-1} with equation (4.8) gives an expression for f_N in terms of known quantities:

$$f_N = \frac{D_t - A_t \beta_{N-1}}{\alpha_{N-1} A_t + B_t}$$

and hence equation (4.8) is again used to generate the remaining values of f. All parameters may assume complex values.

In the following calculations it was found that $N = 1000$ was sufficient to assure rapid and accurate integration over the height range 0 to 40 km. Doubling the number of points caused a change in the numerical value of $F(z)$ of less than 0.1% and comparison with the analytic solutions shows this to be the order of magnitude of the error.

The variable coefficients of the differential equation should be continuous for the method to succeed, and for the height structure equation (2.4) this implies the continuity of static stability B, entropy source S and shear through $d\bar{\psi}/dz$.

(ii) Thermal forcing (Winter)

'Realistic' variation of the mean angular rotation rate of the atmosphere is inferred from the zonal wind distribution given by Newell (1969) (Fig.1.1) and the equivalent mid-latitude zonal wind is shown in Fig.4.1. This profile is not very different from the constant shear profile of zonal wind though has some suggestion of an upper tropospheric maximum. In view of the sensitivity of the transmissive properties of the atmosphere to zonal wind variation, a study of the structure of the thermally-forced $P_2^1(\cos\theta)$ mode is made for various sizes of tropopause wind maxima (Fig.4.3). It must be remembered that the tropopause maximum represents a latitude-average and is much smaller than the January mean sub-tropical jet maximum (~ 35 m s^{-1}).

A realistic vertical profile of static stability B was obtained from the Charney/Drazin paper based on average mid-latitude data (from the U.S. National Bureau of Standards) (shown in Fig.4.2).

(a) Structure of $P_2^1(\cos\theta)$ for different vertical profiles of angular rotation of the atmosphere

Profiles of zonal wind A, B and C in Fig.4.3 represent different

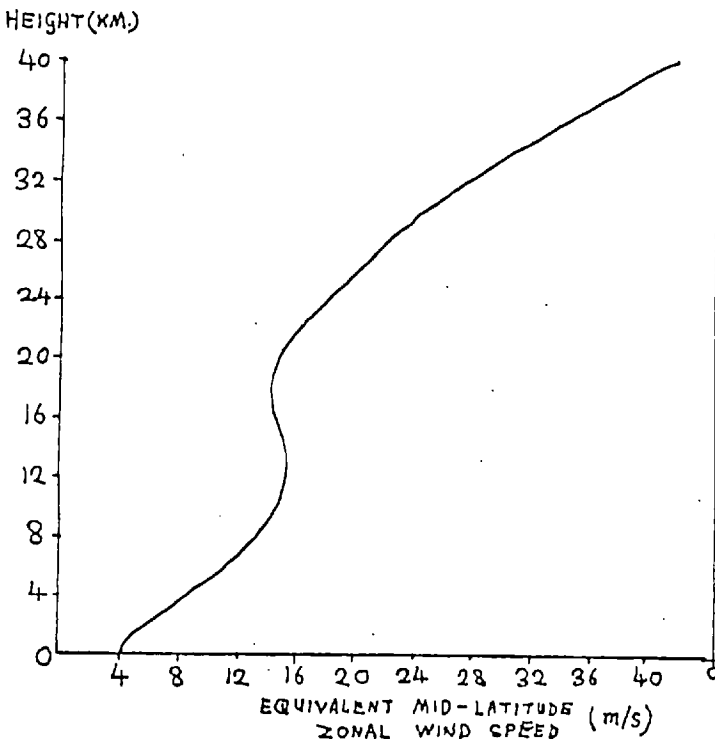

FIG. 4.1 'REALISTIC' ZONAL WIND FIELD FOR JANUARY.

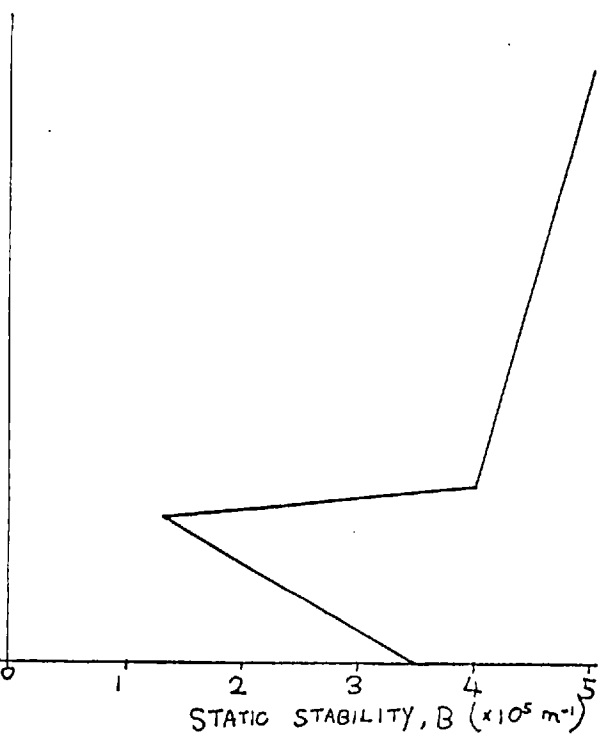

FIG. 4.2 'REALISTIC' STATIC STABILITY VARIATION. (U.S. NATIONAL BUREAU OF STANDARDS)

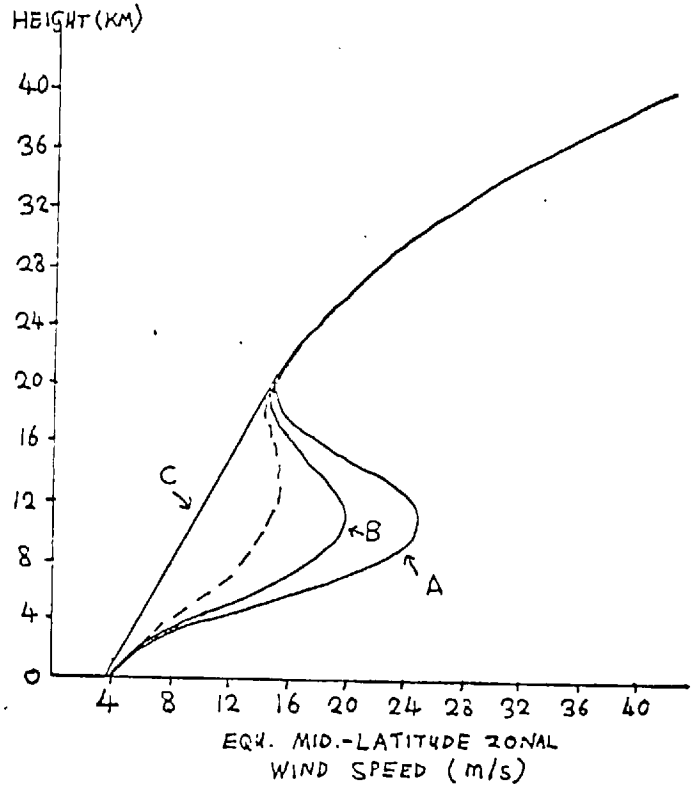

FIG. 4.3 VARIOUS ZONAL WIND PROFILES.

magnitude tropopause peaks of mean westerly wind with the 'realistic' profile given by the dashed curve. The response of these different mean state atmospheres, with static stability profile as given in Fig.4.2, is found for 'exponential thermal forcing' with $S = a \exp(-bz) P_2^1(\cos\theta)\sin\phi$ and $a \equiv 1.5°C/day$, $b^{-1} = 4$ km. As before, an energy-transmitting boundary condition is applied at 40 km.

The corresponding curves of contour height, amplitude and phase are plotted in Fig.4.4 and show some considerable variation in stratospheric wave amplitude. The stronger tropopause wind speed in curve *A* causes more wave energy reflection and a more pronounced minimum of contour height amplitude near 4 km. Westward phase tilt is more rapid in the mid-troposphere for this case and becomes more like the nodal structure of the trapped wave.

These curves for various zonal wind profiles give some idea of the maximum 'error' one might expect through the incorrect choice of wind field that approximates to the real winter distribution of $\bar{u}$. The structure of the contour height field is much more sensitive to changes in the upper boundary condition type than the profile of zonal wind and a reflecting boundary condition would have completely altered the phase variation with height.

Furthermore, the approximate nature of the upper boundary condition in simulating wave energy absorption does not warrant the refinement of the profiles of zonal wind and static stability. In view of this, the zonal wind profile of Fig.4.1 will be considered to be the most satisfactory approximation to the January mean distribution and the structure of forced waves will now be determined for different zonal wavenumbers.

(b) Comparison of low-wavenumber, thermally forced waves ($m = 1$, 2 and 3)

The contour height and temperature fields forced by a heating function

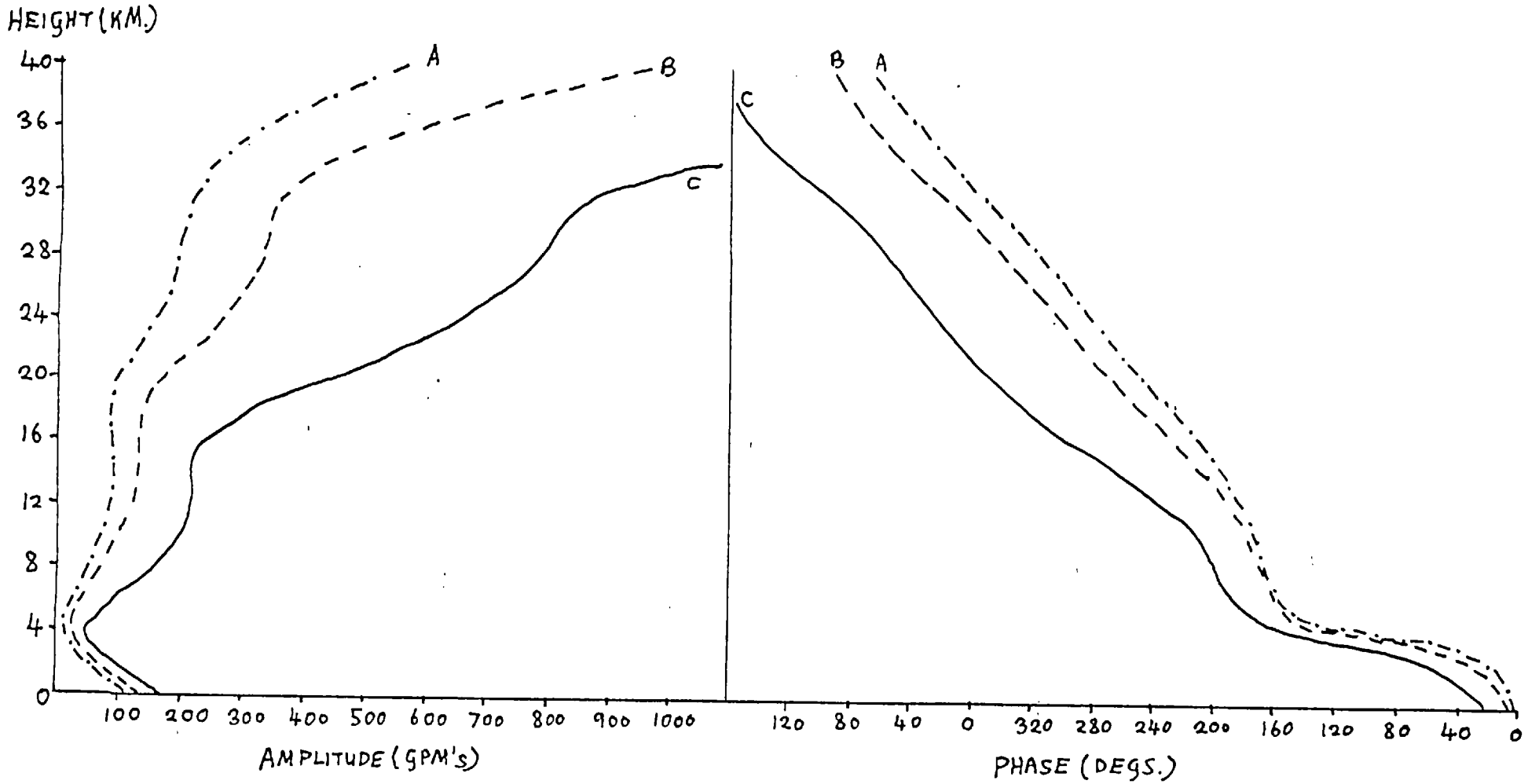

Fig. 4.4 STRUCTURE OF THE P_2^1 MODE CORROSPONDING TO THE DIFFERENT MEAN ZONAL WIND PROFILES OF FIG. 4.3.

$\left(S_o = \left(\frac{1.5°C/DAY}{260°K}\right) \exp\left(\frac{-z}{4\,KM.}\right)\right.$ AND 'REALISTIC' STATIC STABILITY$\left.\right)$

$S = a \sin m\phi \; P^m_{m+1}(\cos\theta)\exp(-z/4\,\text{km})$ is examined for zonal wavenumbers $m = 1$, 2 and 3 with 'realistic' vertical distributions of zonal wind and static stability. Again, a heating function amplitude is chosen so that $a = 1.5°\text{C/day}/260°\text{K}$. Fig.4.5(a) gives the amplitude and phase of the contour height fields and shows that wavenumbers 1 and 2 are untrapped with the characteristic westward slope with height which contrasts with the nodal structure of wavenumber 3.

As in the analytic solutions of the previous chapter, the amplitudes of contour height perturbations are roughly inversely proportional to zonal wavenumber m. Surface amplitudes of 15, 9 and 4 mb are found for $m = 1$, 2 and 3 respectively and are of the correct magnitude to account for the Siberian anticyclone. The maximum of surface perturbation (Siberian High) is about 70° downstream of the region of maximum cooling and is nearly 30° to the west of the surface temperature minimum (Fig.4.5(b)) — similar to the solid rotation atmosphere solutions. It should be noted that for the solid rotation atmosphere solutions, the heating function amplitude a was equivalent to a heating rate of 3°C/day, double the value used here to give a similar surface amplitude wave. This is due almost entirely to the reduced zonal wind speed in the heating region for the realistic zonal wind case. According to the Fourier analyses of Clapp's heating rate calculations, 3°C/day is an overestimate (by a factor of 3) and the values used in the present calculations are more in line with those of his work.

Pronounced minima in contour height amplitude occur near 4 km coinciding with the region of most rapid phase tilt westwards. The trapped wavenumber 3 mode has zero amplitude, associated with nodes at 4 and 17 km. The amplitudes of all three increase steadily with height up to 35 km above which the increase is very rapid and their amplitudes become unrealistically large.

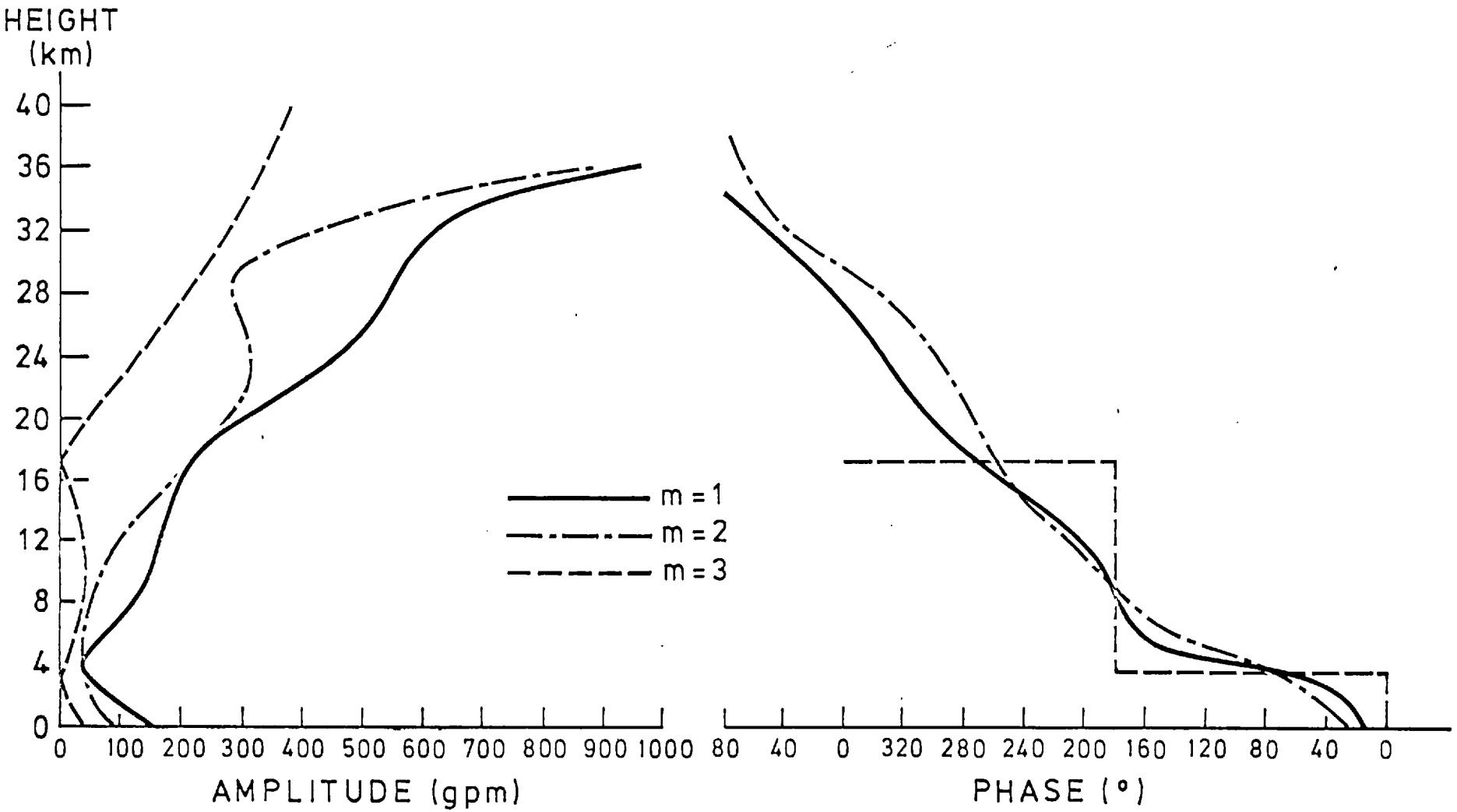

FIG. 4.5(a) CONTOUR HEIGHT FIELD STRUCTURES FOR THE P_2^1, P_3^2 AND P_4^3 MODES IN 'REALISTIC' FLOW. $S_0 = \left(\frac{1.5°C/DAY}{260°K}\right) \exp\left(-\frac{z}{4\,KM.}\right)$

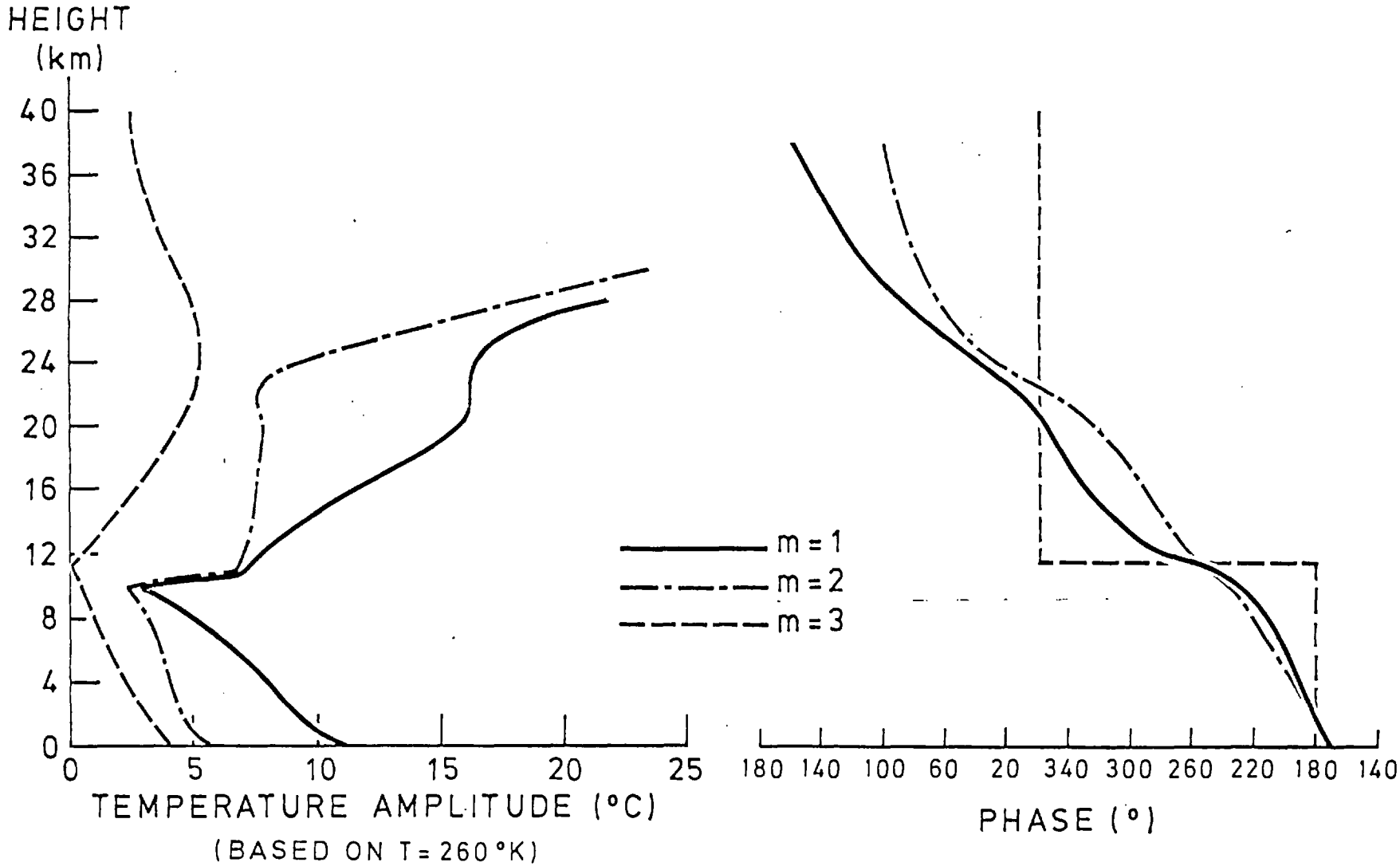

FIG. 4·5(b) STRUCTURE OF THE TEMPERATURE FIELD ASSOCIATED WITH (a).

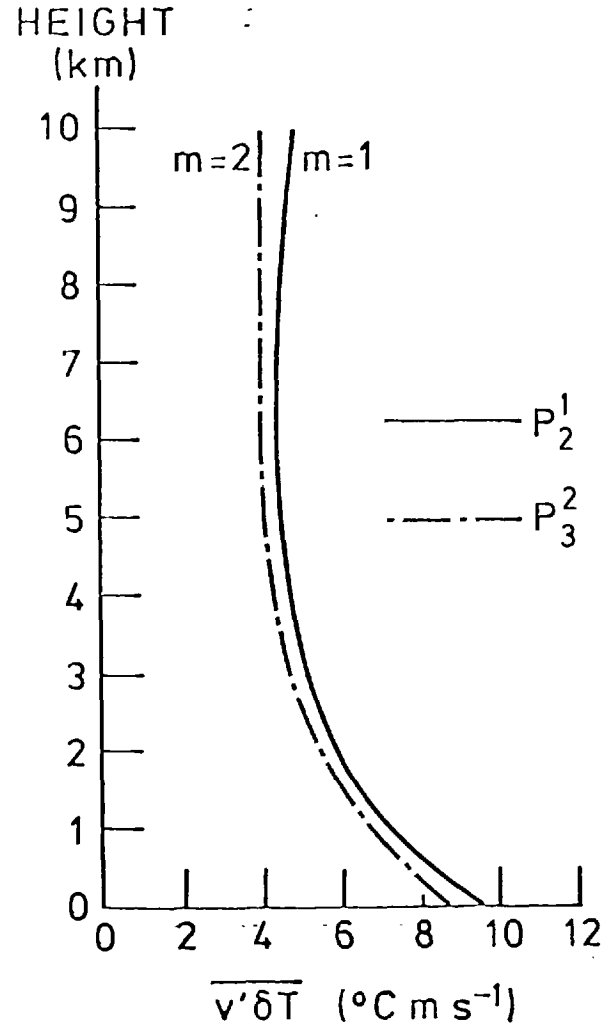

FIG. 4.5(c) $\overline{V'\delta T'}$ ASSOCIATED WITH (a) IN THE TROPOSPHERE.

In Fig.4.6, the wavenumber *1* solution is compared with constant shear solution found in Chapter 3 and the latitudinally-averaged data of Muench for January 1958. Agreement between the calculated wave structure and the observations is striking, particularly in the phase and the constant shear calculation appears to be better than realistic profile case. It must be borne in mind that only the $n = 2$ harmonic mode of wavenumber *1* has to be considered and all the other even n modes will contribute to the structure of wavenumber *1*. In view of this and the neglect of the orographically forced component of wavenumber *1* the good agreement is somewhat surprising.

The phase tilt of wavenumbers *1* and *2* is very similar and of magnitude typically about *9*°/km yet in terms of degrees of longitude, the wavenumber *2* tilt will be half of this. The observed phase variation of wavenumber *1* and *2* in Fig.1.2 shows that the slope of the wavenumber *1* curve is roughly twice as rapid as that of wavenumber *2*.

Another useful rule of thumb to remember from the calculated phase structure is that the phase at *10* km is *180*° different from that at the surface, which compares with *160*° from the Muench data of wavenumber *1*.

The amplitudes of the temperature fields are shown in Fig.4.5(b) and all reveal large surface perturbations in conjunction with the maximum heating rate and steadily decrease with height up to *10* km. The amplitudes increase suddenly at the model tropopause in association with the increase in static stability and become very large above *25* km for the propagating modes. As with the contour height amplitude, this rapid amplification in the stratosphere is due mainly to the inertial effect of density. Wavenumber *3* achieves a maximum in temperature amplitude of about *5*°C at *25* km and decreases above. Phase tilt of the temperature perturbations is much less rapid than that of the contour height field particularly in

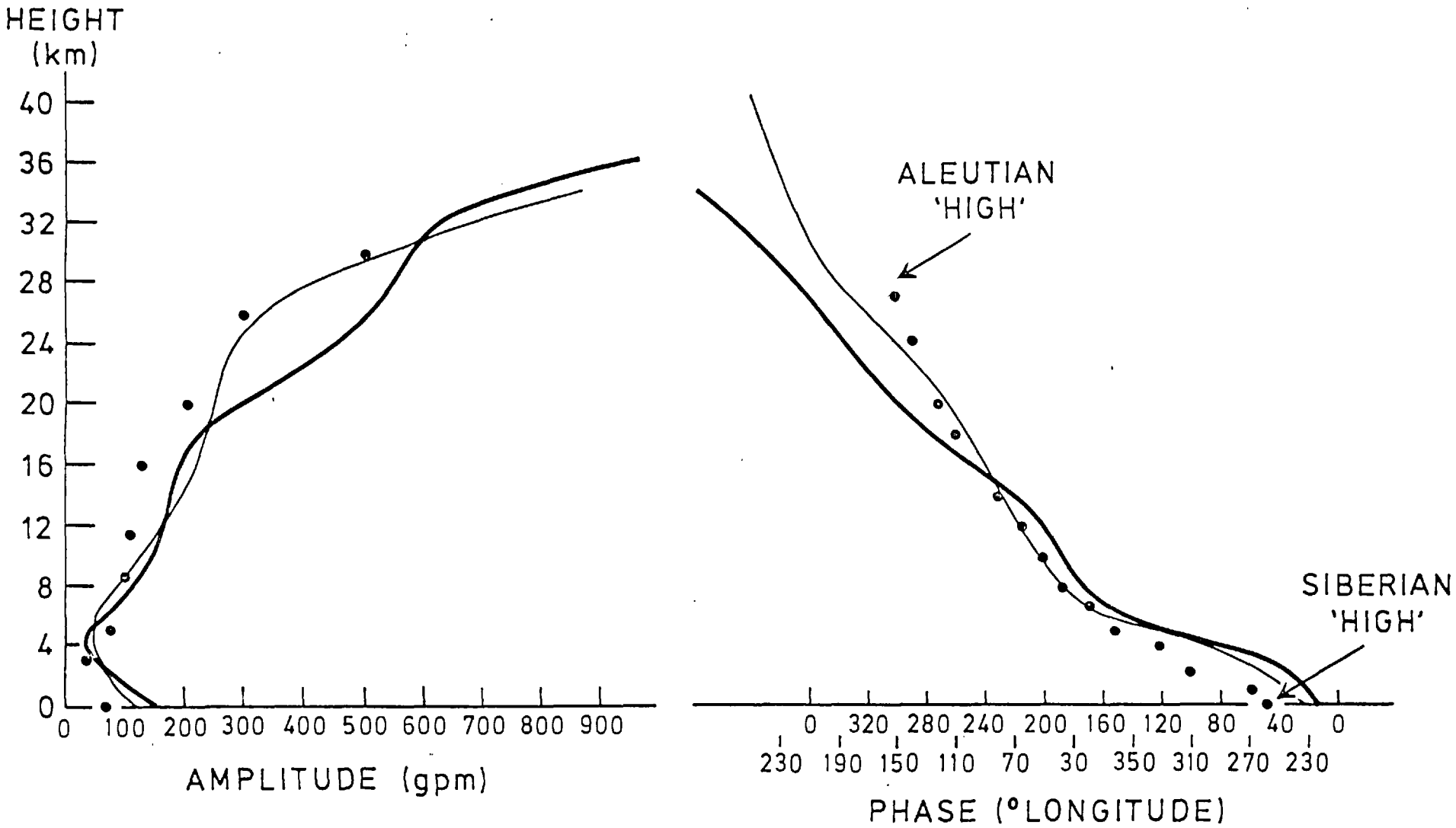

FIG. 4.6 COMPARISON OF THE CALCULATED P_2' MODE (IN REALISTIC PROFILE OF ZONAL WIND AND STATIC STABILITY) WITH THE CONSTANT ANGULAR SHEAR SOLUTION AND LAT. AVERAGE OF MUENCH DATA. BOLD LINE (P_2' IN REALISTIC FLOW), THIN LINE (P_2' IN CONST. SHEAR), MUENCH DATA — SPOTS.

the troposphere where the difference in phase between *0* and *10* km is *60°* compared to *160°* for the height perturbations. Relating this behaviour to the structure of the Siberian anticyclone, we may conclude that although the anticyclone is a shallow feature, its associated temperature anomaly is deep.

Green has shown (unpublished lecture notes) in an analysis of the pressure and temperature deviations over Siberia (compared with the zonal mean) that this is indeed the case.

The negative temperature anomaly was found to vanish (and change sign) near *11* km whereas the positive pressure anomaly vanishes at about *5* km. A quarter of a wavelength phase shift in the temperature field between the surface and *11* km might be inferred from this observation and Fig.4.5(b) shows that this fits in well with the theoretical calculations. Unfortunately, there is no data available at present of the Fourier analyses of the temperature field at selected heights in the troposphere.

A spectral decomposition of the mean January temperature field in the troposphere would help considerably to disentangle the contributions of orographic and thermal forcing to the total stationary wave patterns. Temperature amplitudes in the troposphere associated with orographic forcing are calculated to be ~ a few degrees centigrade and much smaller than those of the thermally-forced waves.

(c) High zonal wavenumber, thermally forced motion (P_5^4, P_6^5 and $P_7^6(\cos\theta)$)

Fig.4.7 gives the amplitude response to forcing at wavenumbers *4*, *5* and *6* with a heating function which peaks at *2.5* km with a heating rate of *2°C/day*. It is evident that even though the forcing function is probably an overestimate the magnitude of the pressure perturbation forced is small and at most gives a surface wave of *4* mb. This is in line with inverse

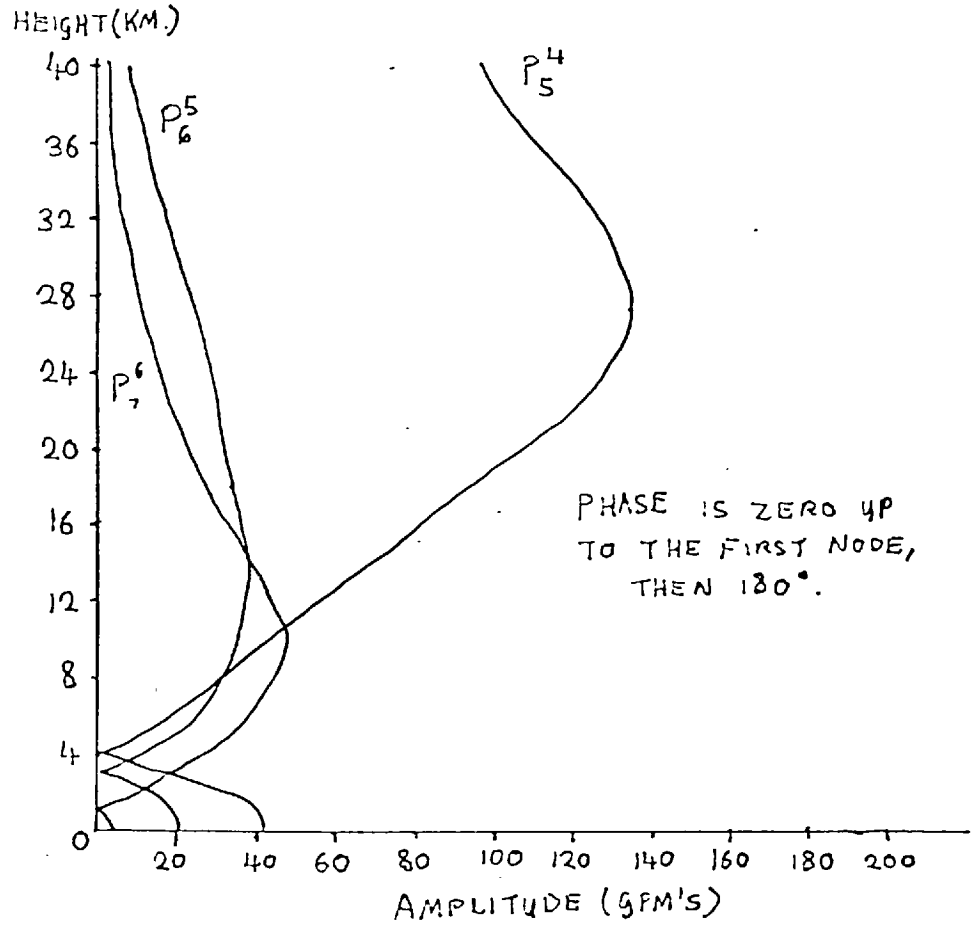

$$S_o = a \sin\left(\frac{\pi z}{5\ \text{KM.}}\right) \qquad a \equiv 2^\circ\text{C/DAY.}$$

$$= 0 \quad \text{IF } z > 5\ \text{KM.}$$

FIG. 4.7 STRUCTURE OF THE THERMALLY-FORCED P_5^4, P_6^5 AND P_7^6 FOR 'REALISTIC WINTERTIME PARAMETERS.

relationship between forcing magnitude and zonal wavenumber as previously discussed. The resulting wave motion quickly becomes evanescent with only one node at *4* km in contrast to the two nodes of wavenumber *3*. Not only is the response much smaller than for wavenumbers *1*, *2* and *3* but the higher n parameters lead to stronger trapping of wave energy and virtual confinement of the disturbances to the troposphere. Zero poleward eddy heat transport is indicated by the presence of vertical phase lines and we conclude that high zonal wavenumber thermally forced waves ($m > 3$) do not play an important part in the large-scale dynamics as anticipated for the low wavenumber waves.

(d) Comparison of the responses to various heating profiles $S_0(z)$

Deviations of the net, time-mean heating rate in the atmosphere from its zonal average are only roughly known and even less is known about its variation in the vertical. The only aspect of the distribution of heating associated with the underlying topography that one can be reasonably sure about is that the bulk of the non-adiabatic effects occur in the lower troposphere below *5* km. If latent heat release contributes strongly to the total longitudinal variation of heating (reflecting the time-mean longitudinal variation of precipitation), one might expect the amplitude of heating to attain a maximum near the condensation level at about *2* km.

The Fourier analysis of longitude distribution of heating calculated by Clapp (1961) revealed average heating rates throughout the *0* to *5* km layer of around *1*°C/day for the low zonal wavenumber components. We chose sinusoidally peaking heating functions $S_0(z)$ such that the vertical average is of this order of magnitude with:

(i)
$$\begin{cases} S_0(z) = \left(\dfrac{2^\circ\text{C/day}}{260^\circ\text{K}}\right)\sin\left(\dfrac{\pi z}{5\,\text{km}}\right) & \text{for } z < 5 \text{ km} \\ S_0(z) = 0 & \text{elsewhere} \end{cases}$$

and

(ii)
$$\begin{cases} S_0(z) = \left(\dfrac{1^\circ\text{C/day}}{260^\circ\text{K}}\right)\sin\left(\dfrac{\pi z}{8\,\text{km}}\right) & \text{for } z < 8 \text{ km} \\ S_0(z) = 0 & \text{elsewhere.} \end{cases}$$

The amplitude and phase of the contour height and temperature fields resulting from the thermal forcing of the P_2^1 and $P_3^2(\cos\theta)$ modes with these heating functions are given in Figs. 4.8 and 4.9, together with the 'exponential' forcing.

Their similarity in height field response is surprising with virtually identical phase structure and all showing minima in their respective amplitude curves near 4 km with only the surface amplitude showing appreciable variation. The apparent indifference of the qualitative amplitude structure to radical alteration of heating function shape probably reflects the dominance of vorticity generation by compression against the rigid lower surface (see the beginning of Chapter 3).

This result is quite gratifying since it provides stronger grounds on which to justify making comparisons with observation in the lower troposphere and knowledge of the vertically integrated heating rate, which is more readily assessed, provides the most important information.

The structure of the temperature field of the P_3^2 mode and the associated poleward transports of heat are given in Figs. 4.9(b) and 4.9(c) for the same profiles of $S_0(z)$ and in marked contrast to the contour height fields show strong differences between each other. The amplitude of the temperature field and poleward heat transport have similar shapes to that of the S_0 profile in the lower troposphere and increase rapidly across the tropopause in response to the sudden increase in static stability. This is in agreement with the relation derived in Chapter 3 which shows that the poleward eddy heat transport should be proportional to the vertical gradient of potential temperature in adiabatic flow for untrapped stationary waves.

The magnitude of stationary wave heat transport calculated, if

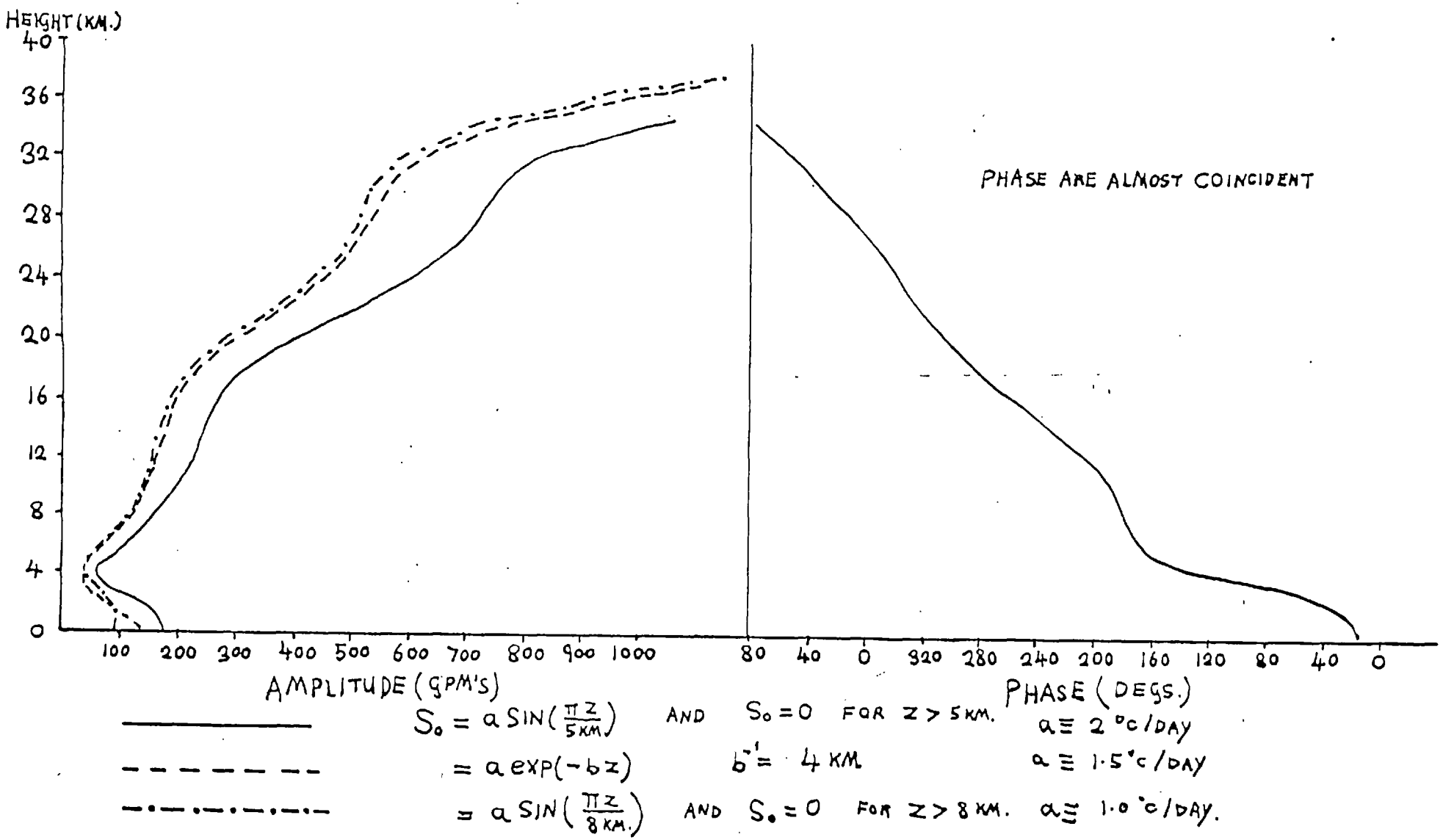

FIG. 4.8 STRUCTURE OF THE P_2^1 CONTOUR HEIGHT FIELD RESULTING FROM DIFFERENT VERTICAL PROFILES OF $S_0(z)$. ('REALISTIC' ZONAL WIND FIELD AND STATIC STABILITY)

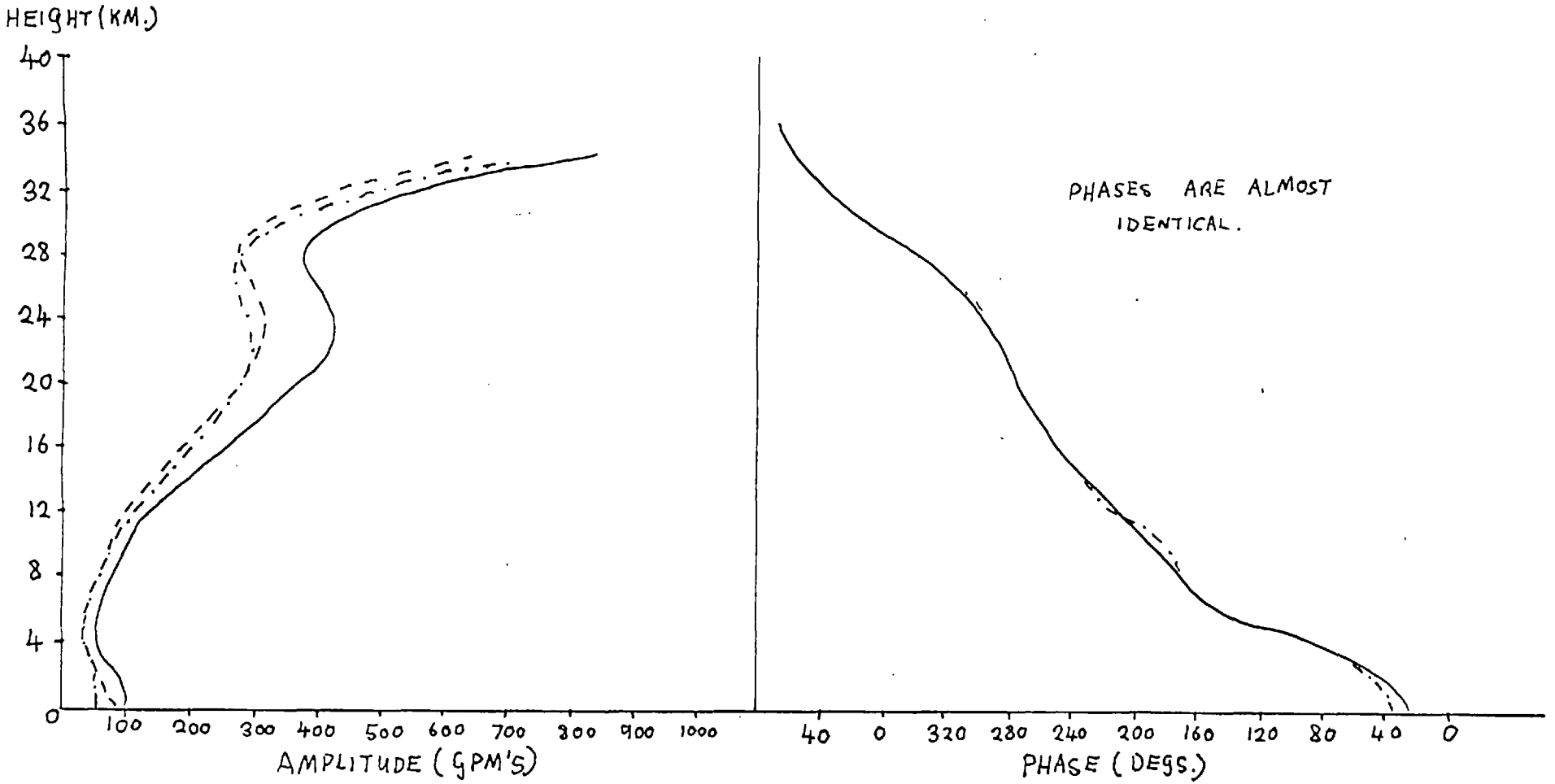

Fig. 4.9(a) STRUCTURE OF THE P_3^2 MODE CONTOUR HEIGHT FIELD RESULTING FROM DIFFERENT VERTICAL PROFILES OF $S_0(z)$. (SHOWN IN FIG. 4.9(c))

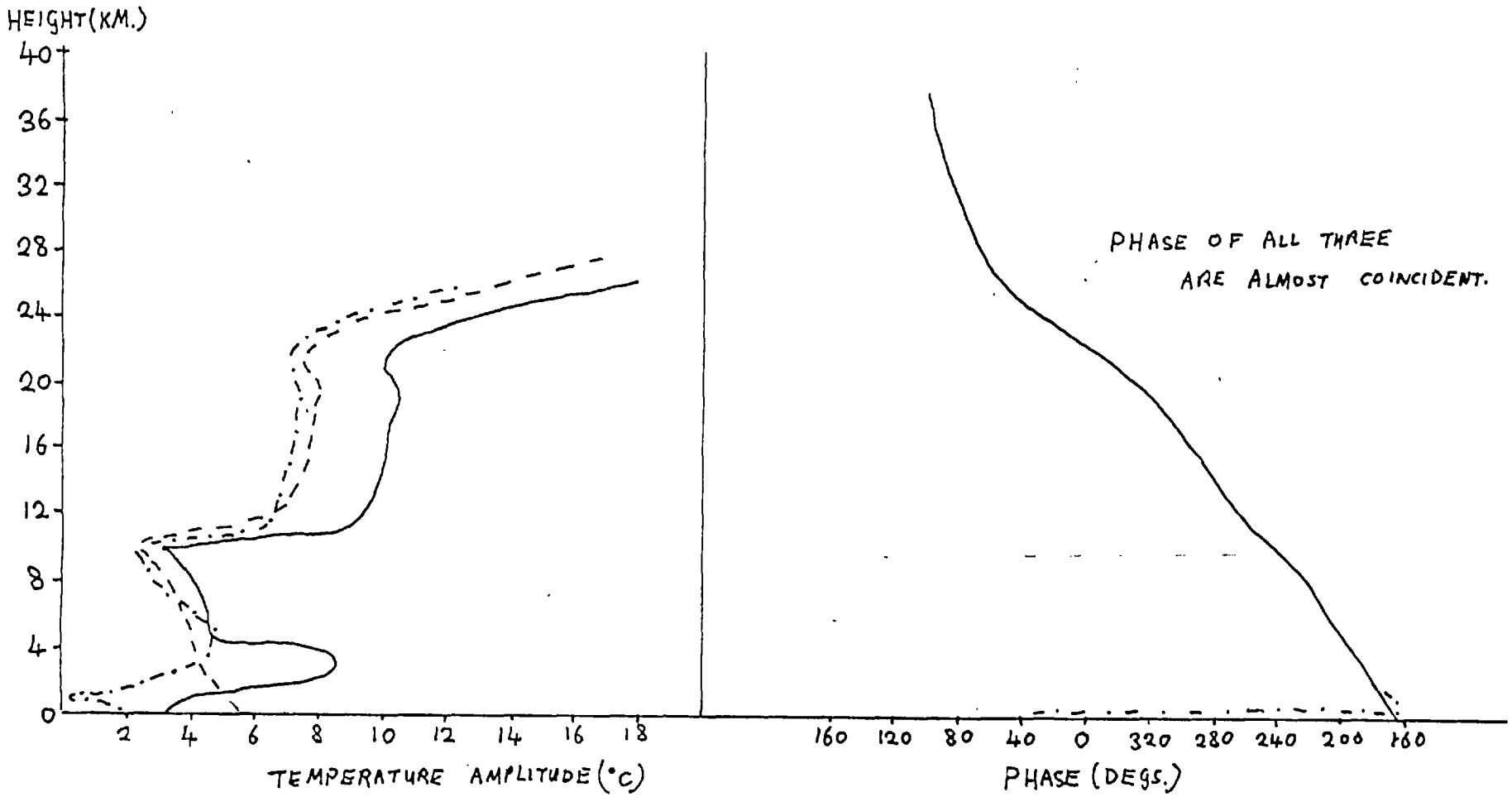

Fig. 4.9 (b) TEMPERATURE FIELD ASSOCIATED WITH (a).

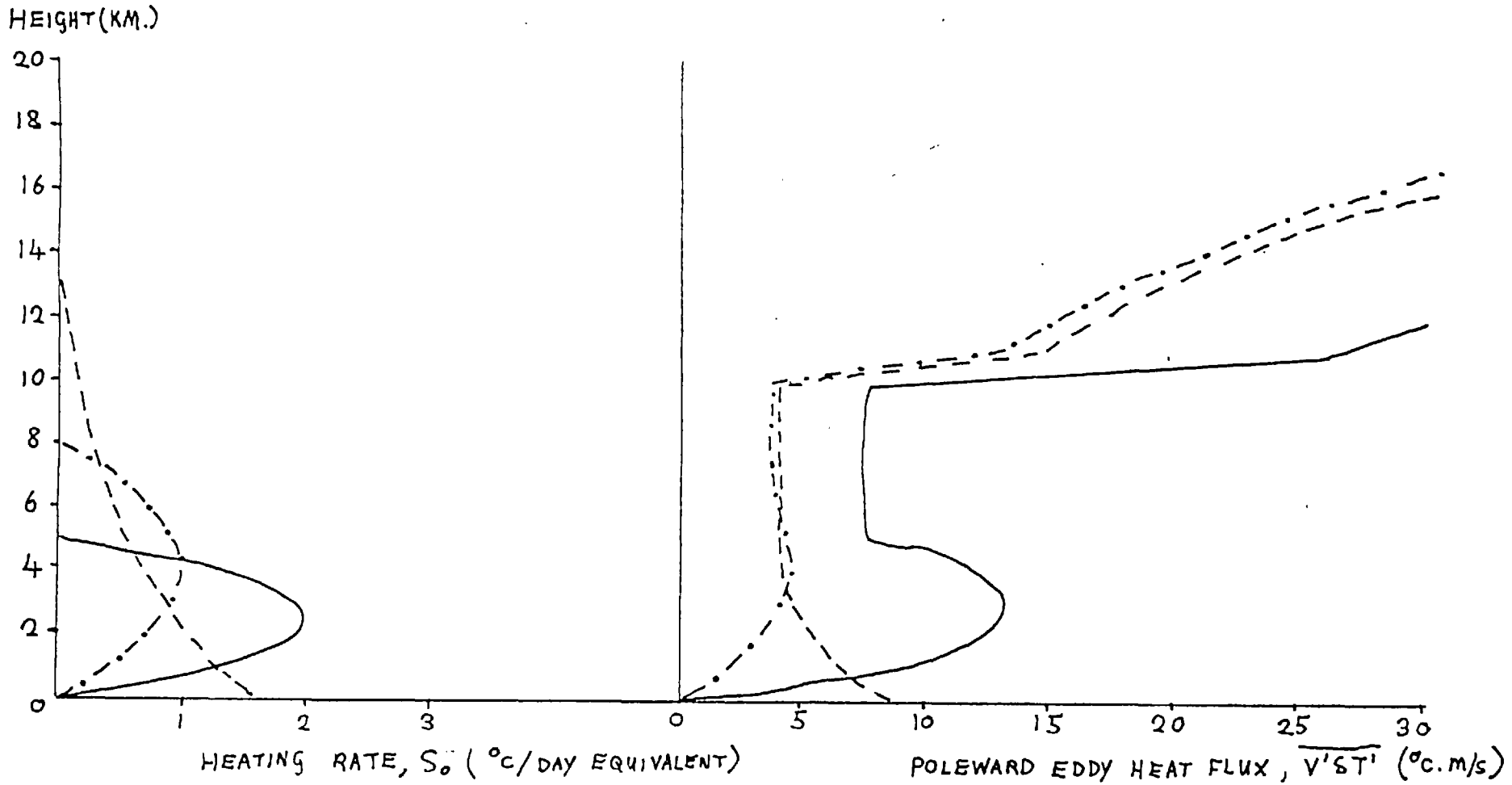

FIG. 4.9 (c) (ON THE LEFT) PROFILE OF HEATING RATE, $S_o(z)$
(" " RIGHT) $\overline{V'\delta T'}$ ASSOCIATED WITH (a).

realistic, leads to the conclusion that this transport mechanism is as important as that arising from unstable baroclinic waves and therefore is an important component of the wintertime general circulation. Unlike the heat transfer properties of baroclinic eddies, the transport by stationary planetary waves is more or less independent of the shear of the zonal wind (and hence the north-south temperature gradient) and for upward energy propagating modes in *negative* shear the heat transport is upgradient and the system behaves as a thermodynamic 'refrigerator'. This situation arises in the region above the tropospheric jet in winter.

Observations of the monthly mean temperature waves ($m = 1$, 2 and 3) in the troposphere would again greatly assist in determining the $S_0(z)$ profile, especially in view of the similarity in shape of the temperature wave amplitude and heating function.

Oort and Rasmusson (1971) have calculated from observations, the total eddy heat flux (or temperature flux $\overline{v'\delta T'}$) averaged around a latitude circle and partitioned it into stationary and transient eddy contributions. The latitude-height distribution of both transient and stationary eddy transports of heat are broadly similar with low-level maxima near *850* mb and it has been argued by White, A. (1975) that the stationary component might represent the organising effect of stationary waves on cyclone scale motion.

However, in so far as there is good agreement between amplitude and phase of the contour height fields and the data of Muench, the untrapped stationary wave contribution to the poleward heat transport must be important.

(iii) Thermal forcing in summer

Previous studies of stationary, planetary wave motion have tended to concentrate on the wintertime structure, particularly in the stratosphere

in connection with the upward transmission of energy. The nature of forced motion in summer poses a more subtle physical and mathematical problem resulting mainly from the transition from zonal westerly to easterly winds in the stratosphere above *20* km. The differential equation (2.4) has a singular point at $\bar{\psi}(z) = 0$ where the zonal wind speed is zero and the numerical integration technique outlined cannot work in its vicinity. The upward propagation of wave energy towards the zero of zonal wind gives rise to the critical layer absorption process at the height corresponding to $\bar{\psi} = 0$.

The problem of the integration of (2.4) in the neighbourhood of the singular point is circumvented by solving analytically in the surrounding region and connecting this solution to the numerical integration region below as a boundary condition. The phenomenon of critical layer absorption can in this way be included yet examination of the nature of the process raises some doubt as to its realism in stationary solutions. The following section will be devoted to the method of solution of the mathematical problem with the critical layer absorption process included and possible ways of eliminating the unphysical aspects of the linearized analysis associated with it.

The introduction of an Ekman boundary layer into the model is found to improve the agreement with existing data of the low-level structure of wavenumbers *1* and *2* in July by providing a sink of wave energy.

(a) Method of solution

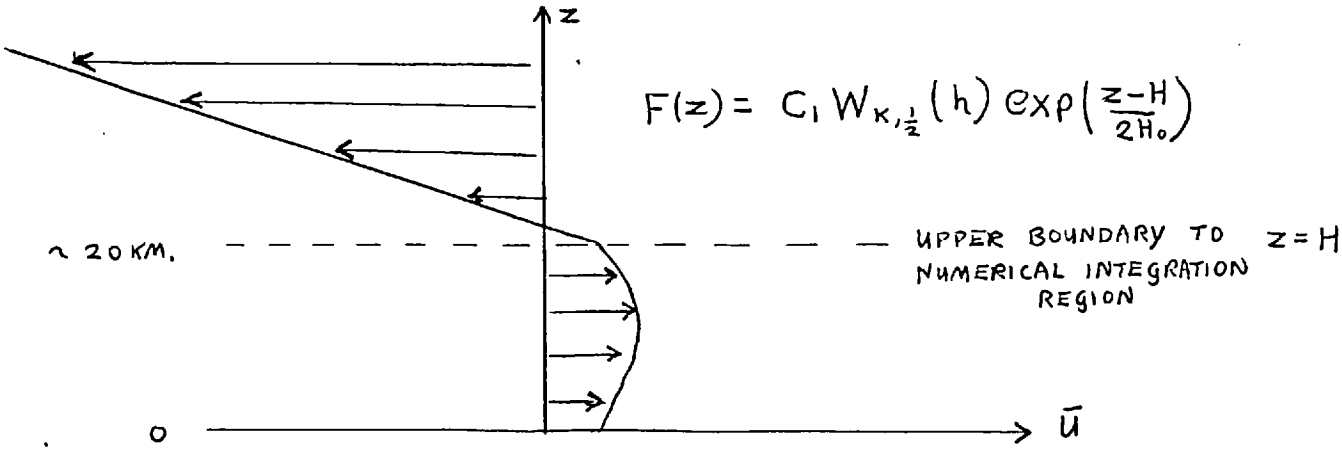

In precisely the same way that the 'radiation' condition was applied, so the connection of the constant negative shear solution above to the numerical solution below can be achieved through the use of interfacial conditions on pressure and vertical velocity. As before, the vertical velocity is expressed in terms of the non-divergent streamfunction through the thermodynamic equation:

$$w' = \frac{f_0}{gB}\frac{1}{R^2}\left\{\frac{\partial\psi'}{\partial\phi}\frac{d\bar{\psi}}{dz} - \bar{\psi}(z)\frac{\partial^2\psi'}{\partial\phi\partial z}\right\}$$

and demanding continuity of pressure ($\rho_0 f\psi'$) and vertical velocity with the constant shear solution above, gives a condition on $F(z)$ at $z = H$ which can be shown to be:

$$\frac{dF}{dz} - \left\{\frac{1}{\chi(H)}\left(\left.\frac{d\bar{\psi}}{dz}\right|_{z=H_-} - \left.\frac{d\bar{\psi}}{dz}\right|_{z=H_+}\right) + \left(\frac{\delta_* W'_{k,\frac{1}{2}}(h_*)}{W_{k,\frac{1}{2}}(h_*)} + \frac{1}{2H_0}\right)\right\}F(z) = 0 \qquad \text{——(4.10)}$$

at $z = H$ or $h = h_*$

with $h = \delta_*\left(\dfrac{\bar{\psi}(H)}{\left.\dfrac{d\bar{\psi}}{dz}\right|_{z=H_+}} + z - H\right)$

for the constant shear solution $\psi_+ = C_1 W_{k,\frac{1}{2}}(h)\exp\left(\dfrac{z-H}{2H_0}\right)P_n^m(\cos\theta)e^{im\phi}$ whose energy density is bounded at infinity.

The solution in the lower region is found by numerical integration with (4.10) as an upper boundary condition and $w' = 0$ giving the lower boundary condition. From the computed solution, the value of $F(z)$ at $z = H$ is used to determine C_1 and hence the solution in the constant shear layer.

The 'realistic' variation of $\bar{\psi}(z)$ was chosen to have a sinusoidal peak at *10* km as given in Fig.4.10(a) and again the static stability variation was taken from average mid-latitude profiles given in Charney and Drazin (1961) (Fig.4.10(b)). Diagrams of amplitude and phase for the $P_{m+1}^m(\cos\theta)$ modes forced by a heating function with vertical profile $S_0(z) = \left(\dfrac{2°C/day}{260°K}\right)\sin\left(\dfrac{\pi z}{4\ km}\right)$ are given in Fig.4.11. All three have similar

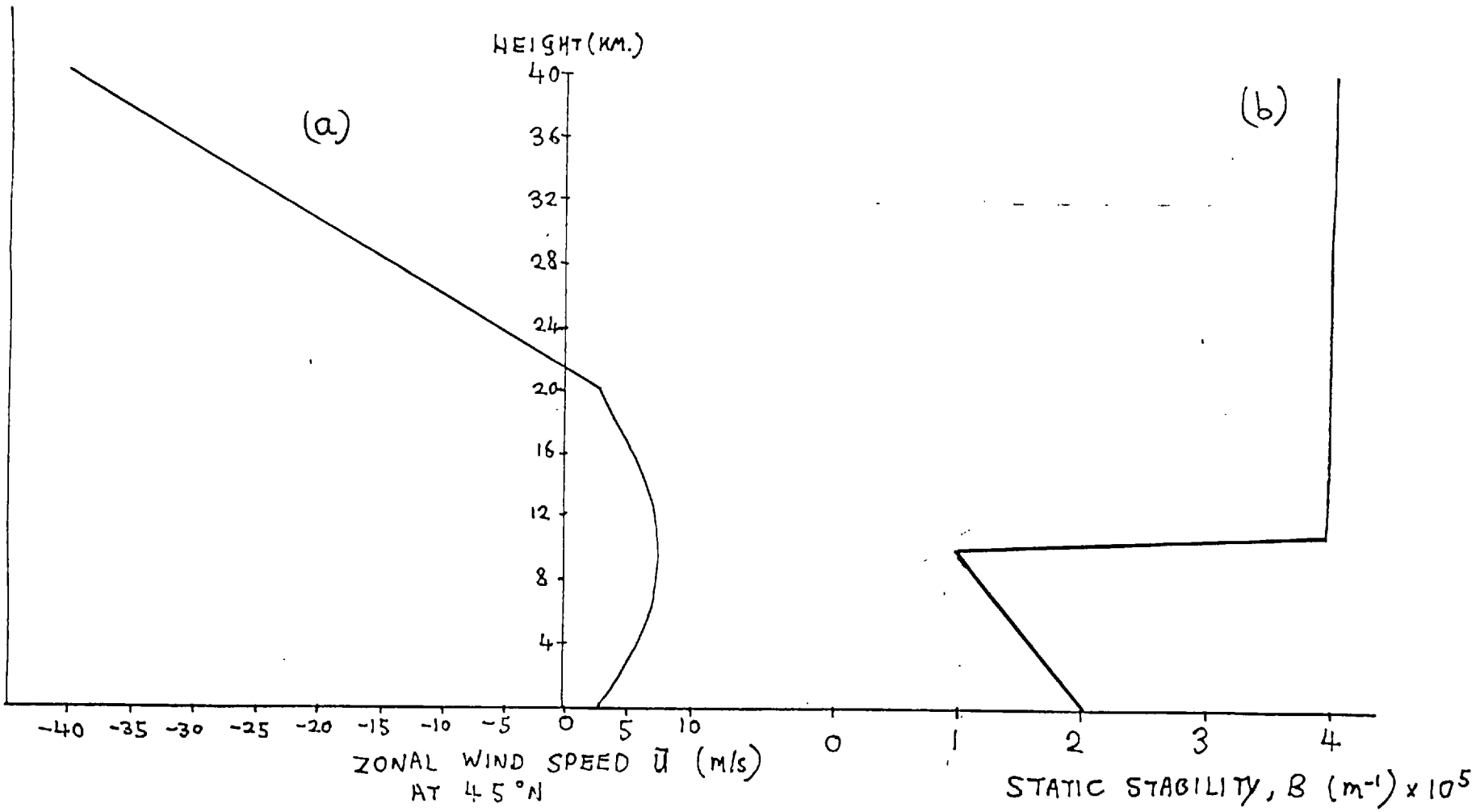

FIG. 4.10 (a) 'REALISTIC' SUMMER ZONAL WIND FIELD. (b) 'REALISTIC STATIC STABILITY' IN SUMMER. (U.S. NATIONAL BUREAU OF STANDARDS)

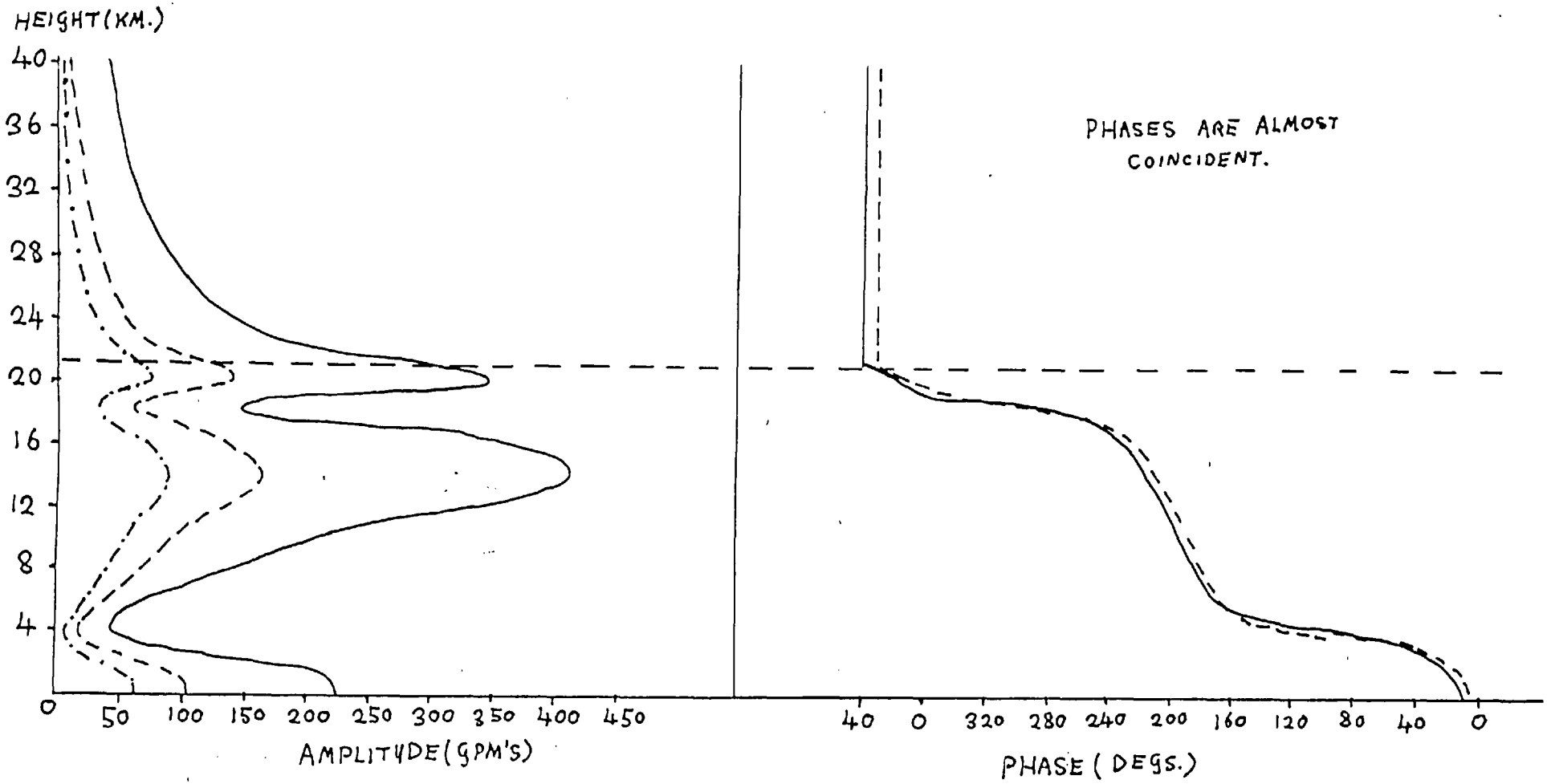

FIG. 4.11 STRUCTURE OF THE P^m_{m+1} MODES FOR $m=1, 2$ AND 3 IN SUMMER.
(WITH REALISTIC MEAN STATE.)

amplitude curve shapes with minima at *4* and *18* km and maxima at *20* and *14* km with a strong surface perturbation. The amplitude decreases rapidly in the easterlies and is virtually insignificant above *30* km unlike in the wintertime stratosphere where the westerlies transmit wave energy. Phase variation with height is virtually identical in all three, with strong westward tilt up to the critical level above which there is no change and the waves are evanescent. This implies upward propagation of wave energy towards the critical level and its subsequent absorption there. Poleward heat transport $\overline{v'\delta T'}$ changes discontinuously at this level and of course is zero in the easterlies above.

Generally, amplitude magnitudes are larger than their wintertime counterparts because the zonal wind speeds in the troposphere are smaller in summer and the $P_2^1(\cos\theta)$ mode is unrealistically large at the surface for this heating function magnitude. Analyses of the observed amplitudes of wavenumbers *1*, *2* and *3* in winter and summer are given by Eliassen, E. (1958) at the *1000* mb, *700* mb and *500* mb levels and show that the July amplitudes are at least half those of the mean January contour charts. This is exactly opposite to what one might have expected given similar heating function magnitudes and so it must be concluded either that the heating rates are much smaller in summer or that the theory breaks down.

(b) Critical-level absorption

The critical-level absorption phenomenon is a feature of the linearized analysis and it is necessary to consider its feasibility in the real atmosphere particularly relating to the behaviour of stationary planetary waves. Geisler and Dickinson (1974) and Murikami (1973) have made numerical studies of the non-linear coupling of wave and mean flow in critical level absorption problems and have found that the resulting accelerations of the zonal flow in the neighbourhood of the critical level

conspire to wipe out the gradient of mean potential vorticity thus causing the eventual reflection of all wave energy. They considered only the horizontal propagation of Rossby wave energy towards a critical layer; though it seems probable that the same qualitative results will hold for vertical propagation.

It will be discussed in some detail in the next chapter on wave/mean flow interaction how the acceleration of the zonal flow due to the 'second-order' effects is proportional to $\frac{\partial}{\partial z}\left(\frac{\rho_0}{B}\,\overline{v'\delta\phi'}\right)$ in the absence of horizontal eddy zonal momentum transport and consequently the discontinuity of heat transport calculated at the zero-wind line implies an infinite drag there. This would be quite inconsistent with the assumption of a steady, balanced mean zonal wind and thus the stationary solution with critical level absorption must be rejected. It is interesting to note that the differential equation property that $\frac{\rho_0}{B}\,\overline{v'\delta\phi'}$ is independent of height found in Chapter 3 is exactly a statement of the non-interaction of stationary wave with the mean flow and holds in all adiabatic flow regions away from critical levels.

One might conjecture that a steady coexistence of wave and mean flow can only be achieved when no wave absorption occurs which, as shown in the numerical experiments of Geisler and Dickinson, is possible if the energy is reflected before it reaches the zero-wind line. The profile of zonal wind only has to be altered in a vanishingly small region about $\bar{u} = 0$ to effect the total reflection of wave energy by destroying the basic state potential vorticity gradient.

The northward gradient of mean potential vorticity Q_* is given by:

$$Q_* = 2\left(\frac{\bar{\psi}}{R^3} + \frac{\Omega}{R}\right) - \frac{f_0^2}{gR}\,\frac{1}{\rho_0}\,\frac{d}{dz}\left(\frac{\rho_0}{B}\,\frac{d\bar{\psi}}{dz}\right)$$

and it vanishes when the zonal wind variation in the vertical is chosen

so as to cause the cancellation of the above terms.

Other small alterations to the zonal wind field in a small finite region about the singular point cause a complete change in the nature of the solution and lead to reflection. For instance, if the zonal wind goes to zero not just at a point but in a layer of any finite depth, then the stationary, linearized potential vorticity equation in this layer reduces to:

$$\frac{Q_\phi}{R}\frac{\partial \psi'}{\partial \phi} = 0$$

and hence the perturbation must vanish in the layer. All wave energy will suffer perfect reflection from the zero wind layer regardless of its thickness.

Also, allowing a discontinuity in zonal wind so as to exclude zonal wind values about $\bar{u} = 0$ causes total reflection as can be inferred from the two layer model solutions in Chapter 2.

That the structure of the stationary planetary wave system should depend on a vanishingly small region about $\bar{u} = 0$ seems physically implausible and in view of the wave/mean flow arguments given, it is concluded that the zero-wind level should reflect wave energy and so the 'summer solutions' are re-calculated with a more appropriate upper boundary condition.

Perhaps the simplest mathematical 'trick' that can be used to avoid critical level absorption while retaining the stratospheric easterlies is to allow a small discontinuity of zonal wind so as to exclude a small region containing the point where $\bar{u} = 0$. The connection of the upper analytic solution to the lower numerical solution is based on the interfacial conditions as derived in Chapter 2 for discontinuous zonal winds. The solution obtained was compared to that arrived at by imposing a rigid lid boundary condition just below the zero-wind level (and integrating numerically)

with the result that there was little difference between them.

The amplitude and phase of the P_2^1 and P_3^2 modes obtained under an upper rigid lid boundary condition are given in Figs. 4.12 and 4.13 respectively and show a pronounced nodal structure.

(c) Introduction of an Ekman boundary layer

Charney and Eliassen (1949) introduced the concept of 'Ekman pumping' whereby the effect of a turbulent boundary layer on the free atmosphere can be crudely incorporated into a lower boundary condition on vertical velocity. For steady, boundary layer flow, approximate balance exists between the stress torque $\text{curl}\left(\frac{1}{\rho_0}\frac{\partial \underline{\tau}_H}{\partial z}\right)$ and the (linearized) stretching term $\frac{f_0}{\rho_0}\frac{\partial}{\partial z}(\rho_0 w)$ (where $\underline{\tau}_H$ is the horizontal component of the stress vector). Integrating over the whole depth of the boundary layer, putting $w = 0$ at the ground and assuming the stress vanishes at the top of the boundary layer gives:

$$\rho_0 w_T = \frac{1}{f_0}\,\text{curl}\,\underline{\tau}_S$$

where w_T is the induced vertical velocity at the top of the boundary layer and $\underline{\tau}_S$ is the surface stress.

It is evident that an upward mass flow occurs for regions of cyclonic surface stress. A form suitable for inclusion as a lower boundary condition in the quasi-geostrophic theory results from the rather crude assumption that the surface stress is proportional to the gesotrophic wind so that $\underline{\tau}_S = \rho_0 c \underline{V}_g$ and gives:

$$w_T = c\frac{\zeta_g}{f_0}$$

with c equal to a constant and ζ_g the geostrophic vorticity. c may be related to the eddy diffusivity K of Ekman-Taylor theory and approximates to $\sqrt{Kf_0}$. Using the non-divergent streamfunction ψ, the expression for the induced upper vertical velocity w_T is given by:

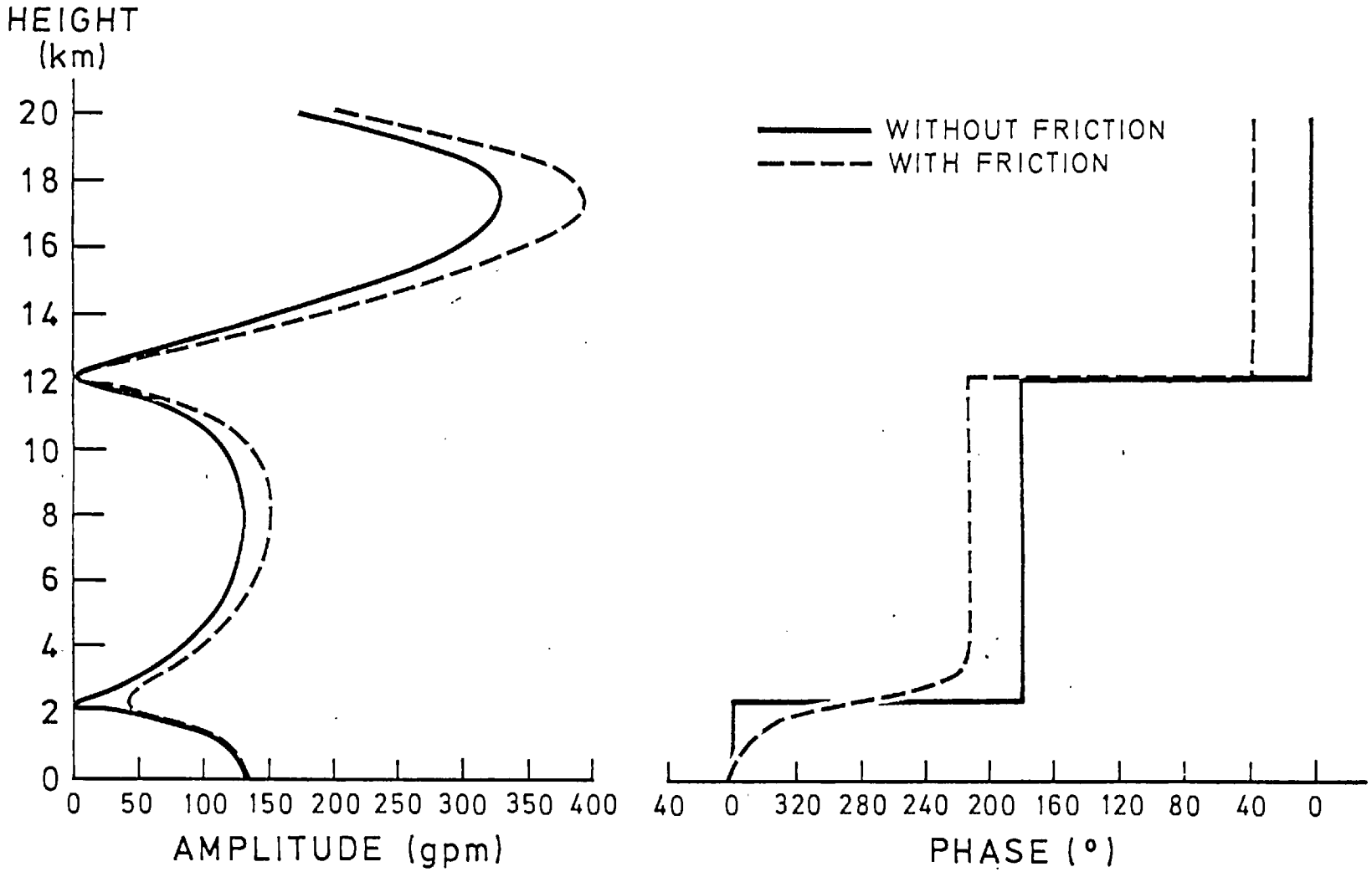

FIG. 4.12 STRUCTURE OF THE P_2' MODE IN SUMMER WITH A 'RIGID LID' AT 20 KM.

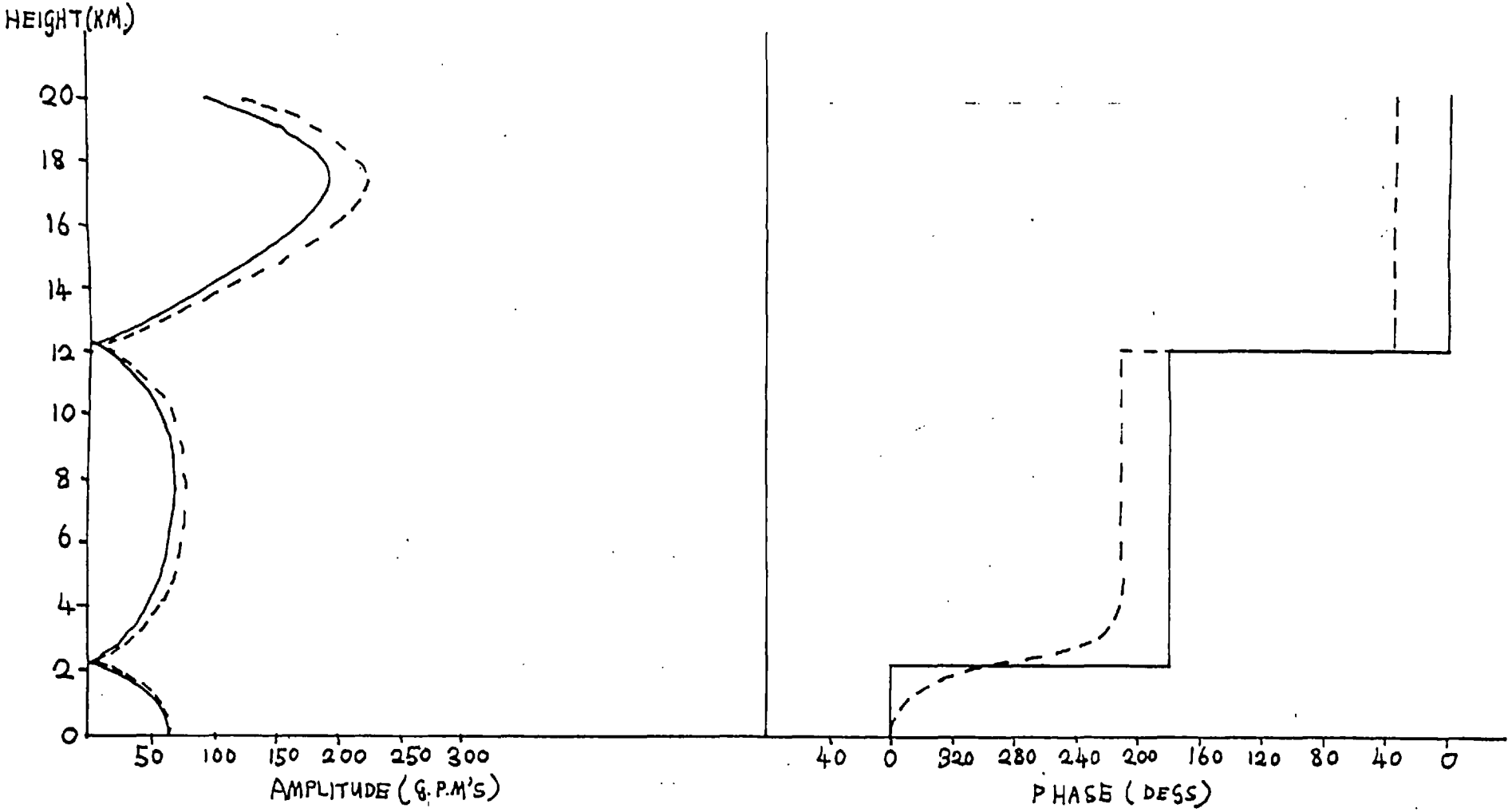

FIG. 4.13 STRUCTURE OF THE P_3^2 MODE IN SUMMER WITH A RIGID LID AT 20 KM.

$$w_T = \sqrt{\frac{K}{f_0}}\,\nabla_H^2\psi$$

and substituting this into the thermodynamic equation yields a lower boundary condition on ψ.

Selecting a typical value of eddy diffusivity of about *10* $m^2 s^{-1}$ (Brunt 1934) and solving the problem of (ii) with this modified boundary condition gives amplitude and phase as in Figs. 4.12 and 4.13 (dashed lines). The structure is very similar to that of the frictionless case except that the phase lines tilt eastward with height in the bottom *4* km.

(d) Interpretation of the planetary wave structure in summer and comparison with observation

The most outstanding difference between the summer and wintertime structure is the rapid attenuation of wave energy above *20* km in summer where the prevailing winds are easterly. At the *40* km level, the predicted amplitudes are small enough to be barely detectable by the sparse network of observing stations that collect rocket data and this is confirmed by the observed contours which are almost parallel to the latitude circles.

Unfortunately, there is insufficient data of amplitude and phase of the low-wavenumber waves to allow a similar comparison with theory to the one made with the January data given by Muench though some Fourier analyses have been made in the troposphere by Eliassen. Amplitude and phase of wavenumbers *1*, *2* and *3* are calculated at the *1000*, *700* and *500* mb levels in July (at *50*°N) by Eliassen (1958) and these form a rough basis for comparison with the theory in the lower troposphere.

As has been noted, the general amplitudes are much smaller than those calculated which probably implies that longitudinal asymmetry of heating is considerably smaller in summer than winter. Wavenumbers *1* and *2* show distinct amplitude minima near *700* mb ($\sim$ *3* km) though the accurate

location of the minimum is impossible from data at only 3 levels. Again, the presence of an amplitude minimum suggests the dominance of thermal forcing in summer.

Strongly eastward sloping phase lines are indicated by the Eliassen data up to 500 mb which is in marked disagreement with those model solutions that allow a critically absorbing layer but compares more favourably with the trapped solutions (Figs. 4.12 and 4.13), especially with the inclusion of a frictional boundary layer.

Oort and Rasmusson (1971) calculate from observations, a small equatorward, stationary eddy transport of heat in summer and if we assume this to be carried mainly by low wavenumber stationary waves, then this is consistent with the eastward slope of the phase lines. It should be noted that the transport of heat in summer is from cold to warm regions constituting a 'refrigerator' and is opposite to what one might expect of a diffusive transport of entropy through fluid instability.

It follows from the Clausius statement of the second law of thermodynamics that an external agency is involved for the system to act as a refrigerator. This is provided by the forcing and the origin of the heating and cooling regions which is external to the atmosphere (i.e. the sun). Note that orographically forced motion could not act in this way for the earth/atmosphere system since no outside perturbing forces are invoked and the overall transfer of heat must be from warm to cold.

The observations of stationary wave heat transport in summer support the hypothesis that the pure, long wave transport of heat dominates any organised, transient wave transfer in the total stationary wave heat transport, since the latter would imply a poleward transfer of heat, contrary to observation.

Wavenumber *3* is observed to have vertical phase lines below *500* mb in winter and summer according to Eliassen and this is in agreement with the theoretical prediction that the wave is trapped.

Clearly, a more detailed analysis of the structure of planetary wave motion in summer is required before a proper evaluation of the role played by stationary planetary waves in the general circulation can be assessed. It is hoped that these calculations provide theoretical guidelines for the interpretation of the observed structure and assessment of the importance of critical level effects.

(iv) Orographic forcing (Winter)

The orographic forcing calculations of Chapter 3 are repeated with realistic winter profiles of zonal wind and static stability for surface elevations given by $z_0 = (200 \text{ gpm}) P^m_{m+1}(\cos\theta)\cos m\phi$ taking $m = 1$, 2 and 3. Amplitudes and phases are given in Fig.4.14 and show that the surface amplitudes are much smaller than those for thermal forcing and are typically ~ 1-2 mb. Contour height amplitudes are generally a good deal smaller than observed magnitudes given in Fig.1.2 and, for instance, the predicted wavenumber *1* amplitude at *30* km is *170* m compared to observed amplitudes of *500* m. The phase slope westward of the propagating wavenumbers *1* and *2* is fairly uniform and implies an average vertical wavelength of ~ 30 km. Nodes appear in the trapped wavenumber *3* structure at about *2* and *17* km.

It should be remembered that only one harmonic component of each zonal wavenumber has been selected and it is instructive to compare the amplitude curves of higher n modes to assess their relative importance. The amplitudes and phases of the P^1_n modes (for $n = 2, 4, 6$) are given in Fig.4.15 and correspond to forcing by the same surface elevation amplitude of *200* gpm. (N.B. these modes have zero amplitude on the equator.)

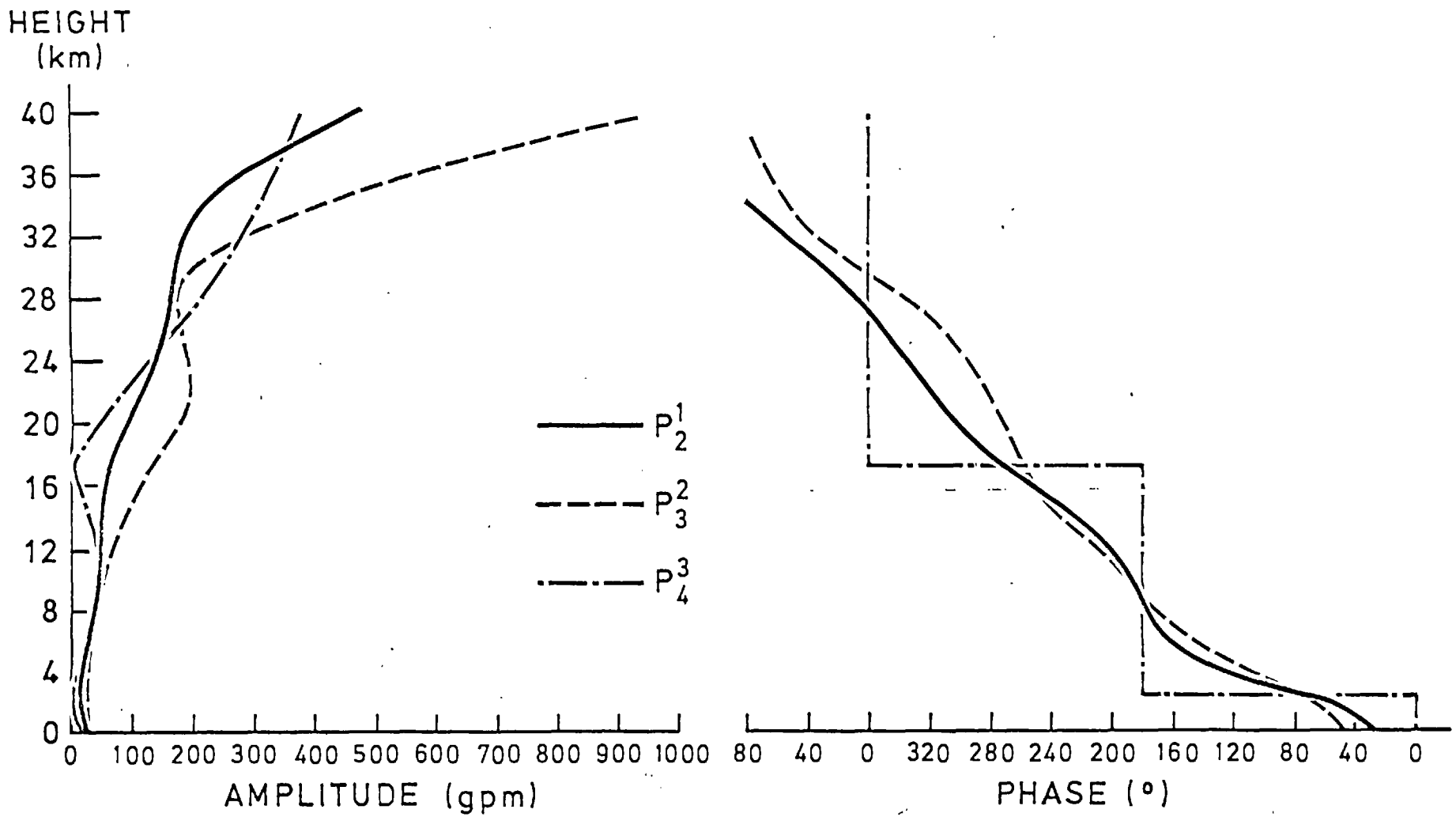

FIG. 4.14 STRUCTURE OF THE OROGRAPHICALLY FORCED P^m_{m+1} MODES FOR $m = 1, 2$ AND 3.

$Z_o = a\, P^m_{m+1}(\cos\theta)\cos m\phi$ WITH $a = 200$ metres.

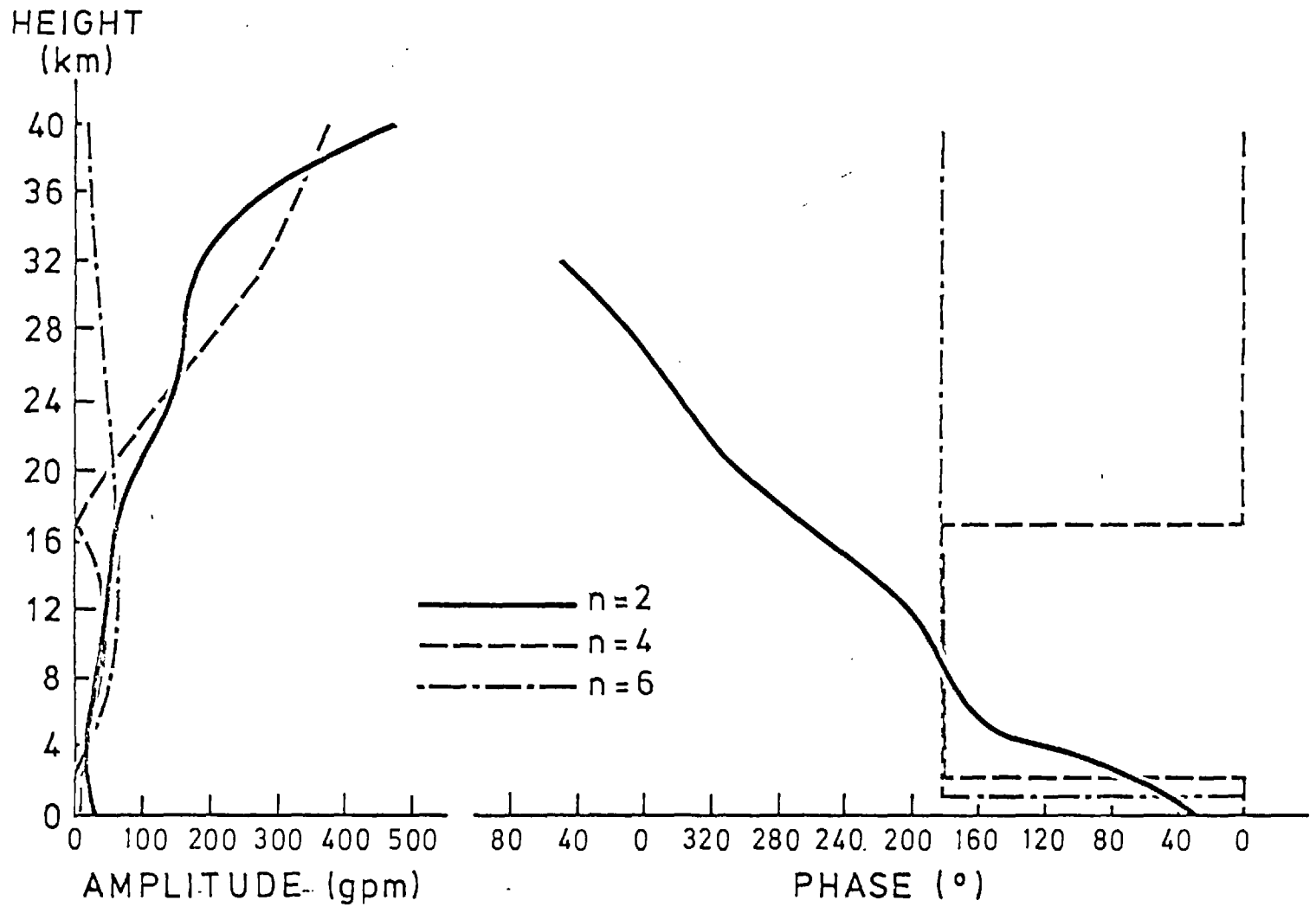

FIG. 4.15 STRUCTURE OF THE P_n^1 OROGRAPHICALLY FORCED MODES WITH $n=2,4$ AND 6.

$z_o = a P_n^1(\cos\theta)\cos\phi$, $a = 200$ m.

The magnitude of the forced contour height amplitude for each mode is similar up to *20* km above which the P_6^1 wave is highly attenuated. Higher n modes are even more strongly attenuated in the stratosphere and it may be concluded that the main contribution to the wavenumber *1* disturbance there comes from the P_2^1 and P_4^1 modes.

The calculated tropospheric poleward heat transport effected by the orographically forced waves P_2^1 and P_3^2 is an order of magnitude smaller than that indicated by their thermally forced counterparts with $\overline{v'\delta T'} \sim 1°C\ m\ s^{-1}$ at most.

(v) Stationary planetary wave forcing: Summary and conclusions

The underlying tenet of the work presented so far is that the upper stratosphere behaves as a wave energy sink for forced, stationary wavenumbers *1* and *2* and that this aspect of the motion has important repercussions on the general circulation and its modelling. The largest planetary scales of quasi-geostrophic motion are highly dispersive which permits the propagation of wave energy away from the regions of forcing for stationary disturbances. This can only be properly accounted in terms of a quasi-geostrophic theory represented in spherical polar geometry since β-plane theories underestimate the ability of planetary wave energy to propagate in strong westerly winds.

It has been deduced from the observations of low wavenumber stationary waves in January that wave energy propagates freely up to about *30* km above which it is strongly absorbed by physical processes that are not clearly understood with the result that the wave energy density decreases rapidly above *50* km. The whole issue of the mechanism of wave energy destruction in this region is circumvented by the use of an energy-transmitting boundary condition at an appropriate height. With this knowledge of the response of the stratosphere to upward propagating Rossby wave energy, we have set up models of orographic and thermal forcing in the troposphere and determined

their structure and heat transferring properties.

General agreement of the vertical structure of wavenumber *1* with observations is very good especially for the thermally forced wave where longitudinal variations of lower tropospheric diabatic heating of the order of *1*°C/day set up a realistic 'Siberian anticyclone' surface disturbance and cause a strong stratospheric wave.

One of the important features of the thermally-forced, untrapped stationary wave is the large poleward transport of heat in the region of diabatic heating.

The strong lower tropospheric stationary wave transport of heat is in good agreement with the stationary eddy heat transfer in January calculated by Oort and Rasmusson from observations. This suggests that the untrapped stationary wavenumbers *1* and *2* in winter carry as much, if not more, of the total poleward eddy heat transport as the transient cyclone waves since the Oort and Rasmusson calculation of stationary eddy heat flux is slightly greater than the transient eddy heat flux.

The main distinguishing characteristics of the thermally-forced wave as compared to the orographically forced wave (N.B. of planetary scale) is the much larger surface disturbance and amplitude minimum near *4* km. Both surface contour height and temperature waves are an order of magnitude larger for thermally forced waves than for planetary waves set up by the continental elevations.

It must be stressed that only those waves of hemispheric extent are referred to in this comparison and locally, near mountain ranges such as the Himalayas, the orographically forced wave may be much larger. We are interested primarily in these continental scale waves that influence the stratosphere through Rossby wave propagation.

The structure of low-wavenumber, stationary waves in summer is quite different from that of the wintertime in the stratosphere with the prevailing easterlies blocking the upward flow of wave energy for all waves. The existence of a critical layer (where $\bar{u} = 0$) in the steady flow description of the wave structure has been treated with scepticism in view of the implied unsteadiness through interaction of the wave with the mean zonal flow. This is backed up by the disagreement between the theoretical solution with a critical level effect and the observed eastward phase tilt. The observed absence of poleward eddy heat flux in the stationary waves (or even a southward transport) in the lower troposphere in summer points to the absence of upward wave energy transmission which one would expect from a theory with critical level absorption. The absorption of wave energy by boundary layer friction might account for the eastward slope of the phase lines with height in the lower troposphere, as found in the calculations. This fundamental difference in planetary wave structure between winter and summer might play an important role in determining the seasonal variation of the zonal mean circulation — primarily through the poleward heat transporting properties.

Year to year fluctuations of the January monthly mean zonal wind of as much as *100 %* occur in the stratosphere and in view of the sensitivity of the transmissive properties of upward propagating Rossby waves to zonal wind speed changes, one might expect some variation in wave structure. Sato (1974) gives the amplitudes and phases of wavenumbers *1*, *2* and *3* between *500* and *10* mb for the winters of 1963 to 1970 at *60*°N and *40*°N. Some interesting differences in vertical phase variation are indicated between years as is exemplified by the years 1963 and 1967 tabulated below:

Wavenumber	Phase (°longitude/km)	
	JAN. 1963	JAN. 1967
1	*10*	*6*
2	*4.4*	*1.6*

Apparently the upward transmission of wave energy was much stronger in January 1963 with steeply westward sloping phase lines which, incidentally, compare very favourably with the calculated slopes of the P_2^1 and $P_3^2(\cos\theta)$ modes for the realistic basic state profile.

The two-layer models of Chapter 2 emphasise the suddenness in transition from the propagating to evanescent regimes with increase of zonal wind and there is good reason to believe that planetary waves near this transition point will be susceptible to small zonal wind changes. This sensitivity to the mean stratospheric zonal wind speed could provide the link between the high atmosphere circulation and the surface climate that has been professed by climatologists for so long, though this is of course, rather speculative (see for example Willet, 1961).

CHAPTER 5 THE INTERACTION OF A STATIONARY WAVE SYSTEM OF SLOWLY VARYING AMPLITUDE WITH THE 'MEAN' FLOW

(i) Theory of wave-mean flow coupling

The previous chapters have been concerned only with stationary ($\partial/\partial t \equiv 0$) solutions to a very specific problem of large-scale forcing without questioning how such a state might be attained or even if it is possible. The time dependent evolution of a stationary wave system from a region of forcing involves a multitude of interactions between the wave and basic state and within the wave itself. It is only for 'very small' amplitude wave motion that it is justified to treat the basic state parameters as unmodified and the questions that arise are 'How small is 'very small'?' and 'What effect does the wave have?'. In a sense, the conventional initial-value problem for the response to a 'switch-on' of forcing produces only half the description of the motion since the very small changes to the basic flow are not calculated. The sudden 'switching-on' of forcing causes a spectrum of 'transient' waves which spread out in all directions with time. We shall only consider the behaviour of the interactions of wave with basic flow under the assumption that the forcing varies slowly in time and that the wave system can always be regarded as a quasi-stationary system (no transients).

Analogous approaches exist in classical mechanics for slow time-varying oscillatory systems (e.g. the pendulum bob on a string pulled over a support) such that the time scale over which the string is shortened is much longer than the period of oscillation.

In the approach given here, we will not be concerned with the type of dispersive motion involved — only that it should be consistent with the linearized Boussinesq equations (hydrostatic). The resulting description is applicable to inertial-gravity wave motion as well as planetary Rossby wave motion.

The following assumptions are essential:

(1) The wave system set up is slowly varying in time.

(2) Changes in amplitude take place slowly in the vertical.

(3) We consider regions away from critical levels ($\bar{U} = 0$).

In general (1) implies (2) since if changes are transmitted upwards with a finite speed (typically the group speed) then the smallness in time variation implies largeness of vertical spread of the changing amplitude. This will not be true near the critical layer where the group speed tends to zero. We shall not be concerned with evanescent wave systems or trapped situations even though the results may be applicable to some extent.

The smallness of variation of z and t and the size of the perturbation quantities is denoted by ε such that we may define new height and time variables $Z = \varepsilon z$ and $T = \varepsilon t$. Also $q' \sim O(\varepsilon)$ where q' represents any perturbation quantity.

Eliassen and Palm (1961) (hereafter EP) derived equations for stationary waves forced by mountains which relate physically significant quantities such as the average perturbation pressure work term to eddy momentum and entropy transport. The procedure for the derivation of their equations will now be re-capped.

The standard Boussinesq set is

$$\frac{Du}{Dt} - fv + \frac{\partial}{\partial x}\left(\frac{\delta p}{\rho_0}\right) = 0 \qquad x\text{-momentum equation}$$

$$\frac{Dv}{Dt} + fu + \frac{\partial}{\partial y}\left(\frac{\delta p}{\rho_0}\right) = 0 \qquad y\text{-momentum equation}$$

$$\frac{\partial}{\partial z}\left(\frac{\delta p}{\rho_0}\right) - g\delta\phi = 0 \qquad z\text{-momentum equation}$$

$$\frac{\partial u}{\partial x} + \frac{\partial v}{\partial y} + \frac{1}{\rho_0}\frac{\partial}{\partial z}(\rho_0 w) = 0 \qquad \text{Continuity of mass}$$

$$\frac{D\delta\phi}{Dt} + wB = 0 \qquad \text{Conservation of entropy.}$$

Linearizing about a basic state of zonal flow with

$$u = \bar{U}(y,z,T) + u'(x,y,z,T)$$

$$v = v'(x,y,z,T)$$

$$w = w'(x,y,z,T) \qquad\qquad T = \varepsilon t$$

$$\delta p = \overline{\delta p} + \delta p'$$

$$\delta\phi = \overline{\delta\phi} + \delta\phi'$$

(overbar indicates x-average)

gives to first order in ε:

$$\bar{U}\frac{\partial u'}{\partial x} + v'\frac{\partial \bar{U}}{\partial y} + w'\frac{\partial \bar{U}}{\partial z} - fv' + \frac{\partial}{\partial x}\left(\frac{\delta p'}{\rho_0}\right) = 0 \qquad \text{——(1)}$$

$$\bar{U}\frac{\partial v'}{\partial x} + fu' + \frac{\partial}{\partial y}\left(\frac{\delta p'}{\rho_0}\right) = 0 \qquad \text{——(2)}$$

$$\frac{\partial}{\partial z}\left(\frac{\delta p'}{\rho_0}\right) - g\delta\phi' = 0 \qquad \text{——(3)}$$

$$\bar{U}\frac{\partial \delta\phi'}{\partial x} + v'\frac{\partial \overline{\delta\phi}}{\partial y} + w'B = 0 \qquad \text{——(4)}$$

$$\frac{\partial u'}{\partial x} + \frac{\partial v'}{\partial y} + \frac{1}{\rho_0}\frac{\partial}{\partial z}(\rho_0 w') = 0 \qquad \text{——(5)}$$

Eliminating w' between (1) and (4) and re-arranging gives

$$\frac{\partial}{\partial x}\left(\bar{U}u' + \frac{\delta p'}{\rho_0} - \frac{\frac{\partial \bar{U}}{\partial z}\bar{U}\,\delta\phi'}{B}\right) + \left(\frac{\partial \bar{U}}{\partial y} - f - \frac{\frac{\partial \bar{U}}{\partial z}\frac{\partial \overline{\delta\phi}}{\partial y}}{B}\right)v' = 0$$

Multiply by $\left(\bar{U}u' + \frac{\delta p'}{\rho_0} - \frac{\frac{\partial \bar{U}}{\partial z}\bar{U}\,\delta\phi'}{B}\right)$ and average with respect to x

$$\left(\frac{\partial \bar{U}}{\partial y} - f - \frac{\partial \bar{U}}{\partial z}\frac{\partial \overline{\delta\phi}}{\partial y}\Big/B\right)\left(\bar{U}\,\overline{u'v'} + \frac{\overline{\delta p'v'}}{\rho_0} - \frac{\partial \bar{U}}{\partial z}\bar{U}\,\overline{\delta\phi'v'}\Big/B\right) = 0$$

if $\quad \frac{\partial \bar{U}}{\partial y} - f - \frac{\partial \bar{U}}{\partial z}\frac{\partial \overline{\delta\phi}}{\partial y}\Big/B \neq 0 \quad$ then

$$\overline{\delta p'v'} = \rho_0\bar{U}\left(\frac{\frac{\partial \bar{U}}{\partial z}}{B}\overline{\delta\phi'v'} - \overline{u'v'}\right) \qquad \text{——(6)}$$

Similarly re-arranging (1) into: $\frac{\partial}{\partial x}\left(\bar{U}u' + \frac{\delta p'}{\rho_0}\right) + \left(\frac{\partial \bar{U}}{\partial y} - f\right)v' + w'\frac{\partial \bar{U}}{\partial z} = 0$

multiplying by $(\bar{U}u' + \delta p'/\rho_0)$ and averaging w.r.t. x gives

$$\left(\frac{\partial \bar{U}}{\partial y} - f\right)\left(\bar{U}\,\overline{u'v'} + \frac{\overline{\delta p' v'}}{\rho_0}\right) + \frac{\partial \bar{U}}{\partial z}\left(\overline{u'w'}\,\bar{U} + \frac{\overline{\delta p' w'}}{\rho_0}\right) = 0$$

Eliminating $\overline{\delta p' v'}$ from the above with equation (6) gives:

$$\overline{\delta p' w'} = \rho_0 \bar{U}\left(\frac{(f - \partial \bar{U}/\partial y)}{B}\,\overline{\delta\phi' v'} - \overline{u'w'}\right) \qquad \text{——(7)}$$

The EP relations (6) and (7) relate the vertical and meridional eddy pressure-work terms to the vertical and meridional flux of momentum and poleward transport of entropy. $\overline{\delta p' w'}$ and $\overline{\delta p' v'}$ are tentatively identified with the rate of transmission of wave energy upwards and in the y-direction.

The zonally-averaged zonal momentum equation is formed and can be re-arranged into:

$$\frac{\partial \bar{U}}{\partial t} + \rho_0 \bar{v}\,\frac{\partial \bar{U}}{\partial y} + \rho_0 \bar{w}\,\frac{\partial \bar{U}}{\partial z} + \frac{\partial}{\partial y}(\rho_0 \overline{u'v'}) + \frac{\partial}{\partial z}(\rho_0 \overline{u'w'}) - f\rho_0 \bar{v} = \qquad \text{——(8)}$$

using the continuity equation and the property that $\overline{\partial q'}/\partial x = 0$ when the x-coordinate is cyclic or if q' vanishes at the end points of the averaging interval.

This expresses that the zonally-averaged zonal momentum changes through advection of mean or eddy momentum or by the coriolis force acting on the north-south drift (representing the conservation of angular momentum).

Zonally-averaged the conservation of entropy equation with the use of the continuity equation yields:

$$\frac{\partial \overline{\delta\phi}}{\partial t} + \frac{\partial}{\partial y}(\overline{\delta\phi v}) + \frac{1}{\rho_0}\,\frac{\partial}{\partial z}(\rho_0 \overline{\delta\phi w}) + \bar{w}B = 0 \qquad \text{——(9)}$$

The convergence of vertical eddy entropy flux is negligible for flows where the product of Richardson and Rossby numbers is much greater than one, and will be omitted hereafter.

It will now be shown that under the assumptions made at the beginning

of this section, the time rate of change of zonal mean entropy is small compared with the convergence of poleward entropy flux, i.e. the first term of (9) may be neglected.

Zonally averaging the y-component of the momentum equation leads to:

$$\frac{\partial}{\partial y}(\overline{v^2}) + \frac{1}{\rho_0}\frac{\partial}{\partial z}(\rho_0 \overline{v\omega}) + f\bar{U} + \frac{\partial}{\partial y}\left(\frac{\overline{\delta p}}{\rho_0}\right) = 0$$

and since $\bar{v}$ and $\bar{\omega}$ are 2nd order quantities at most, $\overline{v^2}$ and $\overline{v\omega}$ can be replaced by $\overline{v'^2}$ and $\overline{v'\omega'}$ respectively. Differentiating with respect to z and t gives:

$$\varepsilon^2\frac{\partial^3}{\partial T\partial Z\partial y}(\overline{v'^2}) + \varepsilon\frac{\partial}{\partial T}\left\{\frac{\partial}{\partial z}\left(\frac{1}{\rho_0}\frac{\partial}{\partial z}(\rho_0\,\overline{v'\omega'})\right)\right\} + \varepsilon\frac{\partial}{\partial Z}\left(f\frac{\partial\bar{U}}{\partial t}\right) + \frac{\partial^2}{\partial t\partial y}\left\{\frac{\partial}{\partial z}\left(\frac{\overline{\delta p}}{\rho_0}\right)\right\} = 0$$

(with the use of $Z = \varepsilon z$ and $T = \varepsilon t$). Notice that it is not necessarily correct to replace $\frac{\partial}{\partial z}$ with $\varepsilon\frac{\partial}{\partial Z}$ when operating on terms involving density since changes in the vertical of density might be more rapid than wave amplitude.

The zonally-averaged hydrostatic relation is:

$$\frac{\partial}{\partial z}\left(\frac{\overline{\delta p}}{\rho_0}\right) = g\,\overline{\delta\phi}$$

and substituting this into the above equation yields:

$$\underset{O(\varepsilon^4)}{\varepsilon^2\frac{\partial^3}{\partial T\partial Z\partial y}(\overline{v'^2})} + \underset{O(\varepsilon^3)}{\varepsilon\frac{\partial}{\partial T}\left\{\frac{\partial}{\partial z}\left(\frac{1}{\rho_0}\frac{\partial}{\partial z}(\rho_0\,\overline{v'\omega'})\right)\right\}} + \underset{O(\varepsilon^3)}{\varepsilon f\frac{\partial}{\partial z}\left(\frac{\partial\bar{U}}{\partial t}\right)} + g\frac{\partial^2\overline{\delta\phi}}{\partial t\partial y} = 0$$

The upper bound on the magnitude of $\frac{\partial\overline{\delta\phi}}{\partial t}$ can be deduced by assuming that it balances the largest term in the equation. The second term is at most $O(\varepsilon^3)$ but in practice scale arguments show that is much smaller than the other terms. The term $\varepsilon f\frac{\partial}{\partial Z}\left(\frac{\partial\bar{U}}{\partial t}\right)$ is of order ε^3 at most since $\partial\bar{U}/\partial t$ is $\leq O(\varepsilon^2)$ and therefore we conclude that $\frac{\partial\overline{\delta\phi}}{\partial t}$ is less than or equal to 3rd order in ε. The above argument would be considerably simplified had we assumed initially that the mean flow is in geostrophic balance.

It is permissible, therefore, to reject this term in equation (9) compared to $\frac{\partial}{\partial y}(\overline{\delta\phi v})$ which is $O(\varepsilon^2)$ and assume that the convergence of poleward entropy flux drives the mean meridional circulation and $\bar{w} \simeq -\frac{1}{B}\frac{\partial}{\partial y}(\overline{\delta\phi v})$.

Using the zonally-averaged continuity equation:

$$\frac{\partial}{\partial y}(\rho_0 \bar{v}) + \frac{\partial}{\partial z}(\rho_0 \bar{w}) = 0$$

$\bar{v}$ can be expressed in terms of poleward entropy flux so that

$$\bar{v} = \frac{1}{\rho_0}\frac{\partial}{\partial z}\left(\rho_0 \frac{\overline{v\delta\phi}}{B}\right)$$

Now $\overline{v\delta\phi} = \overline{v'\delta\phi'} + \bar{v}\,\overline{\delta\phi}$ and if we take $\frac{\partial}{\partial z} = \frac{1}{H_0}$ at most:

$$O(\bar{v}) \sim \frac{\overline{v'\delta\phi'}}{BH_0} + \frac{\bar{v}\,\overline{\delta\phi}}{BH_0} \qquad (O(\ ) \text{ denotes the order of magnitude})$$

Since $\overline{\delta\phi}/BH_0$ is typically $<<1$ it may be assumed that the advection of entropy by the mean meridional circulation is much smaller than that of the eddy transport,

$$\therefore \quad \bar{v} \simeq \frac{1}{\rho_0}\frac{\partial}{\partial z}\left(\rho_0 \frac{\overline{v'\delta\phi'}}{B}\right) \quad \text{and} \quad \bar{w} = -\frac{1}{B}\frac{\partial}{\partial y}(\overline{\delta\phi' v'}) \qquad \text{——(10)}$$

The approximations made so far appear rather stringent though their dependence on the assumptions of slowness of time and height variation is much less critical than implied here. For instance the advection of entropy by the mean meridional circulation is always much smaller than the eddy transport in the stratosphere and one might expect the conclusions to be more generally valid.

Substituting the expressions (10) into equation (8) gives on multiplying by ρ_0

$$\frac{\partial}{\partial t}(\rho_0 \bar{U}) + \frac{\partial}{\partial z}\left(\rho_0 \frac{\overline{v'\delta\phi'}}{B}\right)\frac{\partial \bar{U}}{\partial y} - \frac{\partial}{\partial y}\left(\rho_0 \frac{\overline{v'\delta\phi'}}{B}\right)\frac{\partial \bar{U}}{\partial z} + \frac{\partial}{\partial y}(\rho_0 \overline{u'v'}) + \frac{\partial}{\partial z}(\rho_0 \overline{u'w'}) - f\frac{\partial}{\partial z}\left(\rho_0 \frac{\overline{v'\delta\phi'}}{B}\right) = 0$$

Re-arranging and collecting terms leads to:

$$\frac{\partial}{\partial t}(\rho_0 \bar{U}) + \frac{\partial}{\partial y}\left\{\rho_0 \overline{u'v'} - \rho_0 \frac{\overline{v'\delta\phi'}}{B}\frac{\partial \bar{U}}{\partial z}\right\} + \frac{\partial}{\partial z}\left\{\left(\frac{\partial \bar{U}}{\partial y} - f\right)\rho_0 \frac{\overline{v'\delta\phi'}}{B} + \rho_0 \overline{u'w'}\right\} = 0$$

and on using the EP relations for the terms in { } we have:

$$\frac{\partial}{\partial t}(\rho_0 \bar{U}) = \frac{\partial}{\partial y}\left(\frac{\overline{\delta p' v'}}{\bar{U}}\right) + \frac{\partial}{\partial z}\left(\frac{\overline{\delta p' w'}}{\bar{U}}\right) \qquad \text{——(11)}$$

Notice that in general the zonal momentum field is accelerated in regions of diverging wave energy flow and that the important quantity involved is $\overline{\delta p' \underline{V}'}/\bar{U}$. This expression implicitly contains the acceleration of the mean flow by advection of zonal momentum polewards and upwards by the induced circulation and also the coriolis acceleration due to north-south movement.

Lastly the wave energy equation is formed from the time-dependent, linearized momentum and thermodynamic equations as follows. The perturbation momentum and hydrostatic equations are:

$$\left(\frac{\partial}{\partial t} + \bar{U}\frac{\partial}{\partial x}\right)u' + v'\frac{\partial \bar{U}}{\partial y} + w'\frac{\partial \bar{U}}{\partial z} - fv' + \frac{\partial}{\partial x}\left(\frac{\delta p'}{\rho_0}\right) = 0 \qquad \text{——(12)}$$

$$\left(\frac{\partial}{\partial t} + \bar{U}\frac{\partial}{\partial x}\right)v' + fu' + \frac{\partial}{\partial y}\left(\frac{\delta p'}{\rho_0}\right) = 0 \qquad \text{——(13)}$$

$$\frac{\partial}{\partial z}\left(\frac{\delta p'}{\rho_0}\right) - g\delta\phi' = 0 \qquad \text{——(14)}$$

Multiply (12) by u', (13) by v', (14) by w' and add; using the continuity equation and re-arranging gives:

$$\left(\frac{\partial}{\partial t} + \bar{U}\frac{\partial}{\partial x}\right)\left(\frac{1}{2}\rho_0\left(u'^2 + v'^2\right)\right) + \rho_0 \frac{\partial \bar{U}}{\partial y}u'v' + \rho_0 \frac{\partial \bar{U}}{\partial z}u'w' - \rho_0 g w'\delta\phi'$$
$$+ \frac{\partial}{\partial x}(\delta p' u') + \frac{\partial}{\partial y}(\delta p' v') + \frac{\partial}{\partial z}(\delta p' w') = 0 \qquad \text{——(15)}$$

The linearized equation for entropy conservation is

$$\left(\frac{\partial}{\partial t} + \bar{U}\frac{\partial}{\partial x}\right)\delta\phi' + v'\frac{\partial}{\partial y}\overline{\delta\phi} + w'B = 0$$

and after multiplying by $\rho_0 g \delta\phi'/B$ gives

$$\left(\frac{\partial}{\partial t} + \bar{U}\frac{\partial}{\partial x}\right)\left(\rho_0 \frac{g\,\delta\phi'^2}{2B}\right) - \rho_0 \frac{f}{B} v'\delta\phi' \frac{\partial \bar{U}}{\partial z} + \rho_0 g\,\delta\phi' w' = 0$$

(using the thermal wind equation).

Adding to (15) and averaging w.r.t. x yields:

$$\frac{\partial \bar{E}}{\partial t} + \rho_0 \overline{u'v'}\frac{\partial \bar{U}}{\partial y} + \rho_0 \overline{u'w'}\frac{\partial \bar{U}}{\partial z} - \rho_0 \frac{f}{B}\overline{v'\,\delta\phi'}\frac{\partial \bar{U}}{\partial z} + \frac{\partial}{\partial y}\left(\overline{\delta p' v'}\right) + \frac{\partial}{\partial z}\left(\overline{\delta p' w'}\right) = 0 \qquad \text{——(16)}$$

where $\bar{E} = \frac{1}{2}\rho_0\left(\overline{u'^2} + \overline{v'^2} + \frac{g}{B}\overline{\delta\phi'^2}\right)$.

Using the Eliassen and Palm relations, (6) and (7), equation (16) can be re-arranged into the form:

$$\frac{\partial \bar{E}}{\partial t} = -\bar{U}\left\{\frac{\partial}{\partial y}\left(\frac{\overline{\delta p' v'}}{\bar{U}}\right) + \frac{\partial}{\partial z}\left(\frac{\overline{\delta p' w'}}{\bar{U}}\right)\right\}$$

and after multiplying (11) by $\bar{U}$ and adding to the above expression we have:

$$\frac{\partial}{\partial t}\left(\frac{1}{2}\rho_0 \bar{U}^2 + \bar{E}\right) = 0 \;* \qquad \text{——(17)}$$

This is the main result of this section and expresses the constancy in time of the sum of the specific zonal kinetic energy and total perturbation wave energy at a point in the y-z plane. Summarising the theme of the argument presented: the zonally-averaged momentum and perturbation energy equations are formed and knowledge of the wave-coupled meridional circulation $(\bar{v}, \bar{w})$ (induced by the poleward eddy entropy transport) and the EP relations allows them to be linked. The slowness of variation in time and in the vertical direction are the main assumptions. It can be seen from equation (11) that near $\bar{U} = 0$ the wave stress becomes very large and that the slowness assumptions would be violated. It is important to realise that in making these assumptions and interpreting the above equations, we have had in mind the notion of stationary dispersive waves though nowhere has this been explicitly introduced or the type of wave specified.

The conclusions are valid for any stationary wave disturbance varying slowly in time which satisfies equations (1)-(5).

* Later published work by Andrews D. and McIntyre M. shows that this analysis omits a term $\frac{\partial}{\partial t}(\bar{\eta}\bar{u})$ through the use of the steady E.P. relations. (η = meridional Lagrangian displacement)

Some interesting results follow immediately from (17). The slow propagation of wave energy into an undisturbed region of the atmosphere does so at the expense of the specific zonal kinetic energy so that no net transfer of energy takes place. Changes in the available potential energy of the mean state are possible since the approximation that $\frac{\partial \overline{\delta\phi}}{\partial t}$ is negligible in the thermodynamic equation does not mean that $\overline{\delta\phi}$ cannot change, only that it does so slowly. The change in available potential energy must however be much smaller than the change in zonal kinetic energy and hence little net energy transfer.

The exponential variation of density also produces interesting implications for a stationary wave disturbance propagating into progressively less dense regions. Propagation of waves in a homogeneous medium is characterised by the conservation of disturbance energy following the group velocity and for waves whose propagation properties are unaffected by the local density the specific disturbance energy is conserved even when the density field is non-uniform.

In an atmosphere of constant zonal wind $\overline{U}$ and exponentially decreasing density with height, an upward propagating wave conserving specific energy will have progressively more effect on reducing the local zonal wind strength until the assumptions on which the equation (17) are based become invalid. We might use this as some crude guide to the limit of validity of the linear theory in describing the propagation of Rossby wave energy into the stratosphere. Non-linear effects become important when the specific wave energy is comparable to the specific zonal kinetic energy.

Equation (17) implies that a stationary wave system that does not vary in amplitude with time, cannot accelerate the zonal flow if the motion is adiabatic and without dissipation. This conclusion was also reached by Charney and Drazin in connection with quasi-geostrophic wave/mean flow

interaction. Dickinson (1969) puts forward a theory of wave interaction with the mean flow in the presence of critical layer absorption and dissipation processes in which stationary, time-independent planetary waves *can* interact with the mean flow. The introduction of dissipation into the foregoing analysis only serves to complicate the physical picture and hence is omitted.

Although no net transfer of energy is accomplished by the quasi-stationary wave motion — transfer of momentum is and a simple pictorial representation is suggested (Fig.5.1).

Consider an undisturbed atmosphere of uniform zonal wind and allow a 'wave packet' to be created by the slow application of forcing at a given level for a given length of time (assuming that in this atmosphere, some form of dispersive wave may be excited). In the region of the wave packet where the disturbance energy density is large, equation (17) demands that $\bar{U}$ should have decreased so that a deficit of zonal momentum exists there compared to the undisturbed environment. The deficit of zonal momentum travels with the wave packet and therefore is transported by the disturbance. It is the result of the working of the drag force exerted on the zonal flow during the production of the disturbance wave energy. The action of orography for instance is to convert zonal kinetic energy into perturbation energy by exerting a drag on the flow through the correlation of perturbed pressure with the slope of the orography. High pressure occurs on the windward slope and low pressure on the leeward slope so that zonal (atmospheric) momentum is communicated to the earth. This is in quantitative agreement with equation (11) which gives after integration over the whole atmosphere:

$$\frac{d}{dt}\iint \rho_0 \bar{U}\, dy\, dz = \int_0^{\infty} \left[\frac{\overline{\delta p' v'}}{\bar{U}}\right]_{y=0}^{y=L} dz + \int_0^{L} \left[\frac{\overline{\delta p' w'}}{\bar{U}}\right]_{z=0}^{z=H} dy$$

where the limits $y=0,L$ will be assumed to be rigid walls.

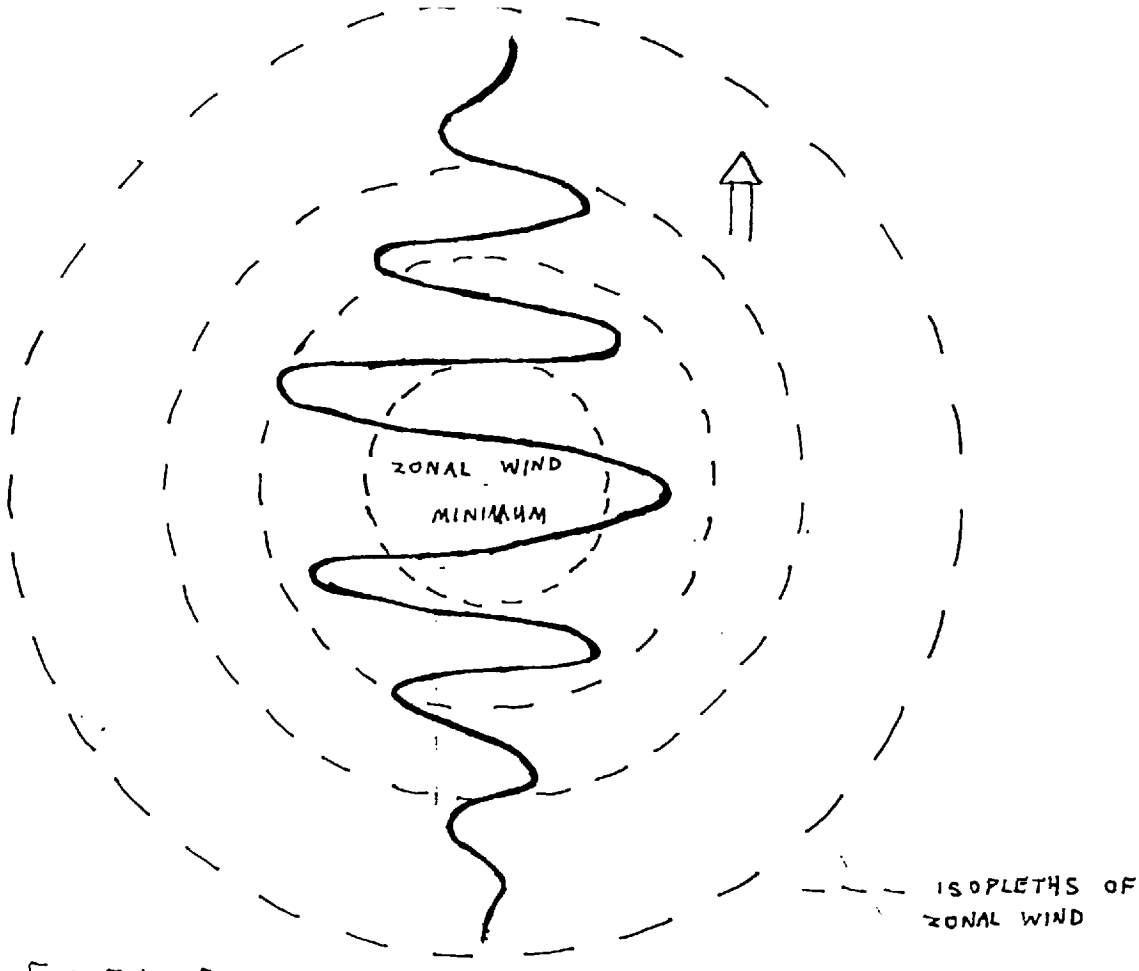

FIG. 5.1 DEFICIT OF ZONAL MOMENTUM CARRIED BY A WAVE PACKET.

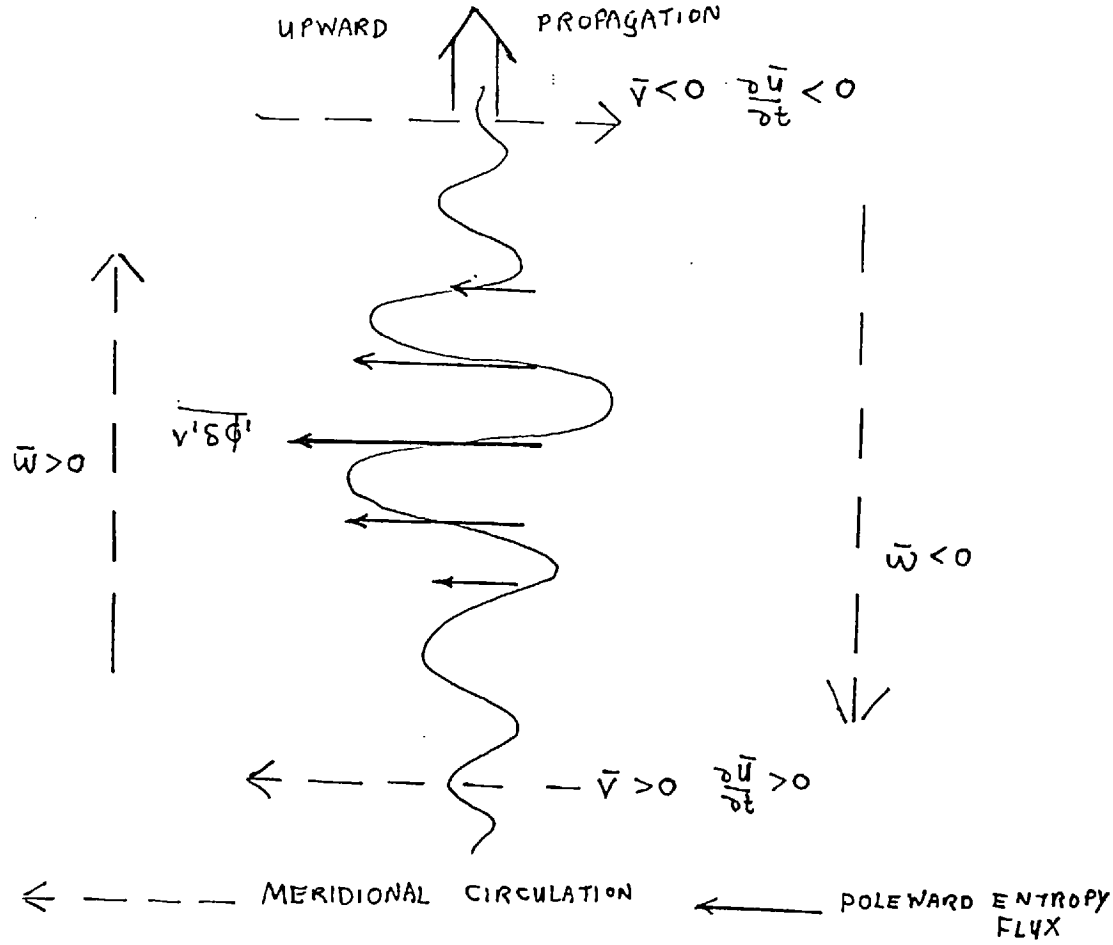

FIG. 5.2 INDUCED CIRCULATION AND HEAT TRANSPORT ASSOCIATED WITH A QUASI-GEOSTROPHIC WAVE DISTURBANCE. (SCHEMATIC)

Assuming that the upper limit $z = H$ is chosen where the vertical pressure-work term is negligibly small, then the above expression reduces to:

$$\frac{d}{dt}\iint \rho_0 \bar{U}\, dy dz = -\int_0^L \frac{\overline{\delta p' w'}}{\bar{U}}(y, z = 0)\, dy \qquad \text{——(18)}$$

noting that v' vanishes at the lateral walls at $y = 0$ and L.

The linearized lower boundary condition for flow over orography of small slopes is:

$$w' = \bar{U}\frac{\partial Z_0}{\partial x} \qquad \text{at } z = 0$$

where $Z_0 = Z_0(x, y)$, the surface elevation function. Substituting this expression for w' at the surface into (18) gives:

$$\frac{d}{dt}\left\{\iint \rho_0 \bar{U}\, dy dz\right\} = -\int_0^L \overline{\delta p' \frac{\partial Z_0}{\partial x}}\, dy$$

$\overline{\delta p' \frac{\partial Z_0}{\partial x}}$ is the net eastward drag exerted on the orography and will be denoted by τ_x so that:

$$\frac{d}{dt}\left\{\iint \rho_0 \bar{U}\, dy dz\right\} + \int_0^L \tau_x\, dy = 0$$

which states that the loss of zonal momentum from the atmosphere is equal to the drag exerted on the orography or the momentum communicated to the earth — as it should be.

It is instructive to look now at how momentum is transported by large-scale quasi-geostrophic waves.

For vertically propagating Rossby waves, the vertical eddy transfer of zonal momentum is small and equation (7) reduces to:

$$\overline{\delta p' w'} = \rho_0 \frac{f\bar{U}}{B}\overline{\delta\phi' v'}$$

so that equation (11) becomes:

$$\frac{\partial}{\partial t}(\rho_0 \bar{U}) = \frac{\partial}{\partial z}\left(\frac{f\rho_0}{B}\overline{\delta\phi' v'}\right) = \rho_0 f \bar{v}$$

Drag is exerted on the zonal flow through the 'coriolis torque' for quasi-geostrophic motion and vertical transfer of momentum is effected by the induced meridional circulation (see Fig.5.2).

For purely horizontal propagation of quasi-geostrophic wave motion equation (6) is well approximated to:

$$\overline{\delta p' v'} = - \rho_0 \bar{U} \overline{u' v'}$$

so that the acceleration of the zonal momentum field is given by:

$$\frac{\partial}{\partial t}(\rho_0 \bar{U}) = \frac{\partial}{\partial y}(\rho_0 \overline{u' v'})$$

Momentum transport is effected primarily through eddy transfer processes.

In small-scale wave motion where the Rossby number is of order unity, the vertcial eddy transfer of momentum becomes important and acts in the same sense as the coriolis acceleration i.e. to decelerate the zonal mean flow. Inertial-gravity waves provide an example of this type of mixed momentum transport.

An obvious consequence of the inferred momentum transport is that wave packets forced in westerly flows carry easterly momentum and vice versa for easterly flows.

(ii) Observational confirmation

Observational evidence of this type of wave/mean flow interaction is generally difficult to ascertain since the zonal flow is accelerated by Reynolds stresses associated with other scales of motion that are strongly time-dependent, particularly baroclinic instability in the troposphere. The stratosphere is apparently free of the baroclinic eddy motion which is so characteristic of tropospheric flow and it is here that the wave/mean flow interaction mechanism should be most prevalent.

Hirota and Sato (1971) analysed observations of zonal wind speed and wave amplitude and found a strong negative correlation between them. Their interpretation of this behaviour was that the decrease in zonal wind speed favoured enhanced upward penetration of tropospheric wave energy consistent with the Charney/Drazin criterion of propagation. Since the critical zonal wind for propagation is ~ 90 m s^{-1} for $n = 2$ modes, typical zonal wind variations of 15 m s^{-1} about the monthly mean will have little effect on the transparency of the stratosphere to upward propagating wavenumber 1 disturbances.

Our conclusions suggest that the phenomenon is completely accounted for by the interaction of quasi-stationary waves with the mean flow and that the negative correlation of zonal wind speed with wave amplitude represents the upward transmission of pulses of easterly momentum accompanying the disturbances. The deposition of the momentum depends ultimately on the fate of the wave disturbance and it might be concluded that since wave energy is absorbed between 30 and 50 km, this region will experience an east-west acceleration. The maintenance of a steady, zonal momentum field poses an interesting problem in view of the constant upward transport of easterly momentum. The accumulation of easterly momentum is probably offset to a large extent by its downward transport by a thermally-driven meridional circulation set up by strong polar night cooling.

(iii) Planetary Rossby wave propagation and wave action conservation

In this section, the wave/mean flow interacting properties of travelling, quasi-geostrophic Rossby waves will be discussed and relations derived in terms of the zonally-averaged wave energy equation, under the assumptions of the slow spatial variation of the mean zonal wind and static stability. When the mean state parameters of the flow on which propagation depends change only slowly over the distance of one wavelength then group velocity and associated wavetrain concepts are useful. The

dispersion relation appropriate to propagation in a weakly non-uniform medium expresses the relationship between frequency, wavenumber and the weak dependence on position i.e. $\sigma = \sigma(\underline{k},\underline{R})$ where σ is the frequency, $\underline{k}$ the wavenumber vector and $\underline{R}$ the position vector.

It will be shown how the eddy-pressure work term, given by the correlation of the perturbed pressure and wind speed, represents the flow of wave energy at the group speed and when substituted into the wave energy equation leads eventually to a conserved quantity, 'wave action', as named by Bretherton (1966).

Consider the quasi-geostrophic, cartesian geometry description of an atmosphere of uniform static stability on a β-plane. Linearizing the quasi-geostrophic potential vorticity equation about a mean zonal wind that is weakly space and time dependent such that $\bar{U} = \bar{U}(\varepsilon z,\varepsilon y,\varepsilon t)$ where ε is a smallness parameter, gives:

$$\left(\frac{\partial}{\partial t} + \bar{U}\frac{\partial}{\partial x}\right)\left\{\nabla_H^2\psi' + \frac{f_0^2}{gB}\frac{1}{\rho_0}\frac{\partial}{\partial z}\left(\rho_0\frac{\partial\psi'}{\partial z}\right)\right\} + \beta\frac{\partial\psi'}{\partial x} = 0 \qquad \text{to order } \varepsilon.$$

Wavetrain solutions are of the form:

$$\psi' = \underline{\text{Real}}\ \psi_0(\varepsilon z,\varepsilon y,\varepsilon t)\exp\left[i(\lambda x + \mu y + \nu z - \sigma t) + \frac{z}{2H_0}\right]$$

and associated with a dispersion relation:

$$\sigma = \bar{U}\lambda - \frac{\beta\lambda}{\lambda^2 + \mu^2 + \frac{f_0^2}{gB}\left(\nu^2 + \frac{1}{4H_0^2}\right)}$$

The Boussinesq equations consistent with the derivation of the quasi-geostrophic potential vorticity equation are:

$$\left(\frac{\partial}{\partial t} + \bar{U}\frac{\partial}{\partial x}\right)u' - fv' + \frac{\partial}{\partial x}\left(\frac{\delta p'}{\rho_0}\right) = 0 \qquad \text{——(a)}$$

$$\left(\frac{\partial}{\partial t} + \bar{U}\frac{\partial}{\partial x}\right)v' + fu' + \frac{\partial}{\partial y}\left(\frac{\delta p'}{\rho_0}\right) = 0 \qquad \text{——(b)}$$

$$\frac{\partial}{\partial z}\left(\frac{\delta p'}{\rho_0}\right) - g\delta\phi' = 0 \qquad \text{——(c)}$$

$$\left(\frac{\partial}{\partial t} + \bar{U}\frac{\partial}{\partial x}\right)\delta\phi' + w'B = 0 \qquad \text{——(d)}$$

$$\frac{\partial u'}{\partial x} + \frac{\partial v'}{\partial y} + \frac{1}{\rho_0}\frac{\partial}{\partial z}(\rho_0 w') = 0 \qquad \text{——(e)}$$

All perturbation quantities are of the form:

$$f' = \underline{\text{Real}}\ f_0(\varepsilon z, \varepsilon y, \varepsilon t)\exp\left\{i(\lambda x + \mu y + \nu z - \sigma t) + \frac{z}{2H_0}\right\}$$

with $u' = -\frac{\partial \psi'}{\partial y}$, $v' = \frac{\partial \psi'}{\partial x}$ and $\delta\phi' = \frac{f_0}{g}\frac{\partial \psi}{\partial z}$

so that to first order in ε, (a) becomes:

$$-i\mu\psi'.\left(-i\sigma + i\lambda\bar{U}\right) - i\lambda f\psi' + i\lambda\frac{\delta p'}{\rho_0} = 0$$

which gives a complex expression for $\delta p'$

$$\frac{\delta p'}{\rho_0} = \underline{\text{Real}}\left\{f + i\mu(\bar{U} - c)\right\}\psi'$$

The zonally-averaged eddy pressure-work term, $\overline{\delta p' v'}/\rho_0$ can be calculated immediately from the complex expressions for $\delta p'$ and v' since:

$$\overline{\delta p' v'} = \frac{1}{2}\underline{\text{Real}}\ (\delta p'\, v'^{*})$$

with the result that:

$$\overline{\delta p' v'} = \frac{1}{2}\rho_0\mu\lambda(\bar{U} - c)\,|\psi_0|^2$$

Similarly the complex expression for w' can be determined from the thermodynamic equation (d) and hence the vertical eddy pressure-work term, $\overline{\delta p' w'}$ becomes:

$$\overline{\delta p' w'} = -\frac{1}{2}\frac{f_0}{gB}(\bar{U} - c)\left\{\frac{\mu\lambda}{2H_0}(\bar{U} - c) - f_0\nu\lambda\right\}|\psi_0|^2$$

The first term in brackets is negligible for large-scale flow since typically $\nu \sim 1/2H_0$

$$\frac{\frac{\mu\lambda}{2H_0}(\bar{U} - c)}{f_0\nu\lambda} \sim \frac{\mu(\bar{U} - c)}{f_0} \sim Ro\ \text{(Rossby No.)} \ll 1$$

so that the vertical pressure-work term is given by:

$$\overline{\delta p' w'} = \frac{1}{2}\rho_0 \frac{f_0^2}{gB}\,(\bar{U}-c)\nu\lambda\,|\psi_0|^2$$

The zonally-averaged specific wave energy $\bar{E} = \frac{1}{2}\rho_0\left(\overline{u'^2 + v'^2 + \frac{g}{B}\delta\phi'^2}\right)$ can be expressed in terms of the streamfunction ψ and gives:

$$\bar{E} = \frac{1}{4}\rho_0\left\{\lambda^2 + \mu^2 + \frac{f_0^2}{gB}\left(\nu^2 + \frac{1}{4H_0^2}\right)\right\}|\psi_0|^2$$

The meridional and vertical group velocity components C_{gy} and C_{gz} can be calculated from the dispersion relation so that:

$$C_{gy} = \frac{2\beta\mu\lambda}{\left\{\lambda^2 + \mu^2 + \frac{f_0^2}{gB}\left(\nu^2 + \frac{1}{4H_0^2}\right)\right\}^2}$$

and

$$C_{gz} = \frac{2\beta\lambda\nu\frac{f_0^2}{gB}}{\left\{\lambda^2 + \mu^2 + \frac{f_0^2}{gB}\left(\nu^2 + \frac{1}{4H_0^2}\right)\right\}^2}$$

From these expressions and those for the pressure-work terms $\overline{\delta p' w'}$ and $\overline{\delta p' v'}$ it can easily be shown that:

$$\overline{\delta p' v'} = \bar{E}\,C_{gy} \qquad \text{and} \qquad \overline{\delta p' w'} = \bar{E}\,C_{gz}$$

demonstrating that wave energy propagates with the group speed.

Neglecting the term $\rho_0 \overline{u' w'}\frac{\partial \bar{U}}{\partial z}$ in the wave energy equation of the last section* gives:

$$\frac{\partial \bar{E}}{\partial t} + \rho_0 \overline{u' v'}\frac{\partial \bar{U}}{\partial y} - \frac{\partial \bar{U}}{\partial z}\cdot\rho_0\frac{f_0}{B}\,\overline{\delta\phi' v'} + \frac{\partial}{\partial y}\left(\overline{\delta p' v'}\right) + \frac{\partial}{\partial z}\left(\overline{\delta p' w'}\right) = 0$$

and expressions for $\overline{\delta\phi' v'}$ and $\overline{u' v'}$ can be obtained in a similar way to those of $\overline{\delta p' w'}$ and $\overline{\delta p' v'}$ giving:

$$\overline{\delta\phi' v'} = \frac{\bar{E}\,C_{gz}}{\rho_0\frac{f_0}{B}(\bar{U}-c)} \qquad \text{and} \qquad \overline{u' v'} = -\frac{\bar{E}\,C_{gy}}{\rho_0(\bar{U}-c)}$$

* justified for quasi-geostrophic motion.

Substituting the expressions derived for $\overline{\delta p' w'}$, $\overline{\delta p' v'}$, $\overline{\delta \phi' v'}$ and $\overline{u' v'}$ into the wave energy equation and re-arranging gives:

$$\frac{\partial \bar{E}}{\partial t} + \mathrm{Div}\left(\bar{E}\,\underline{C}_g\right) = \frac{\bar{E}}{\bar{U} - c}\,\underline{C}_g \cdot \mathrm{grad}\,\bar{U} \qquad \text{——(19)}$$

where Div applies only to the y,z plane.

If $\bar{U}$ is uniform equation (19) reduces to the conservation of wave energy and $\underline{C}_g$ is constant in space. The source term on the right-hand side indicates that wave groups propagating towards stronger zonal winds gain energy at the expense of the mean flow.

Wave groups propagating in non-uniform media have characteristic wavenumbers and frequencies that vary slowly in space and time with the medium properties, and for this case:

$$\sigma = \sigma\left(\underline{K}(T,Y,Z),\ \bar{U}(T,Y,Z)\right)$$

where $\underline{K} = \lambda \underline{i} + \mu \underline{j} + \nu \underline{k}$, $T = \varepsilon t$, $Y = \varepsilon y$ and $Z = \varepsilon z$.

The rate of change of frequency at a point in space, $\partial\sigma/\partial T$ can be expanded by the chain rule for partial differentiation into:

$$\frac{\partial \sigma}{\partial T} = \frac{\partial \sigma}{\partial \lambda}\frac{\partial \lambda}{\partial T} + \frac{\partial \sigma}{\partial \mu}\frac{\partial \mu}{\partial T} + \frac{\partial \sigma}{\partial \nu}\frac{\partial \nu}{\partial T} + \frac{\partial \sigma}{\partial \bar{U}}\frac{\partial \bar{U}}{\partial T}$$

From the dispersion relation, $\partial\sigma/\partial\bar{U} = \lambda$ and after collecting terms, the above equation can be written as:

$$\frac{\partial \sigma}{\partial T} = \underline{C}_g \cdot \frac{\partial \underline{K}}{\partial T} + \lambda \frac{\partial \bar{U}}{\partial T} \qquad \text{——(20)}$$

Redefining σ and $\underline{K}$ by introducing a phase function* χ such that the wavetrain solution becomes:

$$\psi' = \psi_0(Y,Z,T)\exp\left(i\chi + \frac{z}{2H_0}\right)$$

with $\sigma = -\dfrac{\partial \chi}{\partial t}$ and $\underline{K} = \mathrm{grad}\,\chi$

*As suggested by Whitham, 1961.

The slowly varying functions of space and time, σ and $\underline{K}$ satisfy the equation:

$$\frac{\partial \underline{K}}{\partial T} + \underline{\nabla}'\sigma = 0 \qquad \left(\text{where } \underline{\nabla}' = \frac{\partial}{\partial X}\underline{i} + \frac{\partial}{\partial Y}\underline{j} + \frac{\partial}{\partial Z}\underline{k}\right)$$

by definition and this is then known as the 'conservation of wave crests'.

Substituting this into equation (20) for $\partial \underline{K}/\partial T$ gives:

$$\frac{\partial \sigma}{\partial T} + \underline{C_g}.\underline{\nabla}'\sigma = \lambda \frac{\partial \overline{U}}{\partial T}$$

which indicates that the frequency of wave groups changes following the group only when the zonal wind field is being accelerated. λ is a constant since the medium properties are not dependent on x and so the above equation may be re-arranged into the form:

$$\left(\frac{\partial}{\partial T} + \underline{C_g}.\underline{\nabla}'\right)(\overline{U} - c) = (\underline{C_g}.\underline{\nabla}')\overline{U} \qquad \text{with} \quad c = \frac{\sigma}{\lambda}$$

Multiply by $\frac{\overline{E}}{\overline{U} - c}$ and taking it inside the derivative following the group leads to:

$$\left(\frac{\partial}{\partial T} + \underline{C_g}.\underline{\nabla}'\right)\overline{E} - (\overline{U} - c)\left(\frac{\partial}{\partial T} + \underline{C_g}.\underline{\nabla}'\right)\left(\frac{\overline{E}}{\overline{U} - c}\right) = \frac{\overline{E}}{\overline{U} - c}(\underline{C_g}.\underline{\nabla}')\overline{U}$$

Subtracting this from equation (19) leads to the conservation relation:

$$\frac{\partial}{\partial T}\left(\frac{\overline{E}}{\overline{U} - c}\right) + \text{Div}'\left(\frac{\overline{E}}{\overline{U} - c}.\underline{C_g}\right) = 0 \qquad \text{——(21)}$$

(primes denote slow variables)

(after dividing (19) by ε and transforming to the slow variables T, Y and Z).

The conserved quantity $\frac{\overline{E}}{\overline{U} - c}$ is named 'wave action' after Bretherton (1966), who derived it in connection with gravity wave propagation. For all its elegance, it is difficult to interpret and to make use of in this form. It is similar to the 'adiabatic invariant' quantities of classical mechanics that are of the form, energy/frequency.

It has been shown that the zonally-averaged momentum equation for large-scale flow is:

$$\frac{\partial}{\partial t}(\rho_0 \bar{U}) = \frac{\partial}{\partial z}\left(\frac{f\rho_0}{B}\,\overline{\delta\phi' v'}\right)$$

$\frac{f\rho_0}{B}\,\overline{\delta\phi' v'}$ expressed in terms of energy density and group velocity is $\frac{\bar{E}\,C_{gz}}{\bar{U}-c}$

so that: $$\frac{\partial}{\partial t}(\rho_0 \bar{U}) = \frac{\partial}{\partial z}\left(\frac{\bar{E}\,C_{gz}}{\bar{U}-c}\right)$$

Combining this with the wave action equation, neglecting y-variation gives:

$$\frac{\partial}{\partial t}\left(\rho_0 \bar{U} + \frac{\bar{E}}{\bar{U}-c}\right) = 0 \qquad \text{——(22)}$$

Uryu (1974) arrived at a similar relation from the quasi-geostrophic potential vorticity equation and interprets wave action as the momentum carried by the wave group. He points out the similarity in form of the momentum carried by a photon, energy/phase speed of light and wave action though in our case the momentum carried is at right angles to the direction of propagation i.e. east-west momentum.

Here again we see the role of a wave packet in decelerating the zonal wind field. On approaching a critical level, the quantity $\frac{\bar{E}}{\bar{U}-c}$ becomes very large since $\bar{U}-c \to 0$ and the zonal momentum field suffers a correspondingly large deceleration. Uryu uses this as a crude explanation of the sudden warming process. The easterly drag carried by the wave group from the region of forcing causes the greatest effect in the stratosphere where the zonal momentum $\rho_0\bar{U}$ decreases rapidly with height and the downward movement of the zero-wind line caused by the interaction cuts off the transmission of wave energy.

Strictly, the assumptions of slow variations in space and time are violated under these circumstances though some insight is gained.

Acknowledgements

I would like to thank my supervisor, Dr. J.S.A. Green for guidance during this work, Alastair Seaton who provided much computer programming assistance and the 'Climate Group' in general for many interesting discussions and collaboration.

The typing, along with many diagrams, was done by Marion Street to whom I am very grateful.

This work was supported by a NERC research studentship.

References

Abramowitz, M. and Stegun, I. 1964 'Handbook of Mathematical Functions'. Dover Publications.

Bretherton, F.P. 1966 'The propagation of groups of internal gravity waves in a shear flow', *Quart.J.R.Met.Soc.*, 92, p.466.

Brunt, D. 1934 'Physical and Dynamical Meteorology'. Cambridge University Press.

Charney, J.G. 1948 'On the scale of atmospheric motions', *Geofys. Publ.*, 17, 2, pp.1-17.

Charney, J.G. and Drazin, P.G. 1961 'Propagation of planetary scale disturbances from the lower into the upper atmosphere', *J.Geophys.Res.*, 66, pp.83-109.

Charney, J.G. and Eliassen, A. 1949 'A numerical method for predicting the perturbations on the middle latitude westerlies', *Tellus*, 1, pp.38-54.

Clapp, P.F. 1961 'Normal heat sources and sinks in the lower troposphere', *Month.Weath.Rev.*, 89, pp.147-162.

Dickinson, R. 1969 'The theory of planetary wave - zonal flow interaction', *J.Atmos.Sci.*, 26, pp.73-81.

Dickinson, R. 1972 'Motions in the stratosphere', CIAP Survey Conference Proceedings, pp.148-161, (U.S. Dept. Transportation).

Eliassen, E. 1958 'A study of the long atmospheric waves on the basis of zonal harmonic analysis', *Tellus*, 10, pp.206-215.

Eliassen, A. and Palm, E. 1960 'On the transfer of energy in stationary mountain waves', *Geofys.Publ.*, 22, 3, pp.1-23.

Geisler, J.E. and Dickinson, R.E. 1974 'Numerical study of an interacting Rossby wave and barotropic zonal flow near a critical level', *J.Atmos.Sci.*, 31, pp.946-955.

Green, J.S.A. 1972 'Large-scale motion in the upper stratosphere and mesosphere: an evaluation of data and theories, *Phil.Trans.R.Soc.* Lond. A, 271, pp.577-583.

Hadley, G. 1735 *Phil.Trans.R.Soc.*, 29, p.58.

Hirota, I. and Sato, Y. 1969 'Periodic variation of the winter stratospheric circulation and intermittent vertical propagation of planetary waves', *J.Met.Soc. Japan*, 46, pp.418-430.

Lindzen, R.S. and Kuo, H.L. 1969 'A reliable method for the numerical integration of a large class of ordinary and partial differential equations', *Month.Weath.Rev.*, 97, pp.732-734 (correspondence).

London, J. 1952 *J.Meteor.*, 9, p.145.

Mahlman, J. and Manabe, S. 1972 'Numerical simulation of the stratosphere: implications for related climate change problems', CIAP Survey Conference Proceedings, p.186, (U.S. Dept. of Transportation).

Matsuno, T. 1970 'Vertical propagation of stationary planetary waves in the winter Northern Hemisphere', *J.Atmos.Sci.*, 27, pp.871-883.

Möller, F. 1950 *Experientia*, Basel, 6, p.361.

Murikami, M. 1974 'Influence of mid-latitudinal planetary waves on the tropics under the existence of a critical latitude', *J.Met.Soc. Japan*, 52, pp.261-271.

Muench, H.S. 1965 'On the dynamics of the wintertime stratospheric circulation', *J.Atmos.Sci.* 22, pp.349-360.

Oort, A.H. and Rasmusson, E.M. 1971 'Atmospheric circulation statistics', NOAA Prof. Paper 5, U.S. Dept. Commerce.

Sankar-Rao, M. 1965 'Continental elevation influence on the stationary harmonics of the atmospheric motion', *Pure and Appl. Geophys.*, 60, pp.141-159.

Sato, Y. 1974 'Vertical structure of quasi-stationary planetary waves in several winters', *J.Met.Soc. Japan*, 52, pp.272-281.

Simmons, A. 1974 'Planetary-scale disturbances in the polar winter stratosphere', *Quart.J.R.Met.Soc.*, 100, pp.76-108.

Smagorinsky, J. 1953 'The dynamical influence of large-scale heat sources and sinks on the quasi-stationary mean motions of the atmosphere', *Quart.J. R.Met.Soc.*, 79, pp.342-366.

Uryu, M. 1974 'Mean zonal flows induced by a vertically propagating Rossby wave packet', *J.Met.Soc. Japan*, 52, pp.481-490.

Whitham, G.B. 1961 'Group velocity and energy propagation for three dimensional waves', *Commun. on Pure and Appl. Maths.*, XIV, pp.675-691.

White, A.A. 1976 'Modified quasi-geostrophic equations using geometric height as vertical coordinate', submitted to the *Quart.J.R.Met.Soc.*

White, A.A. and Green, J.S.A. 1975 'Parameterised heat transfer in a low-resolution spectral climate model', contributed paper to A.N.M.R.C. Conference, 'Climate and Climatic Change'.

Willet, H.C. 1961 'The pattern of solar-climatic relationships', *Ann. N.Y. Acad.Sci.*, 95, pp.89-106.

APPENDIX Notes on the quasi-geostrophic potential vorticity equation

The following is a brief summary of the derivation of the quasi-geostrophic potential vorticity theorem and the approximations constituting the Boussinesq set. White, A. (1976) derives the normal *Q.G.P.V.* equation from a substantially less approximated set than the standard Boussinesq equations and most of this section is adapted from his work. Although it turns out that the mathematical problem of stationary forcing is unchanged by the increased generality inherent in the modified set, some changes in emphasis in the energetics of the wave motion become apparent which are important in the stratosphere.

Following the procedure of Charney (1948), typical velocity scales, V (horizontal), W (vertical) and length scales L (horizontal), H (vertical) are chosen and associated with these are pressure, density and entropy deviations δp, $\delta\rho$ and $\delta\phi$ from the undisturbed basic state variables $p_0(z)$, $\rho_0(z)$ and $\phi_0(z)$ respectively. All local time derivatives are taken to be of the order of the advective part of the substantial derivative at most and the flow is assumed hydrostatic throughout.

The height scale H of the motion under consideration is typically of similar size to the vertical scales of the static pressure and density fields $\left(-\frac{1}{p_0}\frac{dp_0}{dz}\right)^{-1}$ and $\left(-\frac{1}{\rho_0}\frac{d\rho_0}{dz}\right)^{-1}$ $(=H_\rho)$ respectively and White concludes that the important results are modified only through the replacement of H by the smaller of H and H_ρ.

The equations of motion for inviscid, adiabatic flow in hydrostatic balance are:

$$\left(\frac{\partial}{\partial t} + \underline{V}_H.\underline{\nabla}\right)\underline{V}_H + w\frac{\partial \underline{V}_H}{\partial z} + f\underline{k}\wedge\underline{V}_H + \frac{1}{\rho}\underline{\nabla}_H\delta p = 0 \qquad \text{——(A)}$$

(momentum equation)

$$\frac{\partial p}{\partial z} + \rho g = 0 \quad . \qquad \text{(hydrostatic equation)} \qquad \text{——(B)}$$

$$\left(\frac{\partial}{\partial t} + \underline{V}_H.\underline{\nabla}\right)\delta\rho + \rho\,\underline{\nabla}.\underline{V}_H + \frac{\partial}{\partial z}(\rho w) = 0 \qquad \text{(continuity of mass)} \quad \text{——(C)}$$

$$\left(\frac{\partial}{\partial t} + \underline{V}_H.\underline{\nabla}\right)\delta\phi + w\frac{\partial\phi}{\partial z} = 0 \qquad \text{(conservation of entropy)} \quad \text{——(D)}$$

$$\phi = \frac{1}{\gamma}\log p - \log\rho \qquad \text{(entropy of a perfect gas)} \quad \text{——(E)}$$

(where γ is the ratio of specific heats)

The coriolis term, $2\Omega\cos(\text{lat.})w\underline{i}$ has been omitted from the horizontal momentum equation (A) since $W << V$.

Hydrostatic balance and quasi-geostrophy impose a close relationship between the motion field and thermodynamic variables such that (A), (B) and (E) give:

$$\frac{\delta p}{p}, \quad \frac{\delta\rho}{\rho} \quad \text{and} \quad \delta\phi \sim f\frac{VL}{gH}$$

Motion in rotating, stratified fluids is characterised by the non-dimensional numbers:

$$Ro = \frac{V}{fL} \qquad \text{——Rossby No.}$$

and

$$Ri = \frac{gB}{(V/H)^2} \qquad \text{——Richardson No.}$$

and the order of magnitude of terms is conveniently expressed as a function of them, so that:

$$\frac{\delta p}{p}, \quad \frac{\delta\rho}{\rho} \quad \text{and} \quad \delta\phi \sim \frac{BH}{RiRo}.$$

For large-scale flow, typically:

$$Ro \sim 0.1, \quad Ri \sim 100 \quad \text{and} \quad BH \lesssim 0.3$$

and it can be seen that $\frac{\delta p}{p}$, $\frac{\delta\rho}{\rho}$ and $\delta\phi$ are all very much less than unity.

The conservation of entropy, equation (D), allows estimation of the vertical velocity W and gives:

$$\frac{W}{H} \sim \frac{fV^2}{gBH^2} \sim \frac{V}{L}.(Ri\,Ro)^{-1}$$

which implies physically that knowledge of the slope of isentropic surfaces

and typical horizontal velocities gives the order of the vertical velocity since parcels tend to move along the isentropes (exactly for steady entropy fields, with $(\underline{V}.\nabla)\phi = 0$).

Using the above results to estimate the size of terms in the continuity equation (C) gives:

$$\frac{1}{\rho}\left(\frac{\partial}{\partial t} + \underline{V}_H.\underline{\nabla}\right)\delta\rho \sim \frac{fV^2}{gH} \quad \text{and} \quad \frac{1}{\rho}\frac{\partial}{\partial z}(\rho w) \sim \frac{fV^2}{gH}(BH)^{-1}$$

which implies that $\underline{\nabla}.\underline{V}_H \sim \frac{V}{L}(Ri\,Ro)^{-1}$ and in this sense the flow is almost horizontally non-divergent since $Ri\,Ro >> 1$. Also, it can be seen that horizontal advection $\underline{V}_H.\underline{\nabla}$ is much larger than vertical advection $w\frac{\partial}{\partial z}$ and this allows the rejection of $w\frac{\partial \underline{V}_H}{\partial z}$ in (A) and the replacements $\frac{\partial}{\partial z}(\rho w)$ with $\frac{\partial}{\partial z}(\rho_0 w)$ in (C) and $w\frac{\partial \phi}{\partial z}$ with wB in (D).

The horizontal advection of density is only negligible compared to $\frac{\partial}{\partial z}(\rho_0 w)$ if $BH << 1$ and for deep stratospheric motion this is not a good approximation.

The horizontal wind $\underline{V}_H$ may be partitioned into a rotational component $\underline{V}_\psi$ and divergent component $\underline{V}_\sigma$ with:

$$\underline{V}_\psi = k \wedge \underline{\nabla}\psi$$

and

$$\underline{\nabla}.\underline{V}_H = \underline{\nabla}(\underline{V}_\psi + \underline{V}_\sigma) = \underline{\nabla}.\underline{V}_\sigma$$

Consistent with these approximations, we may form the vorticity equation from (A) giving:

$$\left(\frac{\partial}{\partial t} + \underline{V}_\psi.\underline{\nabla}\right)\left(\nabla_H^2\psi + f\right) + f\,\underline{\nabla}.\underline{V}_\sigma + \frac{k.}{\rho_0}\left(\underline{\nabla}\delta\phi \wedge \underline{\nabla}\delta p\right) = 0$$

Introduction of the scale expressions into the baroclinic and horizontal advection terms gives the ratio:

$$\frac{\underline{k}.\left(\underline{\nabla}\delta\phi \wedge \underline{\nabla}\delta p\right)}{\left(\underline{V}_\psi.\nabla\right)\left(\nabla_H^2\psi + f\right)} \sim \frac{f^2L^2}{gH} \sim BH\left(Ri\,Ro^2\right)^{-1}$$

and for large-scale flow $Ri\,Ro^2 \sim 1$ so that the smallness of the baroclinic term in the vorticity equation depends on the inequality, $BH \ll 1$.

The entropy expression (E) may be approximated to give the perturbation entropy equation: $\delta\phi = \frac{1}{\gamma}\frac{\delta p}{p_0} - \frac{\delta\rho}{\rho_0}$ (since $p \simeq p_0$ and $\rho \simeq \rho_0$) and using this in the perturbation hydrostatic equation, $\frac{\partial \delta p}{\partial z} + g\delta\rho = 0$ gives:

$$\left(\frac{\partial}{\partial z} - B\right)\frac{\delta p}{\rho_0} - g\delta\phi = 0$$

The familiar Boussinesq approximation is based on the smallness of $\frac{\delta p}{p_0}$, $\frac{\delta\rho}{\rho_0}$ and $\delta\phi$, *plus* the change in density following the horizontal motion in (C) and $B\frac{\delta p}{\rho_0}$ in the above hydrostatic relation. Both of these latter assumptions are necessary to form a dynamically consistent set and both are justified by the smallness of BH. The standard derivation of the quasi-geostrophic potential vorticity equation involves the omission of the baroclinic generation term in the vorticity equation which is also based on $BH \ll 1$.

White shows that a dynamically consistent, quasi-geostrophic set may be obtained for motion with $BH \sim 1$ by the retention of all these terms and puts forward the following equations to determine the motion:

$$\left(\frac{\partial}{\partial t} + \underline{V}_H.\underline{\nabla}\right)\left(\nabla_H^2\psi + f\right) + f_0\underline{\nabla}.\underline{V}_\sigma + \frac{\underline{k}}{\rho_0}\cdot\underline{\nabla}\delta\phi \wedge \underline{\nabla}\delta p = 0 \qquad \text{——(1)}$$

$$\psi = \frac{\delta p}{\rho_0 f_0} \qquad \text{——(2)}$$

$$\left(\frac{\partial}{\partial z} - B\right)\frac{\delta p}{\rho_0} - g\delta\phi = 0 \qquad \text{——(3)}$$

$$\left(\frac{\partial}{\partial t} + \underline{V}_\psi.\underline{\nabla}\right)\frac{\delta\rho}{\rho_0} + \underline{\nabla}.\underline{V}_\sigma + \frac{1}{\rho_0}\frac{\partial}{\partial z}(\rho_0 w) = 0 \qquad \text{——(4)}$$

$$\left(\frac{\partial}{\partial t} + \underline{V}_\psi.\nabla\right)\delta\phi + wB = 0 \qquad \text{——(5)}$$

and

$$\delta\phi = \frac{1}{\gamma}\frac{\delta p}{p_0} - \frac{\delta\rho}{\rho_0} \qquad \text{——(6)}$$

As in standard, quasi-geostrophic theory the coriolis parameter is approximated by a constant, mid-latitude value f_0 in the association with the divergence

of the horizontal wind in (1) and the pressure/streamfunction relation (2).

It can be shown that this modified set ((1)-(6)) has well-defined integral conservation properties of mass, entropy, potential vorticity and energy which is desirable if they are to be a suitable approximation to the 'primitive equations'.

The potential vorticity theorem is derived as follows:

Eliminating $\underline{\nabla}.\underline{V}_\sigma$ from (1) and (4) gives:

$$\left(\frac{\partial}{\partial t} + \underline{V}_\psi.\underline{\nabla}\right)\left(\nabla_H^2\psi + f - f_0\frac{\delta\rho}{\rho_0}\right) - \frac{f_0}{\rho_0}\frac{\partial}{\partial z}(\rho_0 w) + \frac{\underline{k}}{\rho_0}.\underline{\nabla}\,\delta\phi \wedge \underline{\nabla}\,\delta p = 0 \qquad \text{——(7)}$$

Multiplying equation (5) by $\frac{\rho_0}{B}$ and differentiating w.r.t. z gives:

$$\left(\frac{\partial}{\partial t} + \underline{V}_\psi.\underline{\nabla}\right)\left\{\frac{\partial}{\partial z}\left(\frac{\rho_0}{B}\delta\phi\right)\right\} + \frac{\rho_0}{B}\frac{\partial \underline{V}_\psi}{\partial z}.\underline{\nabla}\delta\phi + \frac{\partial}{\partial z}(\rho_0 w) = 0 \qquad \text{——(8)}$$

and elimination of $\frac{\partial}{\partial z}(\rho_0 w)$ between (7) and (8) leads to:

$$\left(\frac{\partial}{\partial t} + \underline{V}_H.\underline{\nabla}\right)\left\{\nabla_H^2\psi + f - f_0\frac{\delta\rho}{\rho_0} + \frac{f_0}{\rho_0}\frac{\partial}{\partial z}\left(\frac{\rho_0}{B}\delta\phi\right)\right\} + \frac{f_0}{B}\frac{\partial \underline{V}_\psi}{\partial z}.\underline{\nabla}\,\delta\phi + \frac{\underline{k}}{\rho_0}.\underline{\nabla}\,\delta\phi \wedge \underline{\nabla}\,\delta p = 0 \qquad \text{——(9)}$$

The complete thermal wind equation obtained by applying the operator $\underline{k} \wedge \underline{\nabla}$ to (3) and using (2) results in:

$$\frac{\partial \underline{V}_\psi}{\partial z} = \underline{k} \wedge \underline{\nabla}\left(\frac{\partial \psi}{\partial z}\right) = \frac{\underline{k}}{f_0} \wedge \left(g\,\underline{\nabla}\,\delta\phi + B\,\underline{\nabla}\frac{\delta p}{\rho_0}\right)$$

and on substitution into the second term of equation (9), we find a cancellation with the baroclinic term. Moreover, when $\delta\rho$ and $\delta\phi$ in the remaining part of (9) are written in terms of ψ, the equation simplifies to the conservation theorem:

$$\left(\frac{\partial}{\partial t} + \underline{V}_\psi.\underline{\nabla}\right)\left\{\nabla_H^2\psi + f + \frac{f_0^2}{g\rho_0}\frac{\partial}{\partial z}\left(\frac{\rho_0}{B}\frac{\partial \psi}{\partial z}\right)\right\} = 0$$

which states that the quasi-geostrophic, potential vorticity is conserved following the horizontal projection of the non-divergent motion.

Although the corresponding theorem derived from the standard Boussinesq

set (which includes the subsiding assumption $BH << 1$) is identical, the equation developed here is more general since it implicitly contains virtually exact hydrostatic and continuity equations together with the baroclinic generation of vorticity term.

The equation for the entropy perturbation in terms of ψ is however different and equations (2) and (3) lead to:

$$\delta\phi = \frac{f_0}{g}\left(\frac{\partial}{\partial z} - B\right)\psi$$

as opposed to $\delta\phi = \frac{f_0}{g}\frac{\partial\psi}{\partial z}$ for the standard Boussinesq set.

Upper and lower boundary conditions are usually expressed as conditions on w, which is obtained from the conservation of entropy equation as:

$$w = -\left(\frac{\partial}{\partial t} + \underline{V}_\psi.\underline{\nabla}\right)\left(\frac{f_0}{gB}\frac{\partial\psi}{\partial z} - \frac{f_0\psi}{g}\right)$$

and is different from that obtained from the standard Boussinesq approximation by virtue of the term $\frac{f_0\psi}{g}$. But for all time-independent problems with $\frac{\partial}{\partial t} \equiv 0$, this extra contribution vanishes since $\underline{V}_\psi.\underline{\nabla}\frac{f_0\psi}{g} = 0$ and the boundary condition is not modified.

An expression for the temperature perturbation in terms of the streamfunction can be obtained from the hydrostatic equation:

$$\frac{\partial\delta p}{\partial z} + g\delta\rho = 0$$

by using equation (2), $\psi = \frac{\delta p}{\rho_0 f_0}$ and the differential form of the perfect gas equation:

$$\frac{\delta\rho}{\rho_0} = -\frac{\delta T}{T_0} + \frac{\delta p}{p_0}$$ (where δT is the temperature deviation from the basic state temperature $T_0(z)$)

so that: $$\frac{\delta\rho}{\rho_0} = \frac{f_0}{g}\left(\frac{\psi}{H_0} - \frac{\partial\psi}{\partial z}\right) = -\frac{\delta T}{T_0} + \frac{\delta p}{p_0}$$

and for a constant temperature atmosphere $p_0 = \rho_0 g H_0$, and substitution into

the above equation gives:

$$\frac{\delta T}{T_0} = \frac{f_0}{g}\frac{\partial \psi}{\partial z}$$

The conservation of energy is obtained by multiplying (1) by ψ, using (2) and (4) and integrating over a volume V with zero boundary fluxes giving:

$$\frac{d}{dt}\left\{ \int_V \rho_0 \left[\frac{1}{2}(\underline{\nabla}\psi)^2 - f_0 w \frac{\partial \psi}{\partial z} + f_0 \psi \frac{\partial}{\partial t}\left(\frac{\delta p}{\rho_0}\right)\right] d\tau \right\} = 0$$

(where $d\tau$ is an increment of volume)

which, using (2), (3), (5) and (6), reduces to:

$$\frac{d}{dt}\left\{ \frac{1}{2}\int_V \rho_0 \left[(\nabla\psi)^2 + \frac{g}{B}\delta\phi^2 + \frac{1}{c^2}\left(\frac{\delta p}{\rho_0}\right)^2 \right] d\tau \right\} = 0$$

($c = \sqrt{\gamma R T_0}$, the speed of sound).

The total potential energy of the modified equation set, involves an elastic energy contribution from the term $\frac{1}{c^2}\left(\frac{\delta p}{\rho_0}\right)^2$ which can be seen to be comparable with the kinetic energy term $\frac{1}{2}\rho_0(\underline{\nabla}\psi)^2$, for if $\underline{\nabla} \sim \frac{m}{R}$ (m = zonal wavenumber and R = the earth's radius) then:

$$\frac{\frac{1}{c^2}\left(\frac{\delta p}{\rho_0}\right)^2}{(\nabla\psi)^2} \sim \frac{\frac{f_0^2}{c^2}}{(m/R)^2} \sim \frac{4}{m^2}$$

and the elastic modification is most important for long waves.

In view of the much wider range of validity of the *Q.G.P.V.* equation than implied by the standard Boussinesq approximation we can be confident that the stationary forcing problems of earlier chapters are well-founded.